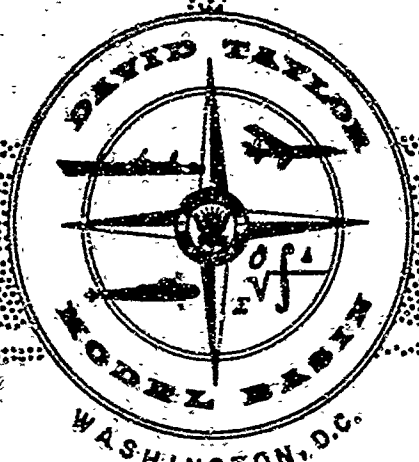

DEPARTMENT OF THE NAVY

HYDROMECHANICS

AERODYNAMICS

STRUCTURAL MECHANICS

APPLIED MATHEMATICS

ACOUSTICS AND VIBRATION

HYDRODYNAMIC ASPECT OF PROPELLER DESIGN BASED ON LIFTING-SURFACE THEORY PART I UNIFORM CHORDWISE LOAD DISTRIBUTION

by

Henry M. Cheng

HYDROMECHANICS LABORATORY
RESEARCH AND DEVELOPMENT REPORT

September 1964

Report 1802

HYDRODYNAMIC ASPECT OF PROPELLER DESIGN BASED ON LIFTING-SURFACE THEORY PART I UNIFORM CHORDWISE LOAD DISTRIBUTION

by

Henry M. Cheng

September 1964

Report 1802

TABLE OF CONTENTS

LIST OF FIGURES

LIST OF TABLES

NOTATION

A_1	Area of a lifting surface
A_2	Area of the helical surface behind the trailing edge of a lifting surface extended to infinity
A_3	Area between a superimposed lifting line and the trailing edge
a_n	Coefficients as defined in Equation [17]
b_n	Coefficients as defined in Equation [21]
C_m	Ordinate of mean line
D	Diameter of propeller
J_s	Advance coefficient based on ship velocity
L	Chordwise coordinate of any point with respect to reference line
L_l	Chordwise coordinate of leading edge
L_t	Chordwise coordinate of trailing edge
L_T	Chord length
n	Revolutions per unit time
P	Point on lifting surface at which mean line is sought
p	Pitch-diameter ratio
$\overline{R}$	Distance vector between two points
r	Radial coordinate
r_h	Radial coordinate of hub
r_0	Radial coordinate of point P
$\overline{dr}$	Length vector of an elementary bound vortex line on a lifting surface; $\overline{dr}/\lvert dr\rvert$ is a unit vector tangent to the bound vortex line
$\overline{ds}$	Length vector of an elementary free vortex line, $\overline{ds}/\lvert rd\phi\rvert$ is a unit vector tangent to the free vortex line

u_a, u_t	Nondimensional axial and tangential components, respectively, of induced velocity from lifting-line calculation based on ship velocity
V	Nondimensional inflow velocity based on ship speed
$\overline{V_B}$	Induced velocity vector at point P due to radial bound circulation
V_{ba}, V_{bt}	Axial and tangential components of $\overline{V_B}$
$\overline{V_F}$	Induced velocity vector at point P due to free circulation
V_{fa}, V_{ft}	Axial and tangential components of $\overline{V_F}$
$\overline{V_L}$	Velocity vector at a lifting line induced by trailing free vortex sheets
$\overline{V_P}$	Total induced velocity vector at point P
$\overline{V_{PL}}$	Total induced velocity vector at point P relative to $\overline{V_L}$
V_s	Ship velocity
V_x	Nondimensional local longitudinal velocity based on ship velocity
$\overline{v}$	Nondimensional induced velocity
v_a, v_t	Nondimensional axial and tangential components, respectively, of induced velocity v based on ship velocity
v_n	Nondimensional induced downwash at point P normal to helical chord line based on ship velocity
v_{ba}, v_{bt}	Axial and tangential components of $\overline{V_B}$ within a strip between r_1 and r_2
v_{fa}, v_{ft}	Axial and tangential components of $\overline{V_F}$ within a strip between r_1 and r_2
x, y, z	Cartesian coordinates
x	Chordwise coordinate
w_x	Local wake fraction
y	Radial coordinate as defined in Equation [17]
Z	Number of propeller blades

β	Advance angle
β_i	Hydrodynamic pitch angle
Γ	Nondimensional circulation = circulation πDV_s
$\Gamma(r)$	Nondimensional bound circulation distribution along a lifting line
$\Gamma_{c.}(r)$	Nondimensional free circulation distribution on free vortex sheet trailing a lifting line or a lifting surface
$\Gamma_f(r, \theta)$	Nondimensional free circulation distribution
$\Gamma_r(r, \theta)$	Nondimensional bound circulation distribution on a lifting surface
$\Gamma_\theta(r, \theta)$	Nondimensional free circulation distribution on a lifting surface
γ	Circulation per unit angle = $\frac{\Gamma(r)}{\theta_T}$
δ_0	Half width of a strip between r_1 and r_2
ξ	$x - x_0$
θ	Angular coordinate = $L \cos \beta_i / r$
θ_l	Angular coordinate of leading edge
θ_0	Angular coordinate of point P
θ_t	Angular coordinate of trailing edge
θ_T	Total chord length in terms of angular coordinate
ϕ	$\theta - \theta_0$
ϕ_l	$\theta_l - \theta_0$
ϕ_m	$\phi + 2\pi(m-1)/Z$

ABSTRACT

This report presents a method of the propeller camber calculations for the case of uniform chordwise load distribution employing the lifting-surface theory. This is essentially a refinement of Pien's published work on propeller lifting-surface theory. Mathematical development pertinent to the numerical computation is reviewed. Details of the computational procedure and method are outlined, and results of sample calculations are included. A detailed instruction for preparation of input data for the computer, samples of the computer input data and output, and the FORTRAN listing of the computer program are also given.

INTRODUCTION

In Reference 1, Pien proposed an improved method for the calculations of marine propellers by applying the lifting-surface theory.[1] Included in Reference 1 was an outline for the numerical computation by means of a high-speed computer, IBM 709. The computation was programmed for the case of uniform chordwise load distribution. After his paper was published, a model propeller (Model 3916) was designed by using this improved method and was tested; the results showed a thrust deficiency of approximately 7 percent.

In the fall of 1962 an active propeller research project was planned and initiated by Pien. The overall program included the formulations and the numerical evaluations for the following cases:

1. Propeller camber calculation method for uniform chordwise load distribution,
2. Propeller camber calculation method for arbitrary (nonuniform) chordwise load distribution,
3. Prediction of performance for a given propeller in steady inflow, and
4. Prediction of performance for a given propeller in unsteady inflow.

This report deals with the first case, the camber calculation method for uniform chordwise load distribution. With the overall project in view, the numerical computation procedure and the programing, reported in Reference 1, were revised. This new program incorporates features that will provide a greater degree of flexibility to facilitate handling of a larger number of parameters and to serve as a basic program for the subsequent works.

A brief discussion of the formulation of the problem and a detailed description of the numerical computation procedure are given in this report. Results of a number of examples with different design parameters such as number of blades and area ratios are also included.

---

[1] References are listed on page 61.

A detailed instruction for preparation of input data, and the FORTRAN listing of the computer program, as well as samples of computer input and output data are given in the appendixes.

FORMULATION

The detailed formulation of the problem is given in Reference 1. For the sake of completeness of presentation, a brief discussion of the mathematical development of the problem and the derivation of the pertinent equations, on which the numerical computations are based, are given.

COORDINATE SYSTEM

A Cartesian (x, y, z) coordinate system, shown in Figure 1, is fixed on the propeller. The x-axis is the axis of the propeller shaft with its positive pointing upstream, the y-axis is an axis on the first blade arbitrarily selected so as to pass through the midchord at $r = 0.7R$ with its positive outward, and the z-axis is the third axis and has its positive in accordance with the right-hand rule. Another coordinate system is also shown in Figure 1. It is a cylindrical coordinate system in which a point in space can be identified by (r, θ, x) where r is the radial coordinate, θ is the angular coordinate (positive clockwise looking forward), and x is the same as defined above. Along a helical line the axial coordinate can be expressed in terms of pitch-diameter ratio $p(r)$, i.e., $x = p(r)\,\theta/\pi$ as shown in Figure 1. This cylindrical coordinate system is used in the formulation of the basic equations.

For convenience in the numerical computations a "moving" cylindrical coordinate is devised. This system has r, ϕ, and ξ as its coordinates, where r is the radial coordinate, ϕ is the new angular coordinate and is defined as $\phi = \theta - \theta_0$, and ξ is a new axial coordinate and is defined as $\xi = x - x_0$, where (r, θ, x) and (r_0, θ_0 , x_0) identify a field point $Q(r, \theta, x)$ and a control point $P(r_0, \theta_0, x_0)$, respectively, in the "stationary" cylindrical coordinate system. Also defined are the unit vectors, $\bar{i}$, $\bar{j}$, $\bar{k}$, in the directions of r_0, ϕ, and ξ, respectively.

In this new "moving" cylindrical coordinate system the control point $P(r_0, \vartheta_0, x_0)$ is identified by the vector $\bar{i}\,r_0$, and the distance vector $\bar{R}$ between a field point $Q(r, \theta, x)$ and P is expressed as follows:

$$\bar{R} = \bar{i}\,(r_0 - r\cos\phi) - \bar{j}\,r\sin\phi - \bar{k}\phi p(r)/\pi$$

Similarly, the vectorial expressions for the element of length of the bound vortex line on the lifting surface, $\overline{dr}$, and for the element of length on the free vortex line, $\overline{ds}$, are as follows:

$$\overline{dr} = dr\,(i\cos\phi + \bar{j}\sin\phi + \bar{k}\phi\,p'(r)/\pi)$$

$$\overline{ds} = d\phi\,(-ir\sin\phi + \bar{j}r\cos\phi + \bar{k}\,p(r)/\pi)$$

These two expressions will be used in the evaluation of the induced velocities.

BASIC EQUATIONS

It is assumed that the propeller is operating in incompressible, inviscid fluid. The thickness of the propeller blade is assumed to be zero. The theory postulates that the propeller blade may be represented by a lifting surface of the same outline. On this surface, vorticity distribution is so placed and with such intensity that for a given design condition, a certain force distribution is developed.

Let r, θ, and x be the coordinates of a field point Q (see Figures 1 and 2) where the intensity of bound vorticity is denoted as $\Gamma_r(r, \theta)$. Then the following relationship holds:

$$\int_{\theta_t(r)}^{\theta_l(r)} \Gamma_r(r, \theta)\, d\theta = \Gamma(r) \qquad [1]$$

where chordwise coordinates $\theta_l(r)$ and $\theta_t(r)$ define, respectively, the leading and trailing edges of the lifting surface, and $\Gamma(r)$ is the radial bound circulation distribution which can be computed from lifting line theory to satisfy certain design thrust or torque conditions.

Because of the variation of $\Gamma(r)$ along the radial direction, a free vortex sheet is shed and trails behind. It is assumed that this trailing vortex sheet is a general helical surface formed by helical lines, neglecting the radial contraction of the slipstream. As an approximation the helical surface is extended to the leading edge of the lifting surface and the lifting surface is assumed to be a part of this helical surface. In the lifting-surface representation there exist two vortex systems: the radial bound system on the surface with an intensity of $\Gamma_r(r, \theta)$, and the free system with an intensity of $\Gamma_f(r, \theta)$. The latter may be considered as consisting of two parts: the part that is on the lifting surface with an intensity designated as $\Gamma_\theta(r, \theta)$, and the part that trails behind the trailing edge in the slipstream which has an intensity of $\Gamma_c(r)$. In the slipstream, the circulation $\Gamma_c(r)$ is

$$\Gamma_c(r) = -\frac{d}{dr}\,\Gamma(r)\, dr \qquad [2]$$

Combining Equations [1] and [2], we have

$$\Gamma_c(r) = -\frac{d}{dr}\left[\int_{\theta_t(r)}^{\theta_l(r)} \Gamma_r(r, \theta)\, d\theta\right] dr \qquad [3]$$

The free circulation on the lifting surface may be expressed as

$$\Gamma_\theta (r, \theta) = - \frac{d}{dr} \left[\int_\theta^{\theta_l} \Gamma_r (r, \theta)\, d\theta \right] dr$$

The induced velocity at any point P on the lifting surface due to these two vortex systems is derived by the use of the law of Biot-Savart. The resulting general expression is as follows:

$$\overline{V_P} = \frac{1}{4\pi} \iint_{A_1} \Gamma_r (r, \theta)\, d\theta\, \frac{\overline{dr} \times \overline{R}}{R^3} + \frac{1}{4\pi} \iint_{A_1 + A_2} \Gamma_f (r, \theta)\, \frac{\overline{ds} \times \overline{R}}{R^3} \qquad [4]$$

where $\overline{V_P}$ = total induced velocity vector at point P on the lifting surface,

$\overline{R}$ = distance vector between a point P and a point where elementary vortex is located,

$\overline{ds}$ = length vector of an elementary vortex line in the free system,

$\overline{dr}$ = length vector of an elementary bound vortex line on the lifting surface,

A_1 = area of the lifting surface, and

A_2 = area of the helical surface behind trailing edge of the lifting surface extended to infinity downstream.

The second term of Equation [4] may be expressed as follows:

$$\frac{1}{4\pi} \iint_{A_1 + A_2} \Gamma_f (r, \theta)\, \frac{\overline{ds} \times \overline{R}}{R^3} = \frac{1}{4\pi} \iint_{A_1} \Gamma_\theta (r, \theta)\, \frac{\overline{ds} \times \overline{R}}{R^3} + \frac{1}{4\pi} \iint_{A_2} \Gamma_c (r)\, \frac{\overline{ds} \times \overline{R}}{R^3} \qquad [5]$$

Substituting Equation [5] into Equation [4] and adding and subtracting a quantity of $\frac{1}{4\pi} \iint_{A_3} - \frac{d}{dr} \Gamma (r)\, dr\, \frac{\overline{ds} \times \overline{R}}{R^3}$, where A_3 is the enclosed area between the line drawn on the lifting surface through the centerline of shaft and the point P and the trailing edge, we obtain the following expression for the induced velocity:

$$\overline{V_P} = \frac{1}{4\pi} \left[\iint_{A_1} \Gamma_r (r, \theta)\, d\theta\, \frac{\overline{dr} \times \overline{R}}{R^3} + \iint_{A_1} \Gamma_\theta (r, \theta)\, \frac{\overline{ds} \times \overline{R}}{R^3} + \iint_{A_3} \frac{d}{dr} \Gamma (r)\, dr\, \frac{\overline{ds} \times \overline{R}}{R^3} \right]$$
$$+ \frac{1}{4\pi} \left[\iint_{A_2} - \frac{d}{dr} \Gamma (r)\, dr\, \frac{\overline{ds} \times \overline{R}}{R^3} + \iint_{A_3} - \frac{d}{dr} \Gamma (r)\, dr\, \frac{\overline{ds} \times \overline{R}}{R^3} \right] \qquad [6]$$

since $\Gamma_c(r) = -\frac{d}{dr}\Gamma(r)\,dr$ by Equation [2].

The second square bracketed term is a function of r only and is denoted as $\overline{V_L}$. It expresses the induced velocity at a lifting line with a bound circulation $\Gamma(r)$. This term plays a very important role in our problem of hydrodynamic aspect of propeller design using lifting surface theory. Consider the case in which the pitch of the lifting surface is constant. If a lifting line with bound circulation $\Gamma(r)$ is superimposed on the surface through the control point P, then it will shed a vortex system with a circulation of $-\frac{d}{dr}\Gamma(r)dr$ and result in an induced velocity at P which is identical to $\overline{V_L}$. The values of this induced velocity $\overline{V_L}$ at various radii may be computed using lifting line theory based on a chosen radial load distribution. From these values the helical surface near the propeller disk is then determined, upon which we place the lifting surface with a chosen blade outline. Since $\overline{V_L}$ is independent of θ, it is convenient to use it as the reference velocity for the induced velocity due to a lifting surface. Let us define the total induced velocity at point P relative to $\overline{V_L}$, $\overline{V_{PL}} = \overline{V_P} - \overline{V_L}$.

If V_{PL} is zero everywhere, then $V_P = V_L$ and the streamline on the lifting surface will coincide with the helical chord at each radius. If V_{PL} is not zero everywhere, then it will induce a mean line with respect to the helical chord at each radius. Since we are only interested in the mean line with respect to the helical chord, $\overline{V_{PL}}$ is the only item that needs to be computed and we can disregard $\overline{V_P}$. Carrying this idea through, we obtain from Equation [6] the following expression for $\overline{V_{PL}}$:

$$\overline{V_{PL}} = \frac{1}{4\pi}\left[\iint_{A_1}\Gamma_r(r,\theta)\,d\theta\,\frac{\overline{dr}\times\overline{R}}{R^3} + \iint_{A_1}\Gamma_\theta(r,\theta)\,\frac{\overline{ds}\times\overline{R}}{R^3} + \iint_{A_3}\frac{d}{dr}\Gamma(r)\,dr\,\frac{\overline{ds}\times\overline{R}}{R^3}\right] = \overline{V_B} + \overline{V_F} \qquad [7]$$

where

$$\overline{V_B} = \frac{1}{4\pi}\iint_{A_1}\Gamma_r(r,\theta)\,d\theta\,\frac{\overline{dr}\times\overline{R}}{R^3} \qquad [8]$$

$$\overline{V_F} = \frac{1}{4\pi}\left[\iint_{A_1} \Gamma_\theta(r,\theta)\frac{\overline{ds}\times\overline{R}}{R^3} + \iint_{A_3}\frac{d}{dr}\Gamma(r)\,dr\,\frac{\overline{ds}\times\overline{R}}{R^3}\right] \qquad [9]$$

If we compare Equation [7] with Equation [6], it is obvious that the amount of numerical computation is reduced quite appreciably. In other words, our problem has been greatly simplified by taking advantage of these shortcuts. This is the unique feature of Pien's approach to the problem.

It should be mentioned here that the foregoing procedure is true only for the case where the pitch of the lifting surface is constant. If the pitch changes with radius, the free vortex sheet of a lifting line may not exactly coincide with that of the lifting surface. However, the influence of this on the induced downwash is rather small, and this procedure, therefore, may also be applied to the cases where the pitch is not constant.

The integrals on the right-hand side of Equation [7] now have bounded limits of integration and can be handled conveniently.

From the axial and tangential components of the relative induced velocity $\overline{V_{PL}}$, the downwash distribution v_n, normal to the chord, is obtained. By integrating this downwash distribution curve, the required mean line relative to the chord is obtained.

$$C_m(r_0,\theta) = \frac{r_0 D}{2V\cos\beta_i}\int_{\theta}^{\theta_l} v_n(r_0,\theta_0)\,d\theta_0 \qquad [10]$$

EQUATIONS FOR NUMERICAL COMPUTATION

The major portion of the work is in the evaluation of the induced velocities. By using Equation [7] as a basis, the following working equations for numerical computations are developed.

Induced Velocity at Point P Due to Bound Vortex System, $\overline{V_B}$

The induced velocity at any control point P due to the bound vortex system is expressed by Equation [8]. To reduce it into a working form, we use the "moving" cylindrical coordinate system for convenience. Making use of the expressions for $\overline{dr}$ and $\overline{R}$ developed previously, we obtain the following equation for induced velocity due to the bound vortex system:

$$\overline{V_B} = \frac{1}{4\pi} \iint_{A_1} \frac{\Gamma_r(r, \phi)}{R^3} \{ \bar{i} [-\phi \sin \phi\, p(r)/\pi + r\phi \sin \phi\, p'(r)/\pi] + \bar{j} [\phi \cos \phi\, p(r)/\pi + \phi (r_0 - r \cos \phi) p'(r)/\pi] + \bar{k} [-r_0 \sin \phi] \}\, d\phi\, dr \qquad [11]$$

where $R = [r^2 - 2 r_0 r \cos \phi + r_0^2 + (\phi\, p(r)/\pi)^2]^{1/2}$.

Induced Velocity at Point P Due to Free Vortex System, $\overline{V_F}$

In a similar manner we put Equation [9] into a working form by substituting the expressions for $\bar{R}$ and $\overline{ds}$ developed previously. It follows that

$$\overline{V_F} = \frac{1}{4\pi} \iint_{A_1} \frac{1}{R^3} [\bar{i} (-\phi \cos \phi + \sin \phi) p(r)/\pi + \bar{j} (r_0 - r \cos \phi - r\phi \sin \phi) p(r)/\pi + \bar{k}\, r (r - r_0 \cos \phi)] [\Gamma_\theta(r, \phi) + \Gamma'(r)\, dr]\, d\phi \qquad [12]$$

where $\Gamma'(r) = \dfrac{d}{dr} \Gamma(r)$ equals zero when $\phi > 0$.

The total induced velocity at point P relative to $\overline{V_L}$, $\overline{V_{PL}}$ is therefore the sum of Equations [11] and [12]. For the present problem the components that are to be evaluated are the axial ($\bar{k}$) and the tangential ($\bar{j}$) components.

To reduce Equation [12] it is necessary to obtain an expression for the intensity of the free vortex system that is on the lifting surface, $\Gamma_\theta(r, \phi)$. This may be obtained by performing the differentiation in Equation [3].

$$\Gamma_c(r) = -\, dr \int_{\theta_t(r)}^{\theta_l(r)} \frac{\partial}{\partial r} \Gamma_r(r, \theta)\, d\theta - \Gamma_r(r, \theta_t) \frac{d}{dr} \theta_l(r)\, dr + \Gamma_r(r, \theta_l) \frac{d}{dr} \theta_t(r)\, dr$$

Then, within the lifting surface, the free circulation $\Gamma_\theta(r, \phi)$ can be expressed as follows:

$$\Gamma_\theta(r, \phi) = -\, dr \int_{\phi}^{\phi_l(r)} \frac{\partial}{\partial r} \Gamma_r(r, \phi)\, d\phi - \Gamma_r(r, \phi) \frac{d}{dr} \theta_l(r)\, dr \qquad [13]$$

For the case of uniform chordwise load distribution, the bound circulation is uniformly distributed along the chord. Its intensity per unit angle is obtained from Equation [1]:

$$\Gamma_r(r, \phi) = \frac{\Gamma(r)}{\theta_l(r) - \theta_t(r)} = \frac{\Gamma(r)}{\theta_T(r)} = \gamma(r) \qquad [14]$$

Then, Equation [13] can be further simplified and becomes

$$\Gamma_\theta(r, \phi) = - dr \left[(\phi_l(r) - \phi) \frac{d}{dr} \gamma(r) + \gamma(r) \frac{d}{dr} \theta_l(r) \right] \qquad [15]$$

With Equation [13] substituted into Equation [11], and Equation [15] into Equation [12], we obtain the following expressions for the axial and tangential components of the induced velocities:

$$V_{ba} = \frac{1}{4\pi} \iint_{A_1} - r_0 \gamma(r) \frac{\sin \phi}{R^3} \, d\phi \, dr \qquad [16a]$$

$$V_{bt} = \frac{1}{4\pi} \iint_{A_1} \frac{1}{\pi} \gamma(r) \frac{\phi}{R^3} [p(r) \cos \phi + (r_0 - r \cos \phi) p'(r)] \, d\phi \, dr \qquad [16b]$$

$$V_{fa} = \frac{1}{4\pi} \iint_{A_1} - \frac{r(r - r_0 \cos \phi)}{R^3} \{[(\phi_l(r) - \phi) \gamma'(r) + \gamma(r) \theta_l'(r)] - \Gamma'(r)\} \, d\phi \, dr \qquad [16c]$$

$$V_{ft} = \frac{1}{4\pi} \iint_{A_1} - \frac{p(r)}{R^3} (r_0 - r \cos \phi - r\phi \sin \phi) \{[(\phi_l(r) - \phi) \gamma'(r) + \gamma(r) \theta_l'(r)] - \Gamma'(r)\} \, d\phi \, dr \qquad [16d]$$

for $\phi > 0$ the $\Gamma'(r)$ term in Equations [16c] and [16d] is equal to zero.

The total axial component of the induced velocity is, therefore, the sum of Equations [16a] and [16c], and the total tangential component is the sum of Equations [16b] and [16d]. These equations are the basic working equations that are to be evaluated numerically.

The Equations [16a] through [16d] are developed for the induced velocity at a point P on the first blade due to a single blade, the first blade itself. Since all the blades may be represented by lifting surfaces, there will be contributions due to each of these surfaces to this induced velocity. The coordinates of a field point on m^{th} blade corresponding to a field

point (r, ϕ, ξ) on the first blade at the same radius is (r, ϕ_m, ξ) where $\phi_m = \phi + 2\pi(m-1)/Z$, $m = 1, 2, 3, \ldots, Z$, assuming the blades are arranged symmetrically with equal angular spacings. To derive an expression for the induced velocity due to the m^{th} blade, it is only necessary then to replace sin ϕ by sin ϕ_m and cos ϕ by cos ϕ_m in Equation [16] since the blades are assumed to be identical to each other. Thus, for example, the axial component of the induced velocity due to the bound vortex system of the m^{th} blade is derived from Equation [16a]:

$$\frac{1}{4\pi} \iint_{A_1} -r_0 \nu(r) \frac{\sin \phi_m}{[r_0^2 - 2r_0 r \cos \phi_m + r^2 + (\phi p(r)/\pi)^2]^{3/2}} d\phi\, dr$$

It follows that if we sum up, we would obtain an expression for this induced velocity due to all the blades:

$$V_{ba} = \frac{1}{4\pi} \sum_{m=1}^{Z} \iint_{A_1} -r_0 \gamma(r) \frac{\sin \phi_m}{[r_0^2 - 2r_0 r \cos \phi_m + r^2 + (\phi p(r)/\pi)^2]^{3/2}} d\phi\, dr$$

Similarly, the various other induced velocity components due to all the blades may be derived for the three remaining equations.

NUMERICAL COMPUTATION

As stated previously, the radial bound circulation distribution and the hydrodynamic pitch ratio distribution are obtained from the lifting-line theory based on certain design conditions. (At the David Taylor Model Basin the program entitled "AML Problem No. 106 – Moderately Loaded Propeller Using Induction Factors" may be used for this purpose.) These quantities along with the blade outline and the chord-length ratios L_l/D and L_T/D, which are chosen based on the considerations of cavitation, blade element efficiency, and strength, are used as input at given radii for the numerical computations.

For the purpose of interpolating these quantities at radii other than those specified in the input, trigonometric series representations in finite number of terms of these quantities are made by using the expression

$$X = \sum_{n=0}^{N} a_n \cos n y \qquad [17]$$

where X denotes any of the preceding quantities

y = radial coordinate defined:

$$\cos y = (1 + r_h - 2r)/(1 - r_h)$$

a_n = coefficients determined from input data

N = number of terms.

From this expression, the quantity X can be calculated at any desired radial position. The derivatives of these quantities with respect to r can be easily expressed as

$$\frac{d}{dr} X = - \frac{2}{(1 - r_h) \sin y} \sum_{n=0}^{N} n\, a_n \sin n\, y \qquad [18]$$

and they can also be computed at any desired radius.

For each radius r_0 at which the blade element mean line relative to the chord line is sought, various values of θ_0 are chosen so that the distributions of components of the induced velocity can be obtained. At any point $P\ (r_0, \theta_0)$ the induced velocities are computed according to Equations [16a], [16b], [16c], and [16d].

It should be noted that in these equations the integrand has a singular point at $r = r_0$ and $\theta = \theta_0$ ($\phi = 0$). The integrations are carried out by isolating the singular point. The integrals are evaluated numerically in the regions of $|r - r_0| \geq \delta_0$, where δ_0 is a quantity that can be made as small as practicable. Within the strip $|r - r_0| < \delta_0$, the region of integration is divided into two parts. The first part is over the portion $|\phi| \geq \epsilon_0$, and the second part is over the portion $|\phi| < \epsilon_0$. The first portion again can be carried out numerically. The second portion, $|r - r_0| < \delta_0$ and $|\phi| < \epsilon_0$, is not evaluated, for when δ_0 and ϵ_0 are very small, the contribution to the camber due to this portion is negligible even though the induced velocity may be infinite at some of the singular points. (See Appendix A.)

The numerical computation for the narrow strip of the lifting surface within which the control point P is located is handled differently from the remaining portions of the lifting surface. Thus, to facilitate the numerical calculation the lifting surface A is divided geometrically into three zones (Figure 2): the "mid-zone," which is the narrow strip with a width of $2\delta_0$ from $r - \delta_0$ to $r_0 + \delta_0$; the "tip-zone," which is the area between $r_0 + \delta_0$ and the tip; and the "hub-zone," which is the area between the hub and $r - \delta_0$. The division of zones varies with the radial position r_0 of the point P. The computation procedures in the tip-zone and the hub-zone are identical. For numerical integration the Simpson method is used. In the tip- and hub-zones, the chordwise integration is performed first, and in the narrow mid-zone, which has a width of $2\delta_0$, the radial direction integration is done first. Within this mid-zone the pitch of the chord $p(r)$, $\frac{d}{dr}\ p(r)$ and the circulation functions $\Gamma_r\ (r, \phi)$, $\Gamma_\theta(r, \phi)$, and $\frac{d}{dr}\ \Gamma(r)$ are considered to be independent of the radial coordinate, and the mean values

evaluated at the midwidth, r_0, of the strip are used. Then the integrations in Equations [16a], [16b], [16c], and [16d] can be carried out for the interval between $r_0 - \delta_0$ and $r_0 + \delta_0$:

$$V_{ba} = \frac{1}{4\pi} \int_{\phi_t(r_0)}^{\phi_l(r_0)} -r_0 \gamma(r_0) \frac{(r - r_0 \cos\phi)\sin\phi}{[r_0^2 \sin^2\phi + (\phi\, p(r_0)/\pi)^2]R} \Bigg|_{r_0-\delta_0}^{r_0+\delta_0} d\phi \qquad [19a]$$

$$V_{bt} = \frac{1}{4\pi} \int_{\phi_t(r)}^{\phi_l(r)} \frac{\phi}{\pi} \gamma(r_0) \frac{1}{r_0^2 \sin^2\phi + (\phi\, p(r_0)/\pi)^2} \left[(p(r_0)\cos\phi + r_0 p'(r_0)) \frac{r - r_0\cos\phi}{R} \right.$$

$$\left. + p' \cos\phi \frac{r_0^2 + (\phi\, p(r_0)/\pi)^2 - r r_0 \cos\phi}{R} \right]_{r_0-\delta_0}^{r_0+\delta_0} d\phi \qquad [19b]$$

$$V_{fa} = \frac{1}{4\pi} \int_{\phi_t(r_0)}^{\phi_l(r_0)} -(SF) \left[\ln(r - r_0\cos\phi + R) - \frac{r}{R} \right]_{r_0-\delta_0}^{r_0+\delta_0} d\phi \qquad [19c]$$

$$V_{ft} = \frac{1}{4\pi} \int_{\phi_t(r_0)}^{\phi_l(r_0)}$$

$$-(SF)\frac{p(r_0)}{\pi} \left\{ \frac{r r_0 (\sin^2\phi - \phi\sin\phi\cos\phi) + r_0^2 \phi\sin\phi + (\phi\, p(r_0)/\pi)^2(\cos\phi + \phi\sin\phi)}{[r_0^2\sin^2\phi + (\phi\, p(r_0)/\pi)^2]R} \right\}_{r_0-\delta_0}^{r_0+\delta_0} d\phi$$

[19d]

where $SF = (\phi_l(r_0) - \phi)\,\gamma'(r_0) + \gamma(r_0)\,\theta_l'(r_0) - \Gamma'(r_0)$

Γ' term equals zero for $\phi > 0$. These chordwise integrations are then computed numerically by the Simpson method.

The contribution of other blades is computed in the same manner with the blade represented by a lifting surface. In the computation for the m^{th} blade the $\sin\phi$ and $\cos\phi$ terms are replaced by $\sin(\phi + 2\pi(m-1)/Z)$ and $\cos(\phi + 2\pi(m-1)/Z)$ respectively, where Z is the number of blades, $m = 2, 3, \ldots, Z$.

The total axial and tangential induced velocity components v_a and v_t are then expressed as

$$v_a = v_{ba} + v_{fa} + v_{ba}' + v_{fa}'$$

$$v_t = v_{bt} + v_{ft} + v_{bt}' + v_{ft}'$$

where the primes denote the velocity components due to other blades.

From these induced velocity components the downwash distributions relative to the chord is calculated by using

$$v_n(r_0, \theta_0) = v_a(r_0, \theta_0) \cos \beta_i - v_t(r_0, \theta_0) \sin \beta_i \qquad [20]$$

For calculating the blade mean line, the downwash is expressed in a power series in terms of a new nondimensional angular coordinate $\frac{\theta_0}{\theta_T}$ as follows:

$$v_n(r_0, \theta_0) = \sum_{n=0}^{M} b_n(r_0) \left(\frac{\theta_0}{\theta_T}\right)^n \qquad [21]$$

where the integer M equals the number of chordwise coordinates minus one, and the coefficients $b_n(r_0)$ are evaluated from $(M + 1)$ simultaneous equations. With this scheme the downwash at any point can be obtained by either interpolation or extrapolation, and the integration of Equation [10] can easily be performed to obtain the blade mean line ordinates:

$$C_m\left(r_0, \frac{x}{L_T}\right) = \frac{L_T(r_0)}{V(r_0)} \sum_{n=0}^{M} \frac{b_n}{n+1} \left(\frac{x}{L_T}\right)^{n+1} \qquad [22]$$

where $V(r_0)$ is the mean resultant velocity. The mean resultant velocity is computed based on the following geometric relationship; see Figure 3.

$$V(r_0) = [(V_x(r_0) + u_a(r_0))^2 + (\pi r_0/J_s - u_t(r_0))^2]^{1/2}$$

where V_x = nondimensional local longitudinal velocity based on ship velocity;

u_a, u_t = nondimensional axial and tangential components, respectively, of induced velocity from lifting-line calculation based on ship velocity; and

J_s = advance coefficient based on ship velocity.

THE COMPUTER PROGRAM

The numerical computation has been programed into the IBM 7090 machine. The computer program is designated as Applied Mathematics Laboratory Problem XPLU. First, the program calculates the angular positions, ϕ, of field points relative to any point P at which the blade element mean line is sought according to the following relationships:

$$\phi_{k,n} = \phi_{1,n-k+1} - \phi_{1,k}$$

with

$$\phi_{1,n} = \phi_{1,n-1} + (n-1)\,(\Delta\phi)_{min}$$

and

$$\phi_{k,1} = 0$$

where $k = 1, 2, 3, \ldots$ and $n = 2, 3, 4, \ldots$ are the indices for the radial and chordwise stations, respectively.

$(\Delta\phi)_{min}$ is the minimum spacing specified, and $(n-1)\,(\Delta\phi)_{min}$ is spacing between the n^{th} and the $(n-1)^{th}$ stations. When it exceeds a prescribed maximum value $(\Delta\phi)_{max}$ in the input, it will take on the value of $(\Delta\phi)_{max}$, i.e., the spacing $\Delta\phi$ is limited to $(\Delta\phi)_{min} \leq \Delta\phi \leq (\Delta\phi)_{max}$. This shows that the field points are so located that they have smaller spacings in the close neighborhood of point P, and the spacing increases as the distance between P and the field point increases. The fineness of the network varies depending upon the $(\Delta\phi)_{min}$ and $(\Delta\phi)_{max}$ specified. For each of these angular positions the sine and cosine of the angles are computed, compiled into tables, and stored. These tables are used for providing ready information of ϕ, $\sin\phi$, and $\cos\phi$, required in the later stage of the computation. Since only one set of angles is computed, a common pattern of network of field points for any point P is thus established. The specified maximum range of angles for which the tables are made is sufficiently large so that they may be used for any propeller of the conventional configuration. Next, the program calculates the coefficients a_n in Equation [17] with the input data supplied. The number of terms, N, depends on the number of intervals of radii r in the input data which can be chosen arbitrarily. A 9-interval of r is recommended, and the present program is programed for 9 intervals.

The computer then selects, according to the input, the radial coordinate (starting from the innermost radius) r_0 of point P at which the blade element mean line is sought. The radial stations where the elemental vortex is located in each of the tip- and hub-zones are calculated according to the spacings specified in the input data.

At each of these radial stations r, quantities that are functions of r and the derivatives required in the computation of the induced velocities are then calculated and stored.

For a given radial station r the factors, which are functions of r and ϕ, appearing in the expressions of the induced velocities are first calculated for various angles at r and then are stored.

The computer proceeds to select a chordwise coordinate (starting from the leading edge) θ_0 of point P according to the specified intervals. The chordwise stations ϕ of the field points are then computed with the aid of the table of ϕ compiled at the beginning of the program at the corresponding radial station. The number of chordwise stations depends on the difference between r and r_0 and the blade outline of the particular propeller involved. This may be better explained by a graphic illustration. Figure 4 shows a pattern of a network of field points for point P, where both the radial and the chordwise stations are symmetrical about the point P. In Figure 5, a propeller blade outline is superimposed on Figure 4 with the point P coinciding. The stations between the line passing P and the leading edge, and between P and the trailing edge at various radial stations, including the stations at the leading and the trailing edges, are the field points at which the vortex elements are assumed to be distributed.

Then the computation of the induced velocity components at point P (r_0, θ_0) follows. This is done by computing the integrands at the selected chordwise stations and integrating them along the chord. The values of the integrations, which represent the contribution of the vortex systems at r to the induced velocities, are stored. It might be instructive to note here that in the calculation of Equations [16c] and [16d] the strength of the free vortex system, which are the factors enclosed in braces in these equations, may be represented graphically as shown in Figure 6. They may be considered to consist of two parts, one is the contribution due to lifting surface and the other due to the superimposed lifting line.

The procedure is repeated for the next θ_0 as point P moves along the chord toward the trailing edge at r_0, and for another r, and so on. Then, the radial integration for various θ_0 is done and the values are stored.

When the calculations for the tip- and hub-zones of the "first blade," and for the other blades are completed, the calculation for the mid-zone of the first blade at various θ_0 follows.

The total induced velocity components at $P(r_0, \theta_0)$ are obtained by adding the values computed for the mid-zone to the radial integrated values previously computed. The entire procedure is then repeated for the next r_0 and so on.

The downwash $v_n(r_0, \theta_0)$ at each point P specified is then computed from the total induced velocity components according to Equation [20]. The downwash at points where mean line ordinates are desired is extrapolated or interpolated by using Equation [21]. Finally, the ordinates of the mean line at any point $\left(r_0, \frac{x}{L_T}\right)$ are calculated based on Equation [22].

Basically, the new computer program is similar to the original program in the method of approach. But there are two areas in which improvements have been made in this new program that are worth mentioning. One is in the method of setting up the network of field points. The other is in the integration of the induced velocity in the tip- and hub-zones.

As noted above, the network of field points is mapped so that it is common to all of the control points, and the field points are located so that they are closely spaced in the

neighborhood of the control point and are symmetrical about it. This feature of symmetry improves the accuracy of numerical computation, especially in the neighborhood of the singular point.

In the original program the lifting surface is divided into strips by cylinders of various radii. Within each of the strips the pitch distribution and the circulation functions are considered to be independent of the radial coordinate. Thus, the integration with respect to the radial coordinate can be carried out first by using the mean values of these quantities and then the chordwise integration is done numerically, whereas in the new program this simplification is made only for the narrow midstrip. The double integrations for the remaining part of the lifting surface are carried out numerically. This again is considered to be an improvement for better accuracy in the evaluation of the integrals.

RESULTS OF SAMPLE CALCULATIONS

The computer program discussed in the previous section has been completed. A number of cases have been worked out by using this new program and the results are reported herein.

NUMBER OF BLADES

The first case is a 5-bladed propeller similar to Propeller 3916, reported in Reference 1, except that the calculation is done by the new computer program. This propeller is designated as Propeller 3916A. The calculated induced velocities and the camber distributions are shown in Table 1 and in Figure 15 (Appendix C), and the maximum mean line ordinates due to all five blades (Curve 1) and due to the one blade (Curve 2) are plotted in Figure 7. For comparison, the results for five blades reported in Reference 1, calculated from the original computing program, is also shown (Curve 3). The difference between Curves 1 and 3 is due to the refinement made in the present computing program.

BLADE OUTLINE

It is worth noting that the camber distribution is affected by the shape of the blade outline selected. When the blade outline of Propeller 3916A is slightly modified, keeping the same expanded area ratio, as shown in the following table, a somewhat different camber distribution is obtained. The maximum mean line ordinates are shown also in Figure 7 (Curve 4). This propeller with the modified blade outline is designated as Propeller 3916B.

	L_T/D	
r/R	Original	Modified
0.2	0.308	0.294
0.3	0.372	0.358
0.4	0.431	0.430
0.5	0.462	0.488
0.6	0.464	0.488
0.7	0.435	0.458
0.8	0.370	0.364
0.9	0.268	0.228
1.0	0.040	0.000

COMPARISON WITH TWO-DIMENSIONAL CASE

The second case is for a propeller having a rectangular expanded outline with an aspect ratio of 10. It has zero hydrodynamic pitch ratio and a uniform bound-circulation distribution along the radius. This fictitious propeller resembles a two-dimensional wing, although the motion involved here is a rotational one rather than a linear translational. The purpose of this calculation is to determine the mean lines at various radii induced by the uniform bound-circulation distribution only and to compare them with a two-dimensional airfoil. The calculated mean line distributions at radii of 0.3, 0.6, and 0.9 are plotted in Figure 8 in which the NACA $a = 1$ mean line distribution is also shown.

In this fictitious case, the mean lines at various radii are quite close to the two-dimensional case. However, for the actual propeller, the means lines at various radii obtained for uniform chordwise loading distribution are somewhat different from the $a = 1$ mean line as shown in Figure 9 for Propeller 3916A. Figure 10 shows the camber distributions of Propeller 3916A at various radii calculated by using the new method compared with those calculated by using the method outlined in Reference 2 for $a = 1$ mean line with camber correction factors k_1 and k_2:

$$\text{Camber ratio, corrected} = 0.05515\, k_1\, k_2\, C_L$$

where C_L is lift coefficient.

SKEWED BLADES

To further demonstrate the effect of blade outline on camber distribution, a third case was worked out. This case is also a 5-bladed propeller (Propeller 3917A). The loading, pitch, and blade chord length distributions are the same as those for Propeller 3916A, except that the blades are skewed. The amount of the skew is the same as that for Propeller 3917.[1] The results are shown in Table 2, and the comparative camber distributions calculated on one blade at various radii are plotted in Figure 11. From these curves, we notice that blade skew not only distorted the mean line but also changed the effective angle of attack. The range of angle of attack for this particular sample problem is in the order of -0.4 degree near the hub and -0.6 degree at the tip.

EXPANDED AREA RATIO

To show the dependence of camber distribution on expanded area ratio (EAR), calculations were made for propellers having the same basic blade outline as Propeller 3916A but with different EAR ranging from 0.5 to 1.2. The results based on one blade are shown in Table 3 and in Figure 12. In this figure, the maximum mean line ordinates due to the bound circulation only are also shown. The contribution due to the other four blades as percentage of the contribution due to one blade is shown in Figure 13 for the various EAR.

LOAD DISTRIBUTION

Calculations were made for a propeller having the same blade outline as Propeller 3916A but with a different loading, i.e., the radial bound circulation distribution is different. The radial load distribution is altered by arbitrarily changing the hydrodynamic pitch ratio to a constant. This constant hydrodynamic pitch propeller is designated as Propeller 3916C. The load and pitch distributions for these two propellers are shown in Figure 14. The camber distributions are shown in Table 4. The comparative camber distributions at various radii are shown in Figure 15.

DISCUSSION

The preceding sample calculations were presented to provide a clearer picture of the information that can be obtained from the program and of the various parameters that affect the mean line distribution.

From the results of these limited sample calculations, we may make the following remarks:

For a uniform chordwise load distribution, as in the case of Propeller 3916A, the three-dimensional mean line distribution differs somewhat from that obtained from the two-dimensional method with correction factors.

The mean line distribution of blades generally depends on the pitch ratio, radial load distribution, blade chord length distribution, and blade outline. Consequently, the expanded area ratio and the skew are very important parameters in the design of mean line, especially the latter, for the skew not only distorts the mean but also changes the effective angle of attack.

The presence of other blades has some effect upon the mean line of a blade. It has more effect in the hub region than it has near the tip. The contribution to the mean line due to other blades also increases as the expanded area ratio increases for propellers having the same blade outline.

It may be of interest to mention that some of the these findings disagree with the conclusions drawn in Reference 3 in which van Manen and Bakker reported the numerical results of a number of propeller design problems using lifting-surface theory. They reported, in part,

that for a uniform pressure distribution along the chord, the three-dimensional camber line of a propeller blade section is identical to the camber line of the two-dimensional profiles and that the effect of radial load distribution is not very pronounced. They also reported that the effect of skew back is negligible. Based on the evidence shown in this report, their conclusions appear to be doubtful.

FUTURE PLANS

To obtain some experimental verification of the theory, tests of model propellers designed by using this method are contemplated. The tests are to be done in conjunction with other research projects that are currently going on at the David Taylor Model Basin. It is also felt that the test of the theory could be easily accomplished by comparing the results from the inverse problem of performance prediction for the steady inflow case with reliable published open-water experimental data. If close agreement between the theoretical and experimental results is obtained, of course, the validity of the theory is firmly established. If, however, some discrepancies are found, we hope to be able to derive some consistent parametric relationships. When this is accomplished, propeller open-water design charts can be constructed with data obtained from computations for a large range of parameters rather than from costly experiments.

With these considerations, we shall proceed with the work on the remaining part of the overall program. The work on the case of an arbitrary chordwise load distribution is already underway and will be reported in the near future. It is anticipated that the work on the inverse problem of predicting performance for a given propeller design will commence shortly.

Also anticipated is the inclusion of the thickness effect in the investigation. Work in this area has been done recently by Kerwin and Leopold; their results are reported in References 4 and 5. Their work may be incorporated in the present computation to take account of the thickness effect.

Finally, from the investigation of the unsteady inflow case, it is hoped that one can estimate the time dependent force fluctuations produced by a propeller operating in a nonuniform wake field behind a ship. Thus, the phenomena of cavitation due to unsteadiness and propeller-induced vibration and noise could be better understood.

ACKNOWLEDGMENTS

The overall project was initiated by Dr. P.C. Pien, who has taken an active interest in the development of this work. The author is grateful for having the opportunity to work with him and wishes to express his sincere thanks to Dr. Pien for his continuing guidance and help. The author also wishes to thank Mr. L. Meuller of the Applied Mathematics Laboratory for his help in the computer work.

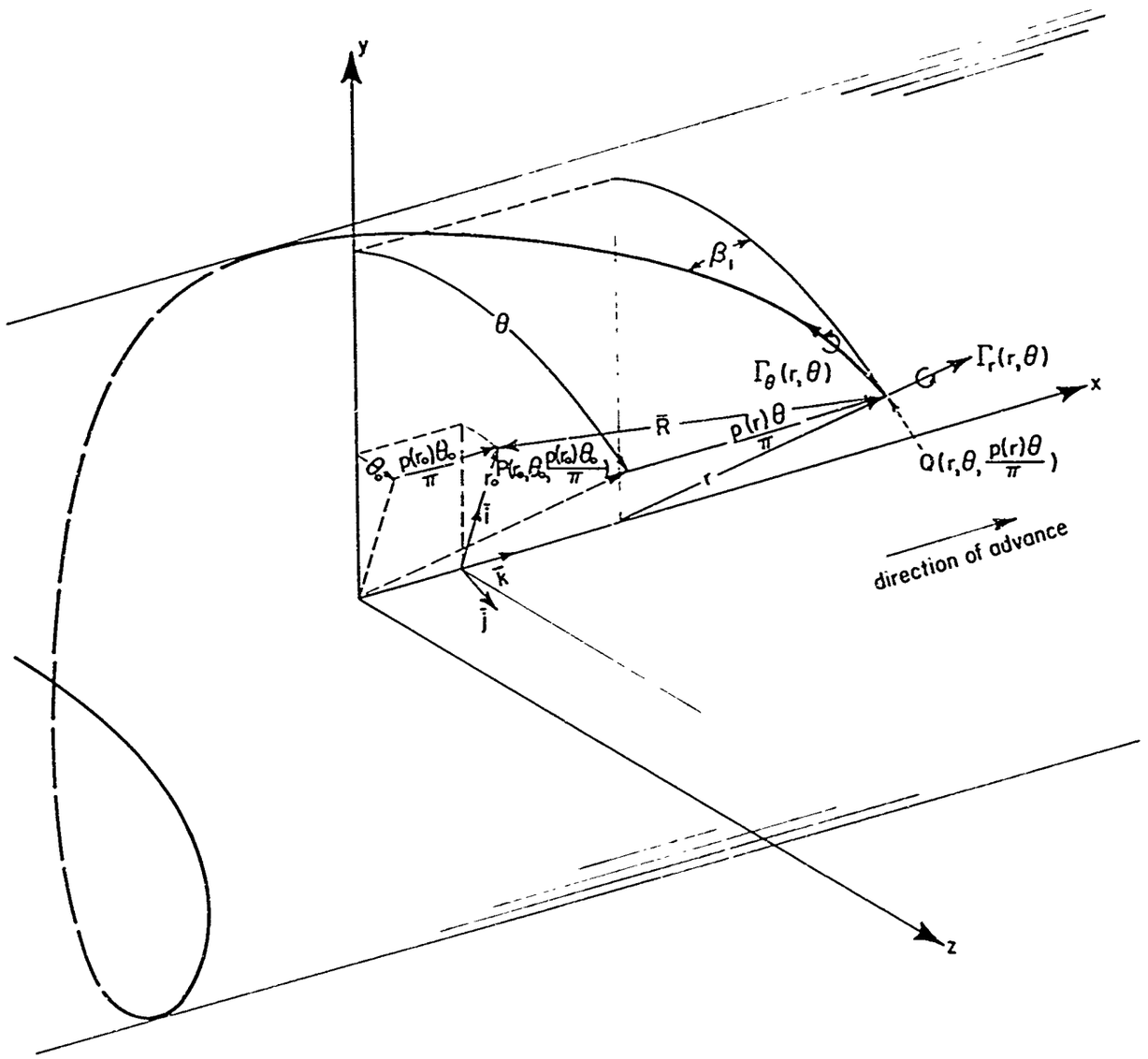

Figure 1 – Coordinate System

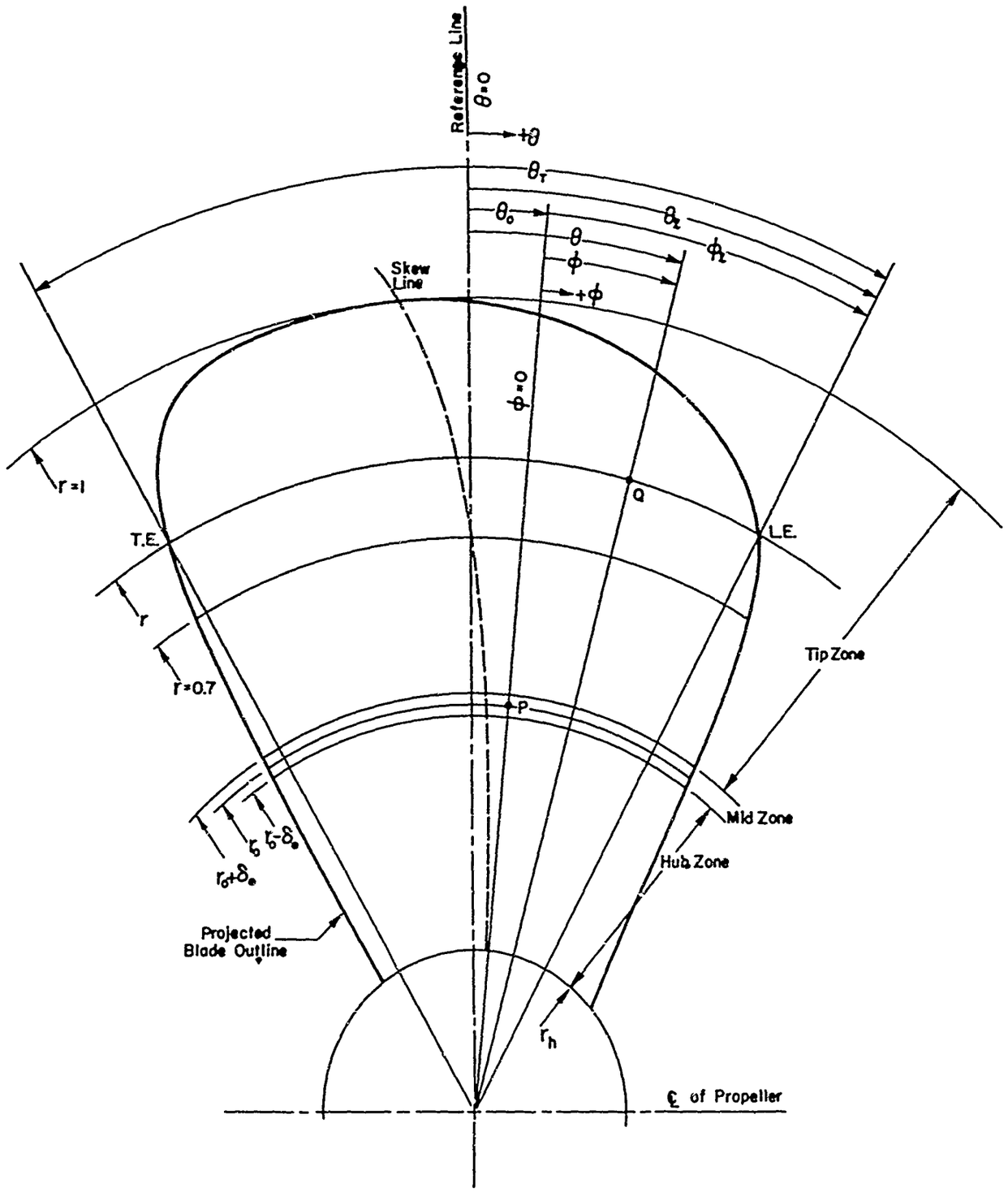

Figure 2 – Coordinate System in Projected Plane and Regions of Integration

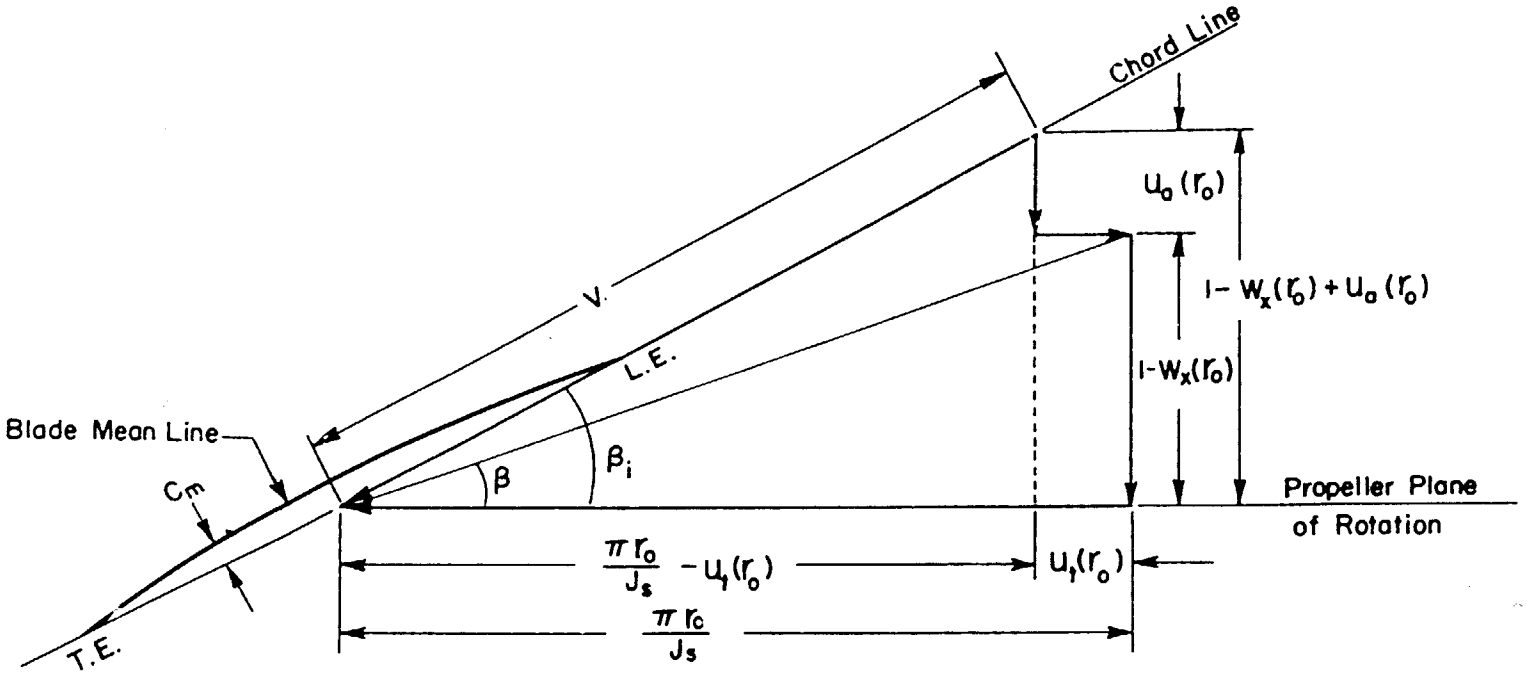

Figure 3 – Velocity Diagram at Radius r_0

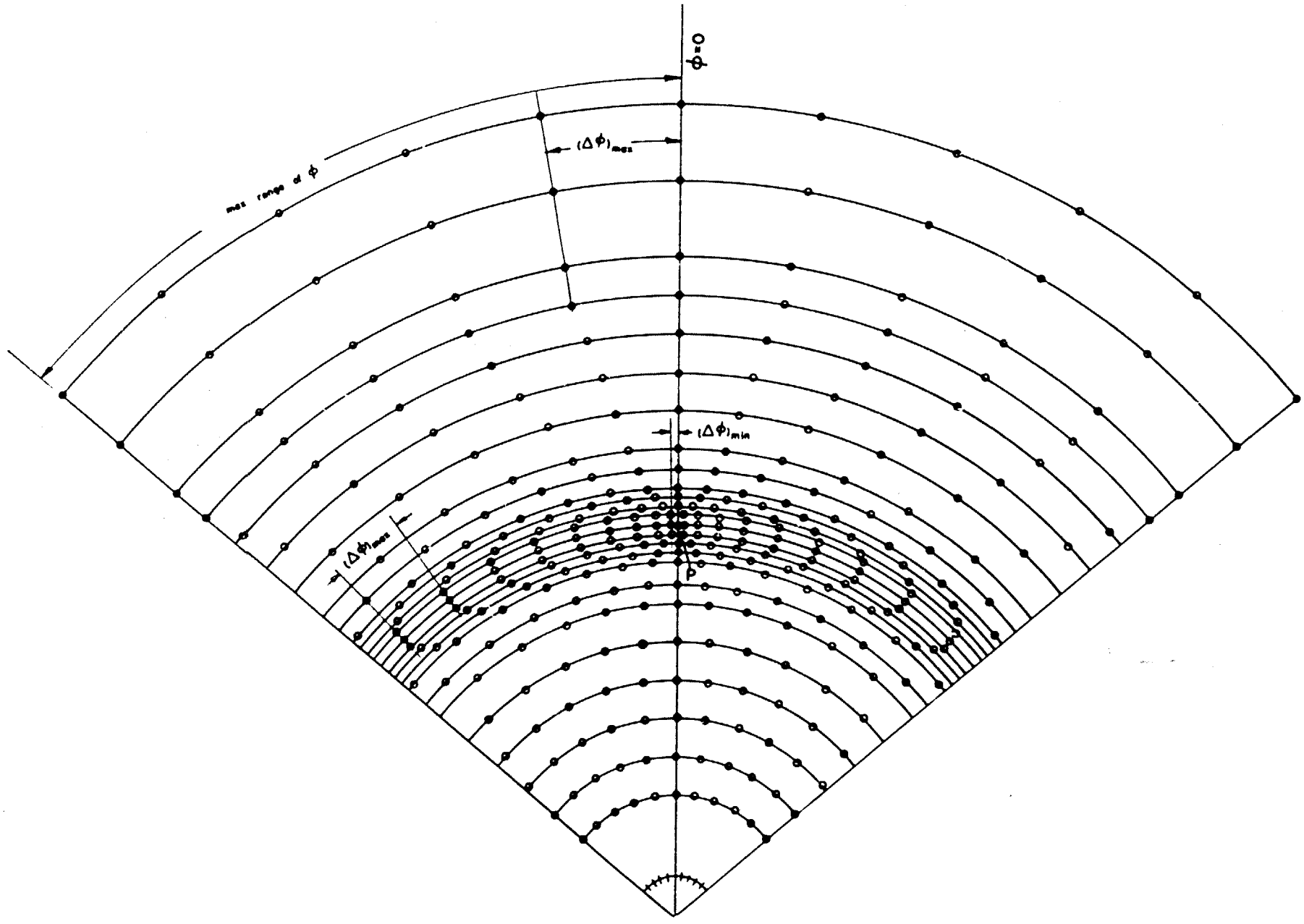

Figure 4 – General Pattern of Network of Field Points for Point *P*

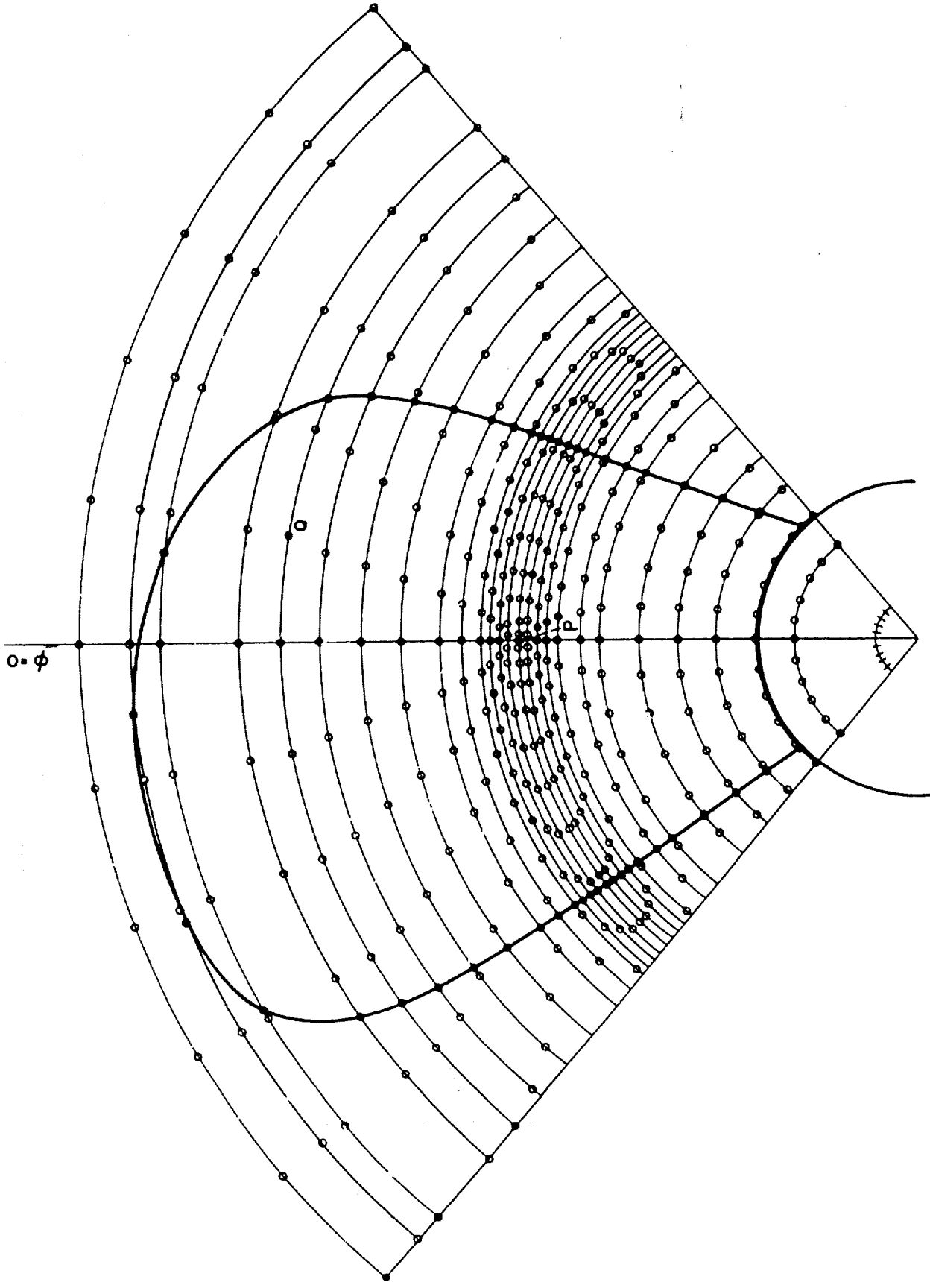

Figure 5 – Field Points for Point P on Blade

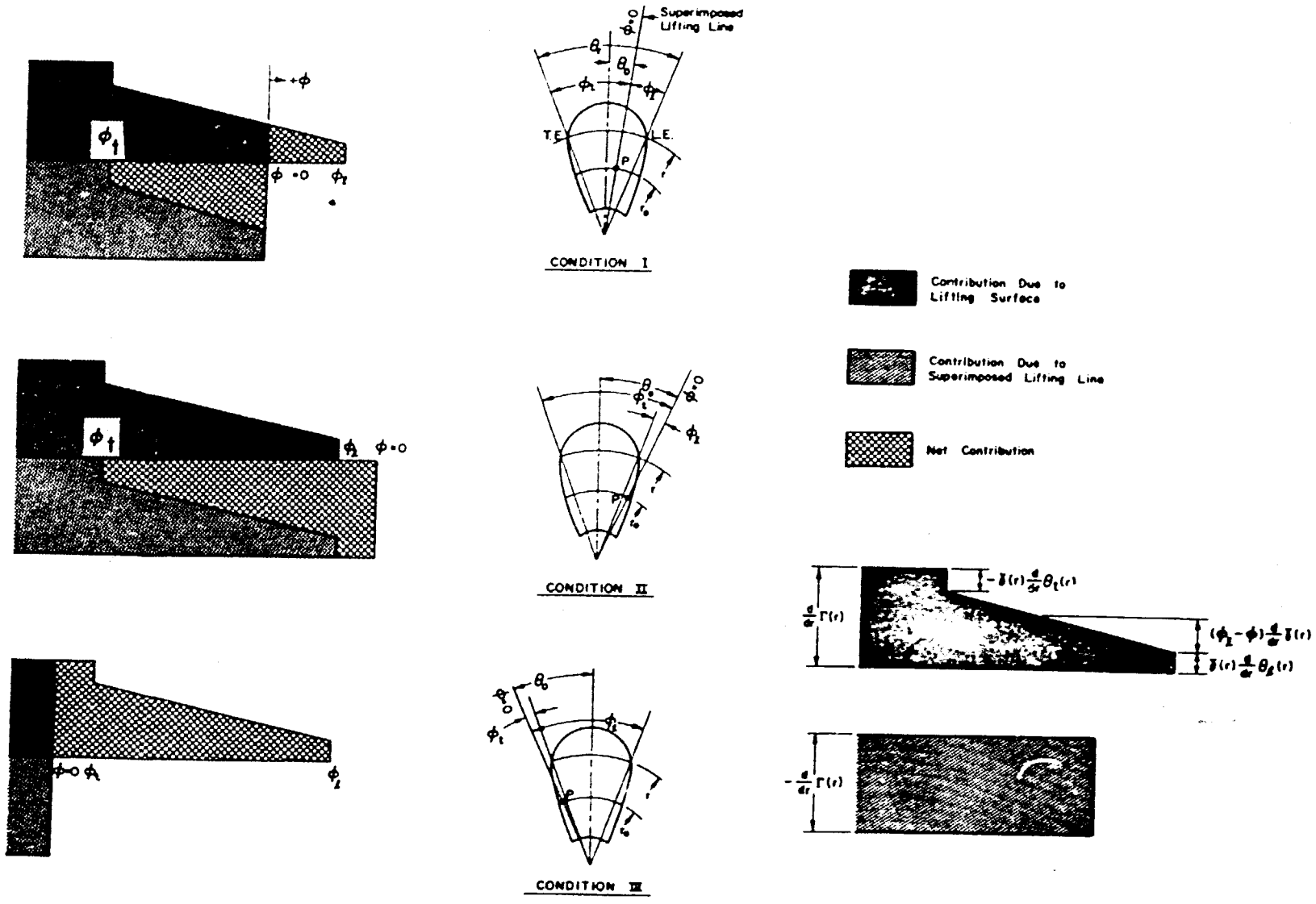

Figure 6 — Graphic Representation of Free Vortex Strength Distribution Along a Helical Line at r Due to a Lifting Surface and a Superimposed Lifting Line at $\phi = 0$

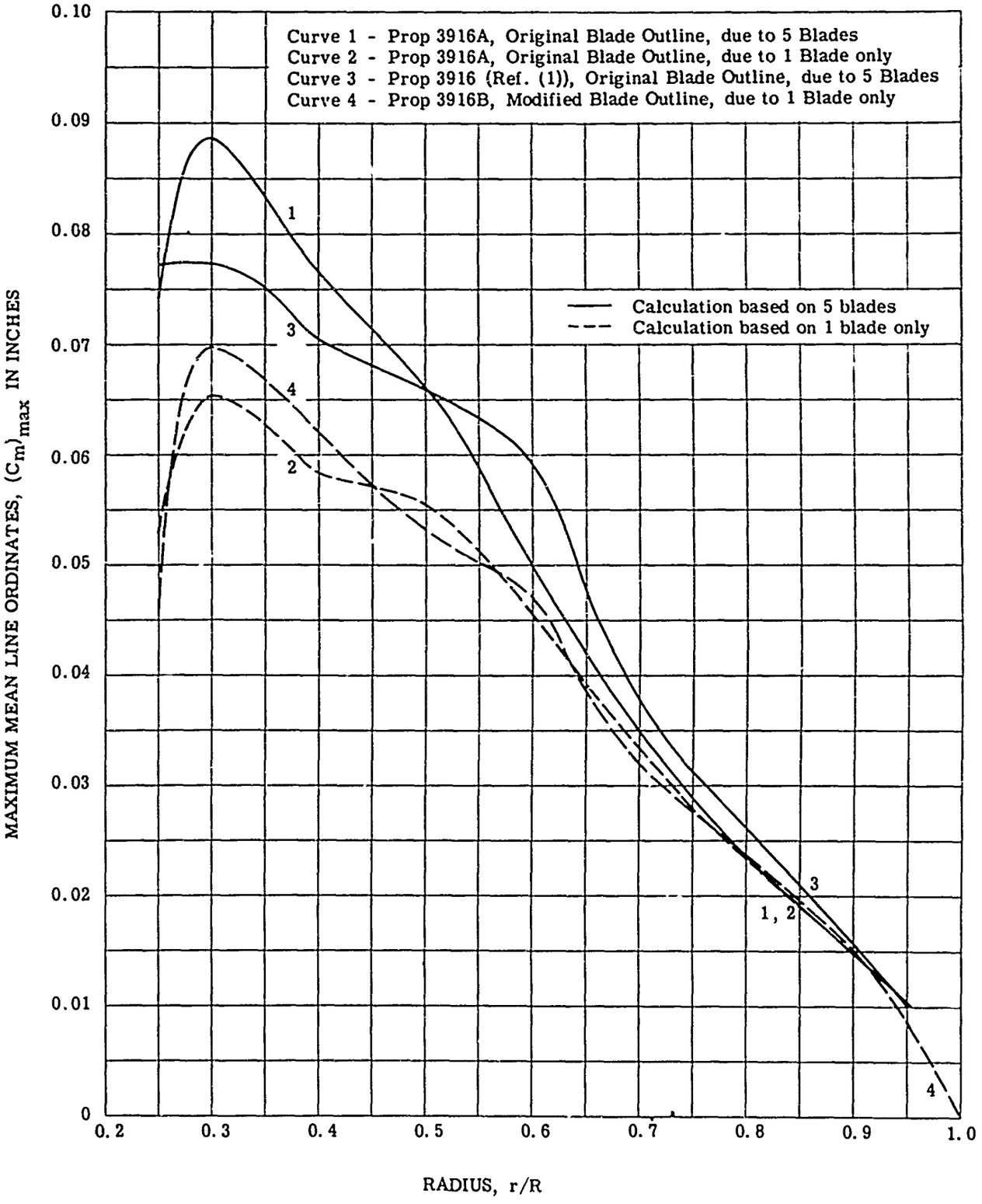

Figure 7 -- Maximum Mean Line Ordinates for Propellers 3916, 3916A, and 3916B

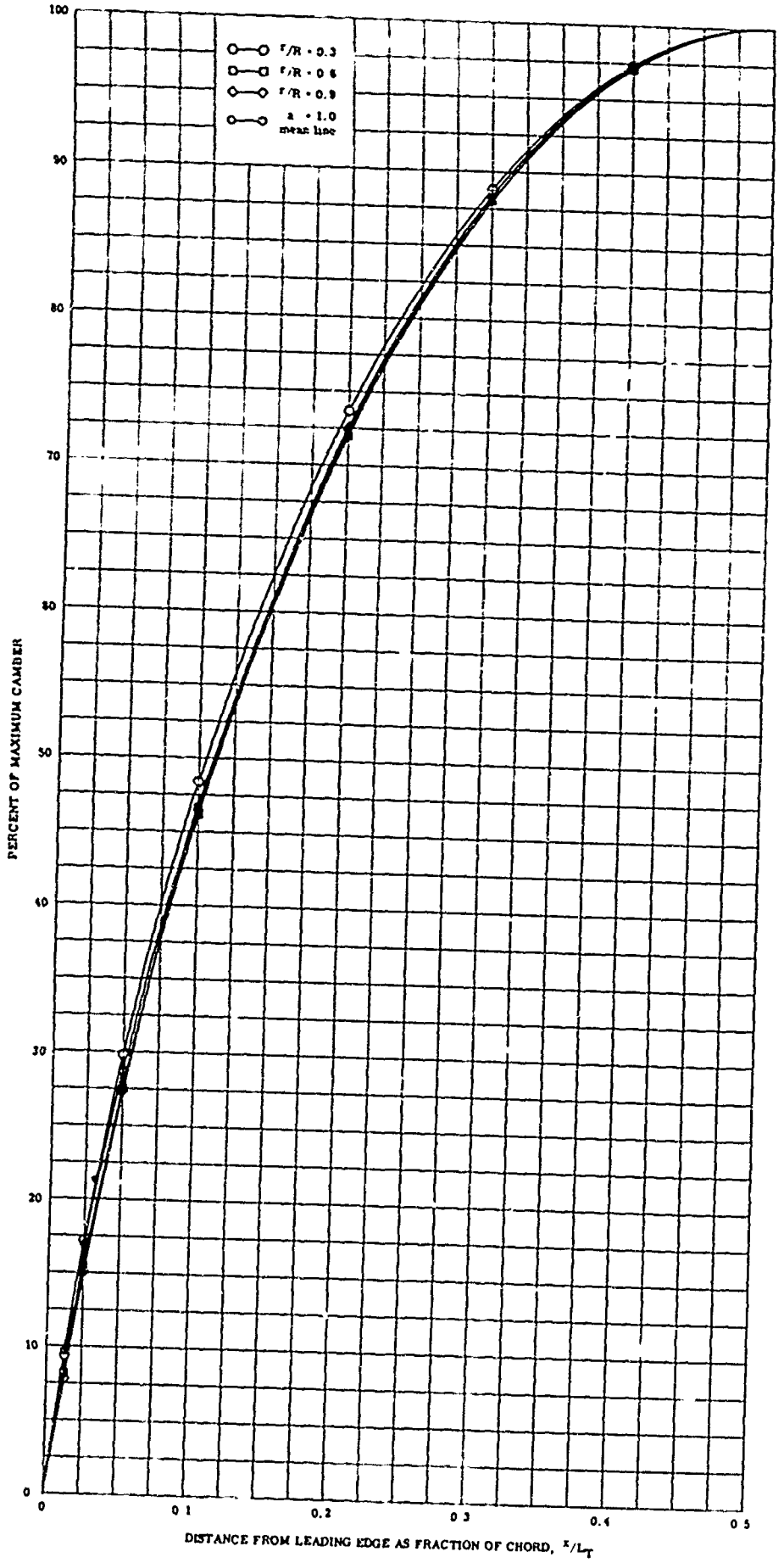

Figure 8 – Camber Line Distribution of a Two-Dimensional Propeller Blade

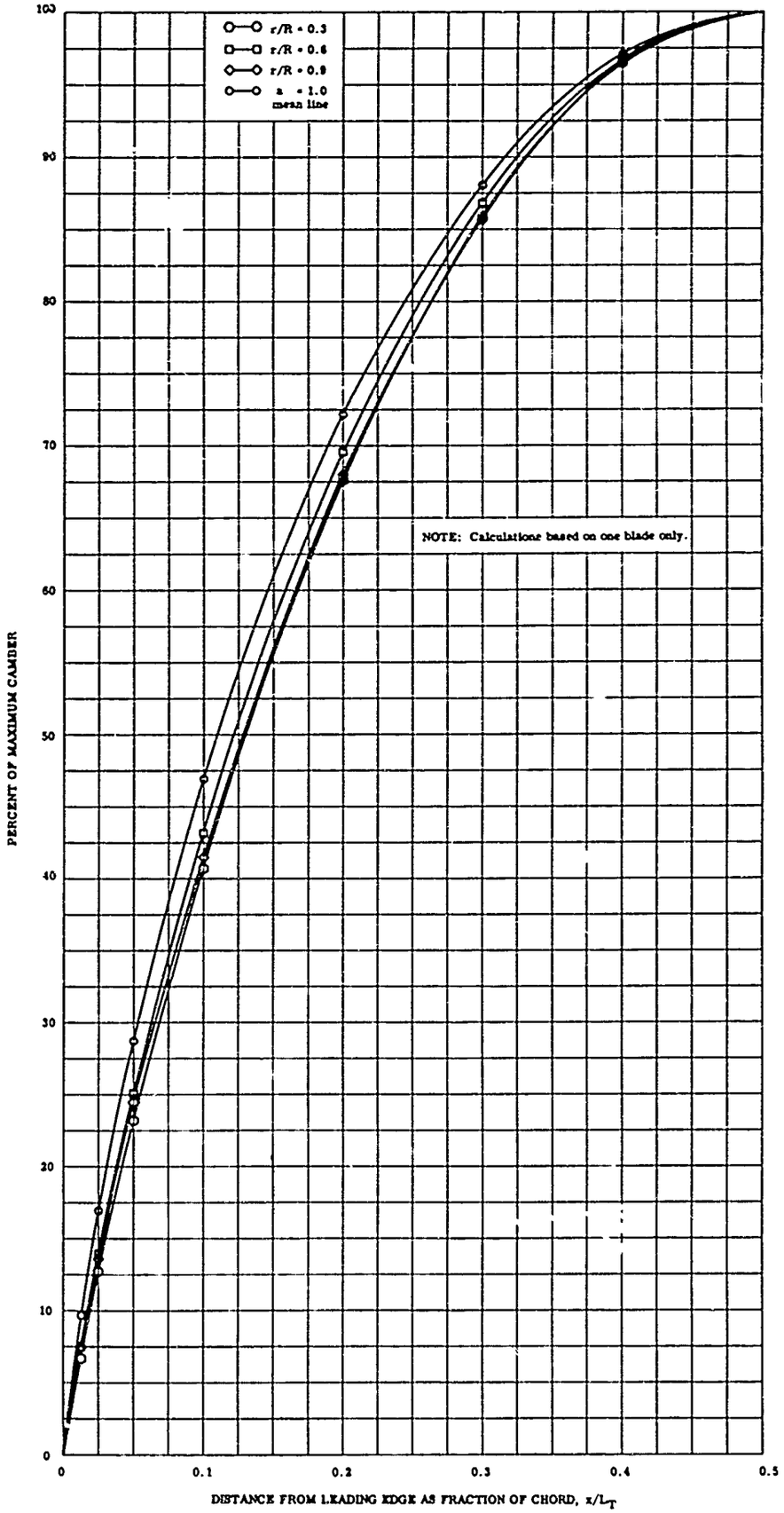

Figure 9 – Camber Line Distribution of Propeller 3916A

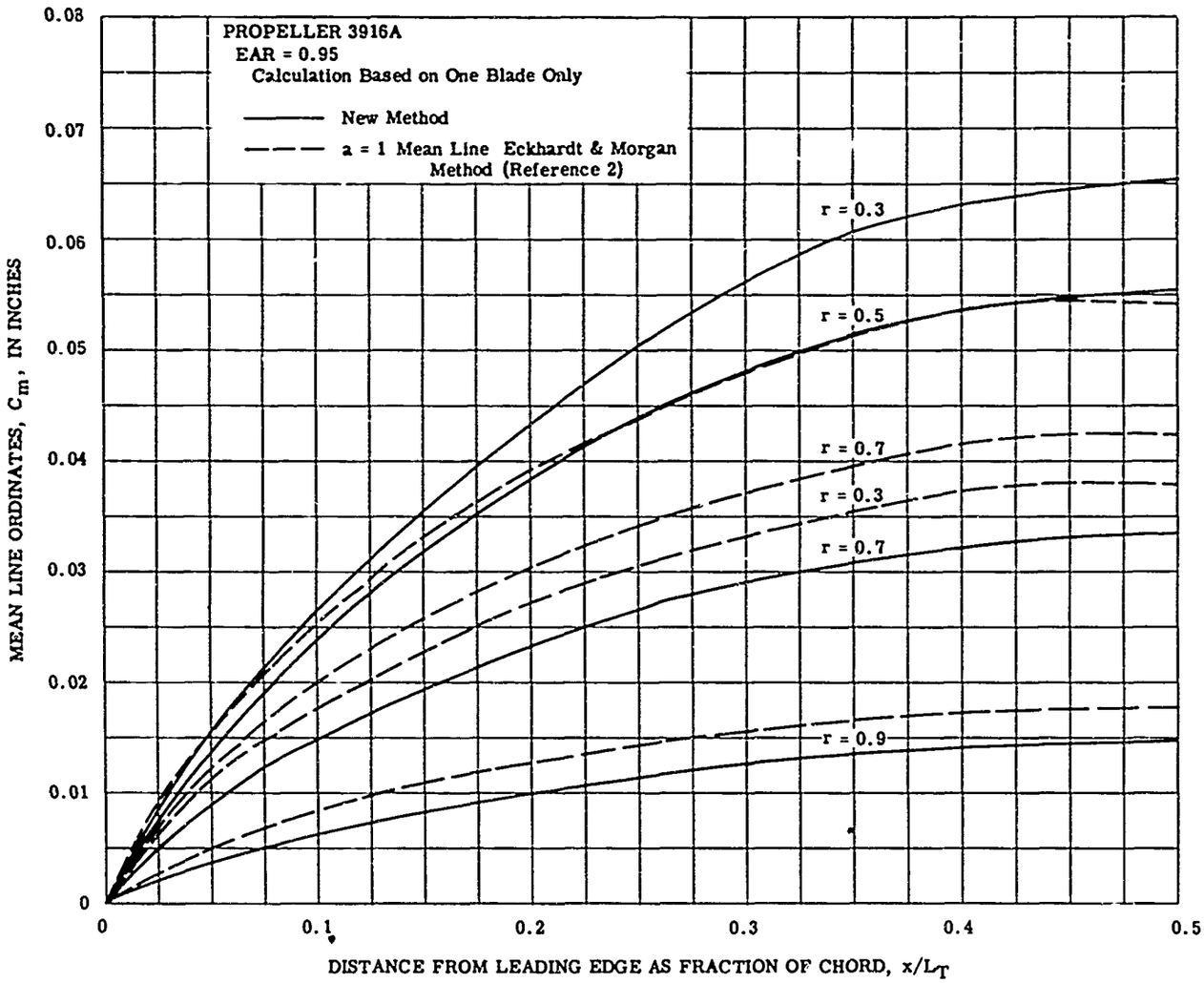

Figure 10 – Comparison of Camber Distribution for Propeller 3916A

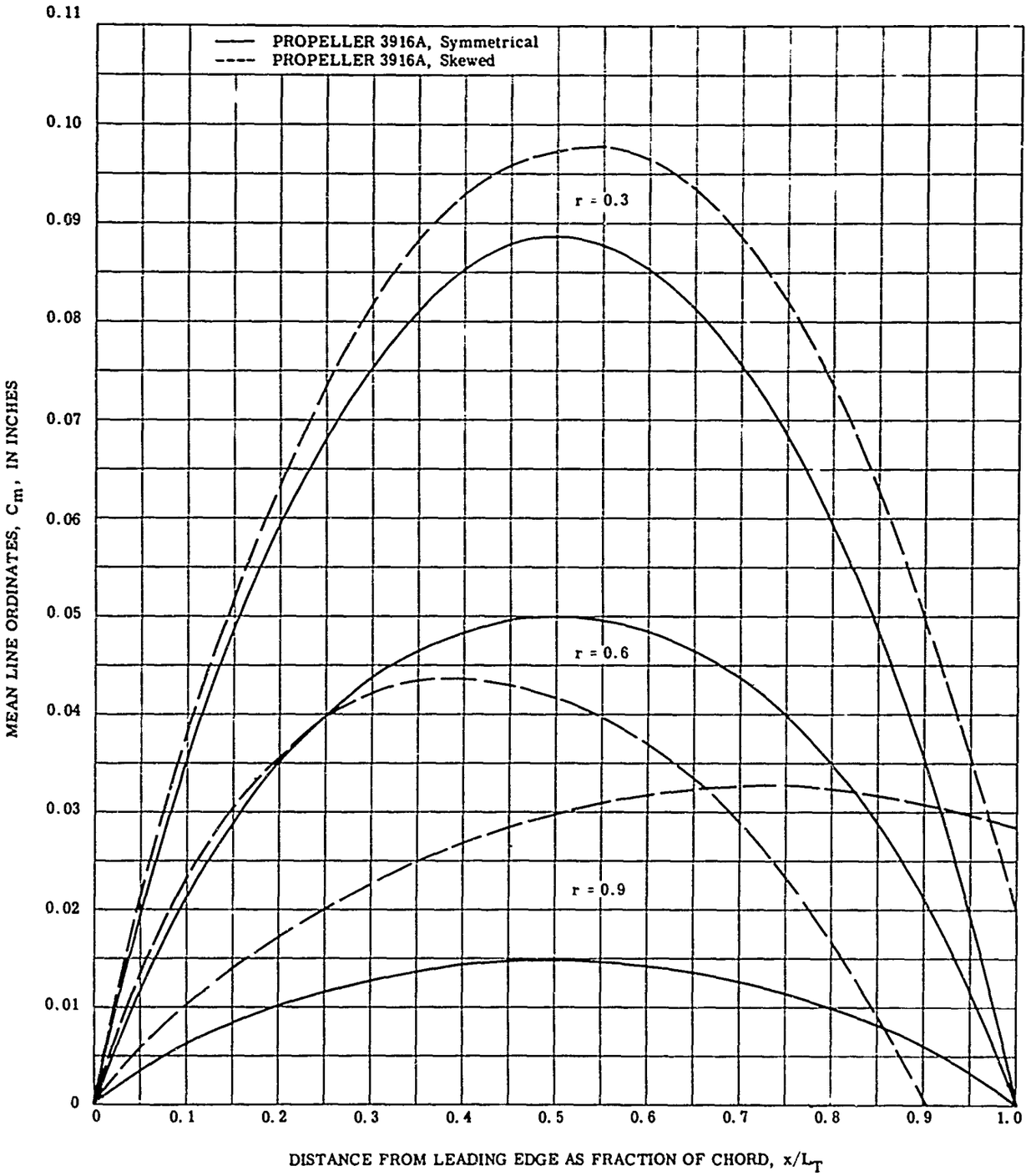

Figure 11 – Comparison of Camber Distributions, Symmetrical versus Skewed Blade Propellers

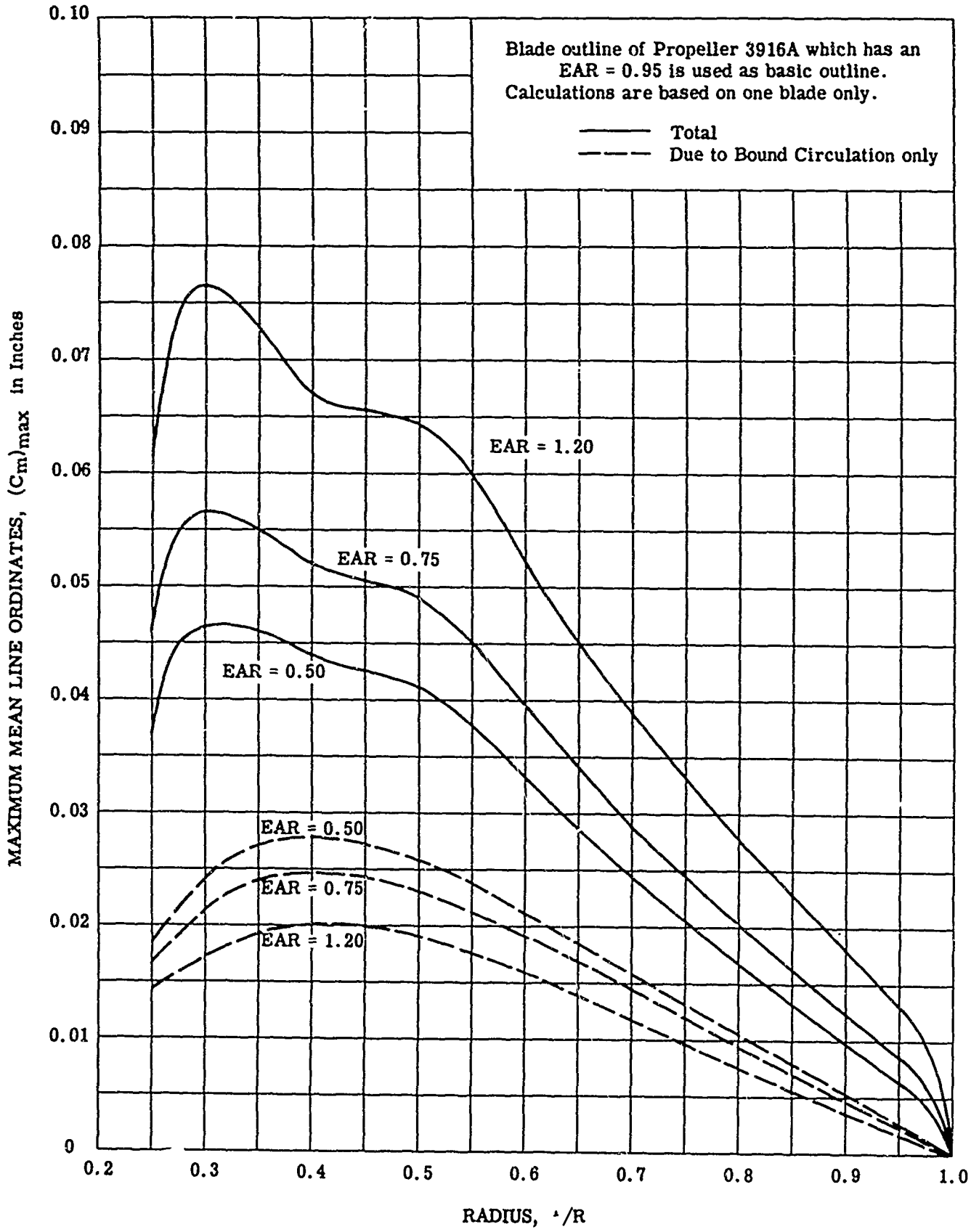

Figure 12 – Maximum Mean Line Ordinates for Propellers with Different EAR

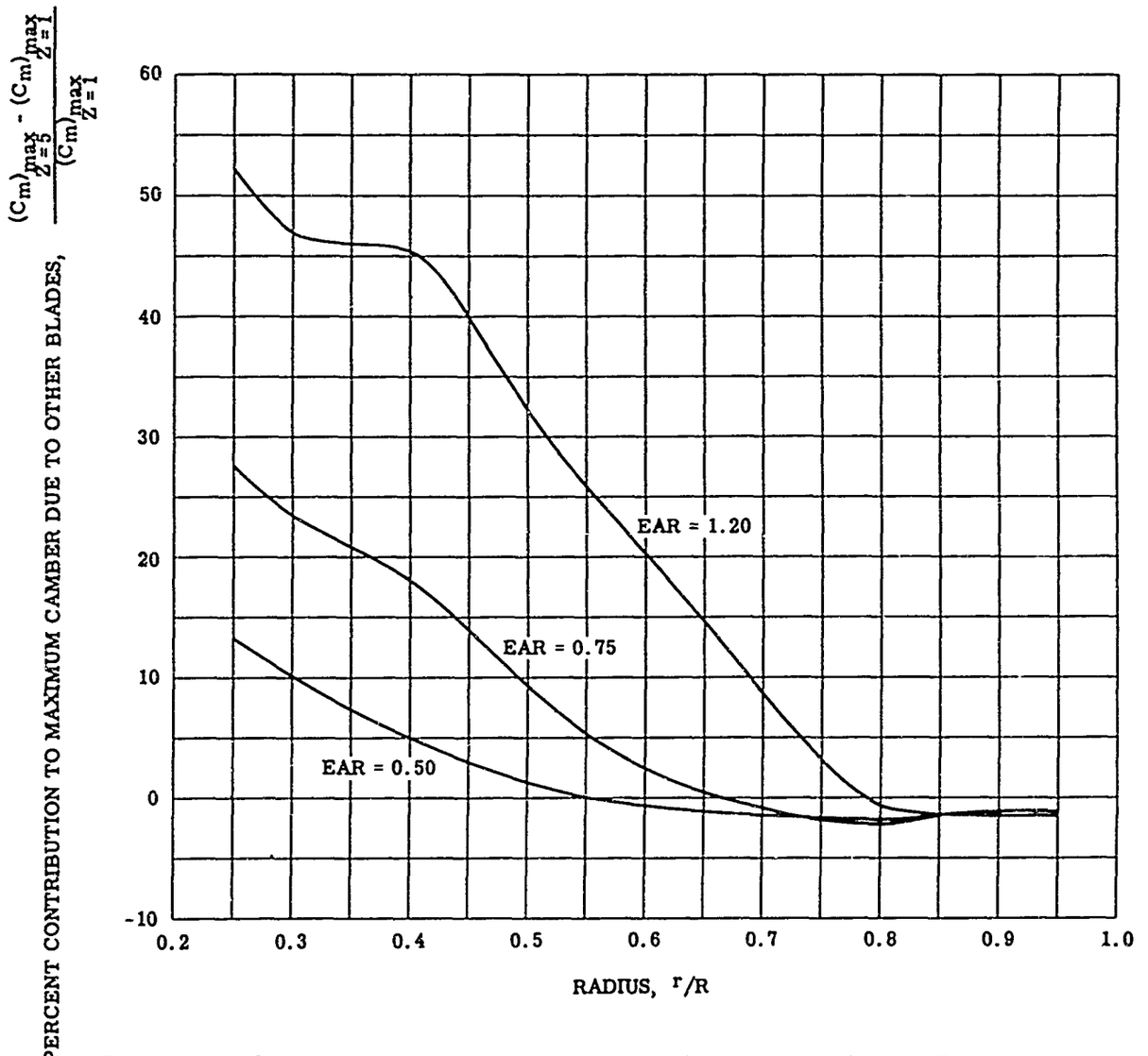

Figure 13 – Percentage Contribution to Maximum Mean Line Ordinates Due to Other Blades for Propellers with Different EAR

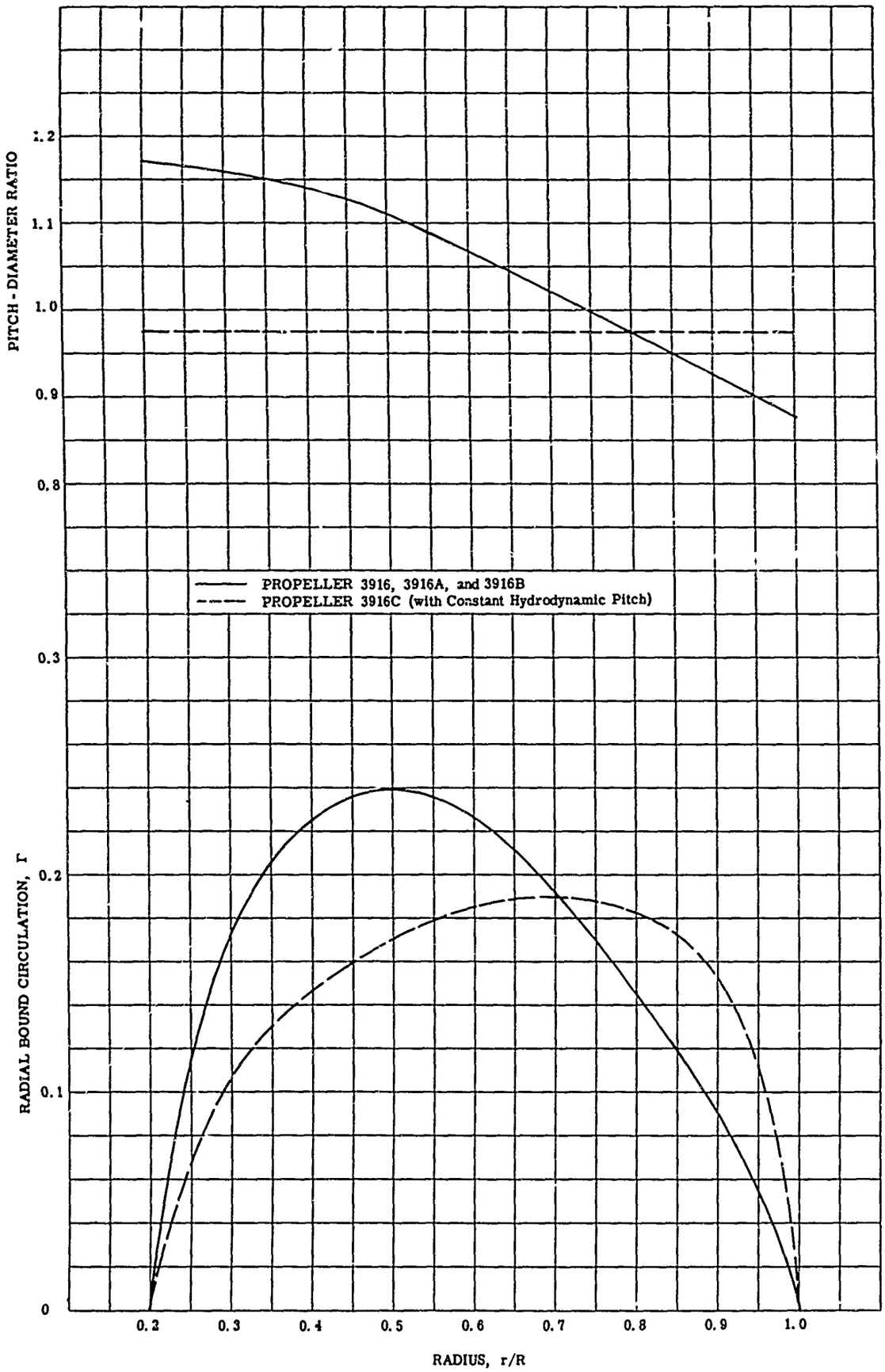

Figure 14 – Pitch Ratio and Bound Circulation Distribution for Propellers 3916 and 3916C

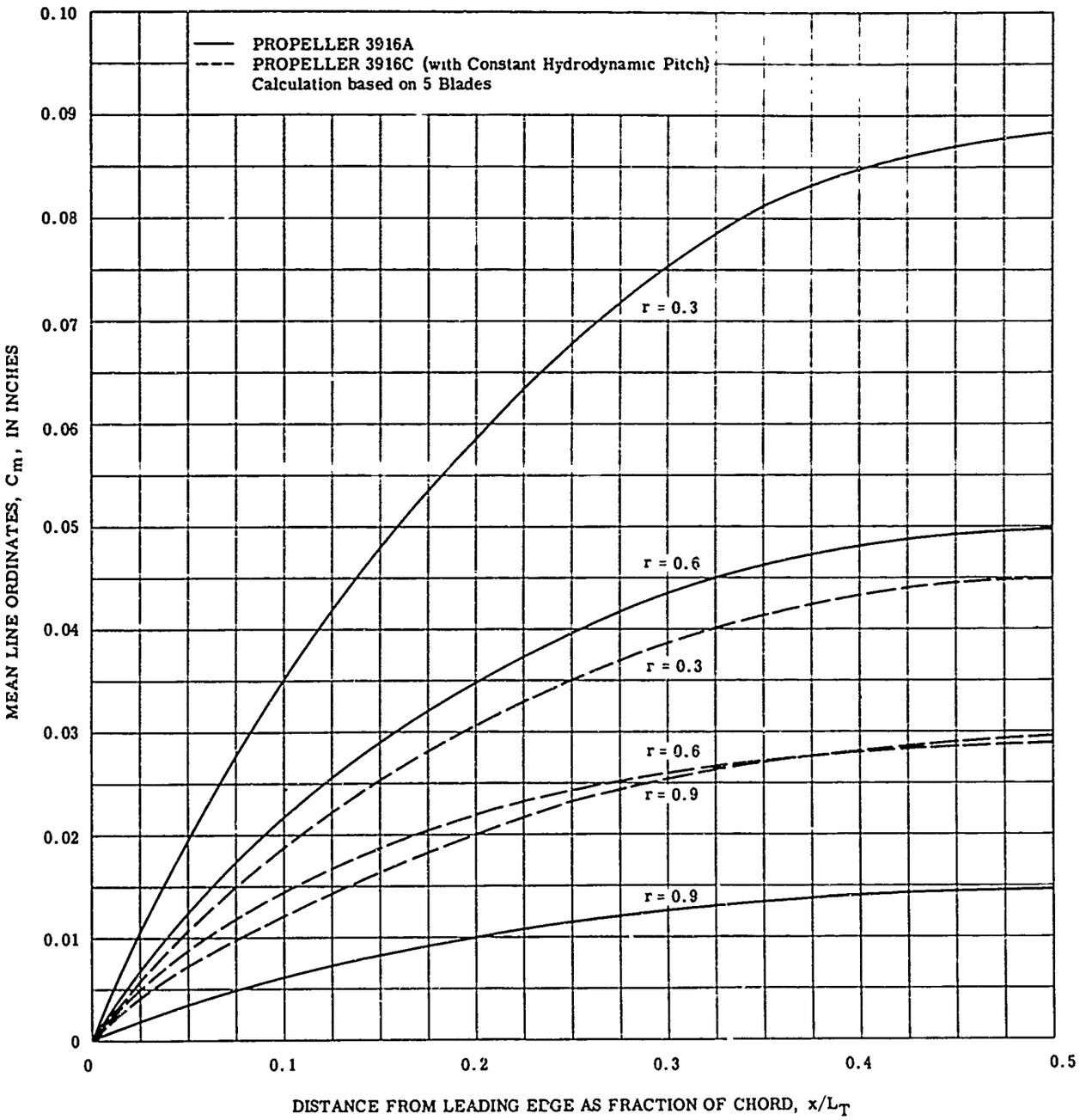

Figure 15 – Comparison of Camber Distribution for Propellers 3916A and 3916C

TABLE 1

Calculated Induced Velocities and Camber Distribution for Propeller 3916A

INPUT DATA

```
      18
 0.00500  0.10000  2.00000150.00000
0.00500 0.01000 0.01600 0.02400 0.03500 0.05000 0.07000 0.09600 0.12900
0.17000 0.22000 0.28000 0.35200 0.44000 0.55200 0.70900 0.94500 1.00000
     1       8       9       0       9      -0      -0
0.00993 0.05083 0.11862 0.20418 0.29586 0.38138 0.44917 0.49007
0.00993 0.01250 0.02500 0.05000 0.10000 0.20000 0.30000 0.40000 0.50000
0.20000 0.30000 0.40000 0.50000 0.60000 0.70000 0.80000 0.90000 1.00000
0.15400 0.18600 0.21550 0.23100 0.23200 0.21150 0.18500 0.13400 0.02600
0.30800 0.37200 0.43000 0.46200 0.46400 0.43500 0.37000 0.26800 0.04000
1.86210 1.22835 0.90786 0.70429 0.56622 0.46342 0.38698 0.32722 0.27950

0.       0.01730 0.02266 0.02428 0.02283 0.01936 0.01463 0.00898-0.
0.25000 0.30000 0.40000 0.50000 0.60000 0.70000 0.80000 0.90000 0.95000
1.00000 1.00000 1.00000 1.00000 1.00000 1.00000 1.00000 1.00000 1.00000
0.14500 0.16902 0.20861 0.22173 0.20765 0.17661 0.13584 0.08937 0.06500
0.16010 0.16678 0.16039 0.13704 0.10517 0.07483 0.04849 0.02767 0.01770
1.00000 0.82600 8.00000 1.00000 1.00000
```

Card 1 (see Appendix B for explanation)
Card 2
Card 3

Card 5
Card 6
Card 7
Card 8 r
$L_f(r)/D$
$L_t(r)/D$
$\tan\beta_i(r)$

$\Gamma(r)$
r_o
$V_x(r_o)$
$u_a(r_o)$
$u_t(r_o)$

Card 9

OUTPUT

AXIAL INDUCED VELOCITY COMPONENT

RX/RO X/LT	0.2500	0.3000	0.4000	0.5000	0.6000	0.7000	0.8000	0.9000	0.9500
0.0099	0.0673	0.1046	0.1276	0.1496	0.1513	0.1487	0.1425	0.1288	0.1164
0.0508	0.0505	0.0775	0.0889	0.1053	0.1086	0.1026	0.0992	0.0913	0.0936
0.1186	0.0389	0.0591	0.0661	0.0758	0.0789	0.0701	0.0688	0.0687	0.0738
0.2041	0.0287	0.0432	0.0465	0.0552	0.0551	0.0521	0.0494	0.0498	0.0581
0.2959	0.0195	0.0289	0.0304	0.0362	0.0363	0.0339	0.0323	0.0336	0.0380
0.3814	0.0116	0.0165	0.0169	0.0206	0.0205	0.0192	0.0184	0.0193	0.0249
0.4492	0.0056	0.0071	0.0068	0.0089	0.0087	0.0081	0.0079	0.0082	0.0111
0.4901	0.0021	0.0015	0.0008	0.0020	0.0017	0.0016	0.0016	0.0014	0.0026

TANGENTIAL INDUCED VELOCITY COMPONENT

RX/RO X/LT	0.2500	0.3000	0.4000	0.5000	0.6000	0.7000	0.8000	0.9000	0.9500
0.0099	-0.1153	-0.1377	-0.1198	-0.1059	-0.0847	-0.0675	-0.0538	-0.0414	-0.0343
0.0508	-0.0894	-0.1040	-0.0856	-0.0758	-0.0609	-0.0466	-0.0373	-0.0293	-0.0275
0.1186	-0.0703	-0.0805	-0.0641	-0.0553	-0.0446	-0.0323	-0.0261	-0.0220	-0.0217
0.2041	-0.0526	-0.0594	-0.0460	-0.0402	-0.0314	-0.0230	-0.0186	-0.0159	-0.0170
0.2959	-0.0359	-0.0399	-0.0302	-0.0266	-0.0207	-0.0156	-0.0121	-0.0107	-0.0111
0.3814	-0.0212	-0.0229	-0.0169	-0.0152	-0.0118	-0.0088	-0.0069	-0.0061	-0.0073
0.4492	-0.0100	-0.0099	-0.0069	-0.0066	-0.0050	-0.0037	-0.0030	-0.0026	-0.0033
0.4901	-0.0033	-0.0020	-0.0009	-0.0015	-0.0010	-0.0007	-0.0006	-0.0004	-0.0008

INDUCED DOWNWASH DUE TO FIRST BLADE ONLY

RX/RO X/LT	0.2500	0.3000	0.4000	0.5000	0.6000	0.7000	0.8000	0.9000	0.9500
0.0099	0.1333	0.1748	0.1750	0.1833	0.1734	0.1634	0.1523	0.1353	0.1213
0.0508	0.1023	0.1296	0.1234	0.1305	0.1245	0.1127	0.1060	0.0959	0.0975
0.1186	0.0803	0.0998	0.0970	0.0938	0.0907	0.0772	0.0736	0.0721	0.0769
0.2041	0.0597	0.0734	0.0693	0.0683	0.0634	0.0573	0.0528	0.0523	0.0605
0.2959	0.0407	0.0492	0.0428	0.0449	0.0418	0.0373	0.0345	0.0353	0.0396
0.3814	0.0241	0.0282	0.0239	0.0256	0.0237	0.0211	0.0197	0.0203	0.0260
0.4492	0.0114	0.0121	0.0096	0.0111	0.0101	0.0090	0.0084	0.0086	0.0116
0.4901	0.0039	0.0025	0.0012	0.0025	0.0020	0.0018	0.0017	0.0015	0.0027

RX/RO	0.2500	0.3000	0.4000	0.5000	0.6000	0.7000	0.8000	0.9000	0.9500
P/D	1.1560	1.1577	1.1406	1.1063	1.0673	1.0232	0.9726	0.9252	0.8976
L.E.	1.3513	1.4880	1.7240	1.8480	1.8560	1.7400	1.4800	1.0720	0.7452
CHORD	2.7213	2.9760	3.4400	3.6960	3.7120	3.4800	2.9600	2.1440	1.4943

CAMBER DISTRIBUTION

X/LT									
0.0099	0.0027	0.0035	0.0035	0.0033	0.0027	0.0021	0.0015	0.0009	0.0005
0.0125	0.0034	0.0044	0.0043	0.0041	0.0034	0.0026	0.0018	0.0011	0.0006
0.0250	0.0064	0.0083	0.0081	0.0077	0.0063	0.0049	0.0034	0.0020	0.0012
0.0500	0.0118	0.0152	0.0145	0.0139	0.0114	0.0088	0.0062	0.0036	0.0022
0.1000	0.0209	0.0266	0.0249	0.0238	0.0196	0.0147	0.0104	0.0061	0.0040
0.2000	0.0351	0.0442	0.0404	0.0383	0.0316	0.0232	0.0165	0.0100	0.0068
0.3000	0.0448	0.0561	0.0505	0.0480	0.0394	0.0290	0.0205	0.0126	0.0088
0.4000	0.0507	0.0631	0.0563	0.0536	0.0439	0.0322	0.0228	0.0142	0.0100
0.5000	0.0529	0.0654	0.0581	0.0555	0.0454	0.0333	0.0236	0.0147	0.0105

CAMBER RATIO

X/LT									
0.0099	0.0010	0.0012	0.0010	0.0009	0.0007	0.0006	0.0005	0.0004	0.0003
0.0125	0.0012	0.0015	0.0013	0.0011	0.0009	0.0007	0.0006	0.0005	0.0004
0.0250	0.0024	0.0028	0.0024	0.0021	0.0017	0.0014	0.0012	0.0009	0.0008
0.0500	0.0043	0.0051	0.0042	0.0038	0.0031	0.0025	0.0021	0.0017	0.0015
0.1000	0.0077	0.0089	0.0072	0.0064	0.0053	0.0042	0.0035	0.0029	0.0027
0.2000	0.0129	0.0148	0.0117	0.0104	0.0085	0.0067	0.0056	0.0047	0.0046
0.3000	0.0165	0.0188	0.0147	0.0130	0.0106	0.0083	0.0069	0.0059	0.0059
0.4000	0.0186	0.0212	0.0164	0.0145	0.0118	0.0093	0.0077	0.0066	0.0067
0.5000	0.0194	0.0220	0.0169	0.0150	0.0122	0.0096	0.0080	0.0069	0.0070

NOTES: 1. Calculation based on one blade only.

2. Calculated camber in inches.

TABLE 2

Calculated Induced Velocities and Camber Distribution for Propeller 3917A (Skewed)

```
INPUT DATA
     18
 0.00500  0.10000  2.00000150.00000
0.00500 0.01000 0.01600 0.02400 0.03500 0.05000 0.07000 0.09600 0.12900
0.17000 0.22000 0.28000 0.35200 0.44000 0.55200 0.70900 0.94500 1.00000
      5       8       9       0       9      -0      -0
0.01250 0.10166 0.23724 0.40828 0.59172 0.76276 0.89834 0.98014
0.01250 0.02500 0.05000 0.10000 0.20000 0.40000 0.60000 0.80000 0.95000
0.20000 0.30000 0.40000 0.50000 0.60000 0.70000 0.80000 0.90000 1.00000
0.12500 0.20900 0.26400 0.28600 0.27300 0.22700 0.14900 0.03300-0.11300
0.30800 0.37200 0.43000 0.46200 0.46400 0.43500 0.37000 0.26800 0.04000
1.88210 1.22835 0.90766 0.70429 0.56622 0.46392 0.38698 0.32722 0.27960

0.      0.01730 0.02266 0.02428 0.02283 0.01936 0.01463 0.00898-0.
0.25000 0.30000 0.40000 0.50000 0.60000 0.70000 0.80000 0.90000 0.95000
1.00000 1.00000 1.00000 1.00000 1.00000 1.00000 1.00000 1.00000 1.00000
0.14500 0.16902 0.20861 0.22173 0.20765 0.17661 0.13584 0.08937 0.06500
0.16010 0.16678 0.16039 0.13704 0.10817 0.07483 0.04889 0.02767 0.01770
1.00000 0.82600 0.00000 1.00000 1.00900
```

Card 1 (see Appendix B for explanation)
Card 2
Card 3
Card 5
Card 6
Card 7
Card 8 r
$L_f(r)/D$
$L_t(r)/D$
$\tan \beta_i(r)$

$\Gamma(r)$
r_o
$V_x(r_o)$
$u_a(r_o)$
$u_t(r_o)$
Card 9

OUTPUT

AXIAL INDUCED VELOCITY COMPONENT

RX/RO	0.2500	0.3000	0.4000	0.5000	0.6000	0.7000	0.8000	0.9000	0.9500
X/LT									
0.0125	0.0809	0.1115	0.1158	0.1427	0.1642	0.1770	0.1818	0.1922	0.1680
0.1017	0.0573	0.0669	0.0604	0.0713	0.0820	0.0872	0.0984	0.1257	0.1343
0.2372	0.0450	0.0400	0.0232	0.0200	0.0320	0.0430	0.0480	0.0844	0.1036
0.4083	0.0341	0.0163	-0.0067	-0.0122	-0.0049	0.0090	0.0213	0.0558	0.0720
0.5917	0.0228	-0.0065	-0.0322	-0.0425	-0.0355	-0.0201	-0.0067	0.0253	0.0335
0.7628	0.0126	-0.0310	-0.0575	-0.0718	-0.0650	-0.0480	-0.0339	-0.0038	-0.0005
0.8983	-0.0133	-0.0589	-0.0876	-0.1049	-0.0975	-0.0783	-0.0620	-0.0333	-0.0323
0.9801	-0.0429	-0.1002	-0.1296	-0.1512	-0.1446	-0.1231	-0.1031	-0.0729	-0.0927

TANGENTIAL INDUCED VELOCITY COMPONENT

RX/RO	0.2500	0.3000	0.4000	0.5000	0.6000	0.7000	0.8000	0.9000	0.9500
X/LT									
0.0125	-0.1953	-0.2042	-0.1637	-0.1423	-0.1226	-0.0994	-0.0758	-0.0662	-0.0479
0.1017	-0.1479	-0.1418	-0.1073	-0.0890	-0.0718	-0.0547	-0.0418	-0.0436	-0.0375
0.2372	-0.1068	-0.0934	-0.0632	-0.0480	-0.0374	-0.0288	-0.0201	-0.0289	-0.0279
0.4083	-0.0562	-0.0372	-0.0153	-0.0069	-0.0052	-0.0063	-0.0064	-0.0179	-0.0179
0.5917	-0.0022	0.0231	0.0346	0.0335	0.0243	0.0139	0.0075	-0.0044	-0.0060
0.7628	0.0485	0.0794	0.0806	0.0703	0.0511	0.0325	0.0206	0.0046	0.0045
0.8983	0.0952	0.1291	0.1217	0.1038	0.0763	0.0486	0.0334	0.0153	0.0144
0.9801	0.1404	0.1795	0.1653	0.1404	0.1052	0.0732	0.0401	0.0289	0.0326

INDUCED DOWNWASH DUE TO ALL BLADES

RX/RO	0.2500	0.3000	0.4000	0.5000	0.6000	0.7000	0.8000	0.9000	0.9500
X/LT									
0.0125	0.2073	0.2228	0.1958	0.1986	0.2033	0.2024	0.1969	0.2033	0.1747
0.1017	0.1548	0.1522	0.1168	0.1095	0.1050	0.1021	0.1049	0.1330	0.1398
0.2372	0.1135	0.0977	0.0597	0.0449	0.0462	0.0511	0.0520	0.0892	0.1072
0.4083	0.0657	0.0391	0.0053	-0.0060	-0.0017	0.0108	0.0221	0.0585	0.0741
0.5917	0.0145	-0.0220	-0.0471	-0.0540	-0.0429	-0.0241	-0.0089	0.0260	0.0338
0.7628	-0.0332	-0.0812	-0.0968	-0.0997	-0.0818	-0.0572	-0.0390	-0.0050	-0.0017
0.8983	-0.0863	-0.1373	-0.1466	-0.1455	-0.1224	-0.0923	-0.0699	-0.0364	-0.0351
0.9801	-0.1405	-0.2025	-0.2071	-0.2044	-0.1777	-0.1425	-0.1143	-0.0763	-0.0981

RX/RO	0.2500	0.3000	0.4000	0.5000	0.6000	0.7000	0.8000	0.9000	0.9500
P/D	1.1560	1.1577	1.1406	1.1063	1.0673	1.0202	0.9726	0.9252	0.8976
L.E.	1.3624	1.6720	2.1120	2.2880	2.1840	1.8160	1.1920	0.2640	-0.3133
CHORD	2.7213	2.9760	3.4400	3.6960	3.7120	3.4800	2.9600	2.1440	1.4943

CAMBER DISTRIBUTION

X/LT									
0.0125	0.0052	0.0058	0.0048	0.0045	0.0040	0.0033	0.0024	0.0016	0.0009
0.0250	0.0101	0.0112	0.0093	0.0086	0.0076	0.0062	0.0046	0.0031	0.0017
0.0500	0.0194	0.0210	0.0171	0.0158	0.0138	0.0112	0.0084	0.0057	0.0034
0.1000	0.0357	0.0375	0.0299	0.0270	0.0232	0.0187	0.0143	0.0102	0.0063
0.2000	0.0628	0.0630	0.0476	0.0411	0.0351	0.0284	0.0218	0.0170	0.0114
0.4000	0.1004	0.0928	0.0624	0.0497	0.0435	0.0372	0.0293	0.0264	0.0189
0.6000	0.1160	0.0962	0.0544	0.0394	0.0367	0.0355	0.0306	0.0315	0.0233
0.8000	0.1100	0.0730	0.0248	0.0109	0.0166	0.0245	0.0254	0.0323	0.0241
0.9500	0.0873	0.0354	-0.0144	-0.0246	-0.0093	0.0068	0.0164	0.0294	0.0223

CAMBER RATIO

X/LT									
0.0125	0.0019	0.0020	0.0014	0.0012	0.0011	0.0009	0.0008	0.0007	0.0006
0.0250	0.0037	0.0038	0.0027	0.0023	0.0020	0.0018	0.0015	0.0014	0.0012
0.0500	0.0071	0.0071	0.0050	0.0043	0.0037	0.0032	0.0025	0.0027	0.0023
0.1000	0.0131	0.0126	0.0087	0.0073	0.0063	0.0054	0.0048	0.0048	0.0042
0.2000	0.0231	0.0212	0.0138	0.0111	0.0095	0.0082	0.0074	0.0079	0.0076
0.4000	0.0369	0.0312	0.0181	0.0134	0.0117	0.0107	0.0099	0.0123	0.0127
0.6000	0.0426	0.0323	0.0158	0.0107	0.0099	0.0102	0.0103	0.0147	0.0156
0.8000	0.0404	0.0245	0.0072	0.0030	0.0045	0.0071	0.0086	0.0150	0.0162
0.9500	0.0321	0.0119	-0.0042	-0.0067	-0.0025	0.0025	0.0055	0.0137	0.0150

NOTES: 1. Calculation based on five blades.

2. Calculated camber in inches.

TABLE 3

Camber Distribution for Propellers with Different Expanded Area Ratios

EAR = 0.50

RX/RO	0.2500	0.3000	0.4000	0.5000	0.6000	0.7000	0.8000	0.9000	0.9500
P/D	1.1560	1.1577	1.1406	1.1063	1.0673	1.0202	0.9726	0.9252	0.8976
L.E.	0.7119	0.7827	0.9068	0.9720	0.9763	0.9152	0.7785	0.5639	0.3920
CHORD	1.4314	1.5654	1.8074	1.9441	1.9525	1.8305	1.5570	1.1277	0.7860
CAMBER DISTRIBUTION									
X/LT									
0.0099	0.0022	0.0028	0.0028	0.0026	0.0021	0.0015	0.0010	0.0006	0.0003
0.0125	0.0027	0.0035	0.0035	0.0033	0.0026	0.0019	0.0013	0.0007	0.0004
0.0250	0.0050	0.0065	0.0065	0.0061	0.0049	0.0036	0.0024	0.0013	0.0007
0.0500	0.0071	0.0116	0.0116	0.0108	0.0088	0.0065	0.0043	0.0024	0.0014
0.1000	0.0157	0.0198	0.0195	0.0181	0.0148	0.0109	0.0074	0.0042	0.0026
0.2000	0.0257	0.0321	0.0309	0.0288	0.0235	0.0172	0.0117	0.0067	0.0043
0.3000	0.0325	0.0402	0.0382	0.0357	0.0289	0.0213	0.0146	0.0084	0.0054
0.4000	0.0365	0.0449	0.0425	0.0397	0.0322	0.0236	0.0162	0.0094	0.0061
0.5000	0.0379	0.0463	0.0438	0.0410	0.0332	0.0244	0.0157	0.0097	0.0064

EAR = 0.75

RX/RO	0.2500	0.3000	0.4000	0.5000	0.6000	0.7000	0.8000	0.9000	0.9500
P/D	1.1560	1.1577	1.1406	1.1063	1.0673	1.0202	0.9726	0.9252	0.8976
L.E.	1.0664	1.1725	1.3585	1.4562	1.4625	1.3711	1.1662	0.8447	0.5872
CHORD	2.1444	2.3451	2.7107	2.9124	2.9251	2.7422	2.3325	1.6895	1.1775
CAMBER DISTRIBUTION									
X/LT									
0.0099	0.0025	0.0032	0.0032	0.0030	0.0025	0.0018	0.0013	0.0007	0.0004
0.0125	0.0030	0.0039	0.0039	0.0037	0.0030	0.0022	0.0016	0.0009	0.0005
0.0250	0.0058	0.0074	0.0074	0.0069	0.0057	0.0042	0.0029	0.0017	0.0010
0.0500	0.0106	0.0135	0.0132	0.0124	0.0102	0.0076	0.0052	0.0031	0.0019
0.1000	0.0185	0.0235	0.0224	0.0212	0.0174	0.0128	0.0088	0.0053	0.0033
0.2000	0.0307	0.0385	0.0361	0.0341	0.0277	0.0200	0.0141	0.0085	0.0057
0.3000	0.0391	0.0485	0.0450	0.0424	0.0344	0.0251	0.0176	0.0107	0.0073
0.4000	0.0442	0.0546	0.0501	0.0472	0.0383	0.0279	0.0195	0.0120	0.0083
0.5000	0.0460	0.0565	0.0516	0.0489	0.0395	0.0288	0.0202	0.0124	0.0086

EAR = 1.20

RX/RO	0.2500	0.3000	0.4000	0.5000	0.6000	0.7000	0.8000	0.9000	0.9500
P/D	1.1560	1.1577	1.1406	1.1063	1.0673	1.0202	0.9726	0.9252	0.8976
L.E.	1.7052	1.8749	2.1722	2.3285	2.3386	2.1924	1.8648	1.3507	0.9389
CHORD	3.4289	3.7498	4.3344	4.6570	4.6771	4.3848	3.7296	2.7014	1.8829
CAMBER DISTRIBUTION									
X/LT									
0.0099	0.0030	0.0040	0.0038	0.0038	0.0032	0.0024	0.0017	0.0010	0.0006
0.0125	0.0038	0.0049	0.0048	0.0047	0.0039	0.0030	0.0022	0.0013	0.0007
0.0250	0.0072	0.0094	0.0090	0.0088	0.0073	0.0057	0.0040	0.0024	0.0014
0.0500	0.0133	0.0172	0.0163	0.0157	0.0128	0.0102	0.0072	0.0044	0.0027
0.1000	0.0238	0.0305	0.0283	0.0271	0.0219	0.0170	0.0122	0.0075	0.0050
0.2000	0.0403	0.0512	0.0462	0.0442	0.0359	0.0269	0.0194	0.0122	0.0085
0.3000	0.0517	0.0653	0.0579	0.0555	0.0450	0.0337	0.0241	0.0153	0.0110
0.4000	0.0586	0.0737	0.0647	0.0621	0.0503	0.0375	0.0267	0.0172	0.0125
0.5000	0.0613	0.0764	0.0667	0.0643	0.0520	0.0388	0.0277	0.0179	0.0131

NOTES: 1. Blade outline of Propeller 3916A which has an EAR = 0.95 is used as basic blade outline.
2. Calculations are based on one blade only.
3. Calculated camber distributions are in inches.

TABLE 4

Calculated Induced Velocities and Camber Distribution for Propeller 3916C

INPUT DATA

16									Card 1	(see Appendix B for explanation)
0.00500	0.10000	2.00000150.00000							Card 2	
0.00500	0.01000	0.01600	0.02400	0.03500	0.05000	0.07000	0.09600	0.12900	Card 3	
0.17000	0.22000	0.28000	0.35200	0.44000	0.55200	0.70900	0.94500	1.00000		
5	8	9	1	9	-0	-0			Card 5	
0.00993	0.05083	0.11862	0.20414	0.29586	0.38138	0.44917	0.49007		Card 6	
0.00993	0.01250	0.02500	0.05000	0.10000	0.20000	0.30000	0.40000	0.50000	Card 7	
0.20000	0.30000	0.40000	0.50000	0.60000	0.70000	0.80000	0.90000	1.00000	Card 8	r
0.15400	0.18600	0.21550	0.23100	0.23200	0.21750	0.18500	0.13400	0.02000		$L_l(r)/D$
0.30800	0.37200	0.43000	0.46200	0.46400	0.43500	0.37000	0.26800	0.04000		$L_t(r)/D$
1.57165	1.04777	0.78583	0.62866	0.52388	0.44904	0.39291	0.34926	0.31433		$\tan \beta_i(r)$
0.	0.01067	0.01451	0.01698	0.01841	0.01897	0.01833	0.01537	0.		$\Gamma(r)$
0.25000	0.30000	0.40000	0.50000	0.60000	0.70000	0.80000	0.90000	0.95000		r_o
1.00000	1.00000	1.00000	1.00000	1.00000	1.00000	1.00000	1.00000	1.00000		$V_x(r_o)$
0.07500	0.09239	0.12034	0.13957	0.15287	0.16215	0.16890	0.17973	0.17900		$u_a(r_o)$
0.09550	0.09793	0.09510	0.08817	0.08041	0.07308	0.06661	0.06302	0.06000		$u_t(r_o)$
1.09000	0.82600	8.00000	1.00000	1.00000					Card 9	

OUTPUT

AXIAL INDUCED VELOCITY COMPONENT

RX/RO	0.2500	0.3000	0.4000	0.5000	0.6000	0.7000	0.8000	0.9000	0.9500
X/LT									
0.0099	0.0214	0.0559	0.0649	0.0861	0.1089	0.1346	0.1777	0.2487	0.2667
0.0508	0.0104	0.0370	0.0389	0.0556	0.0687	0.0885	0.1209	0.1802	0.2215
0.1186	0.0050	0.0246	0.0232	0.0346	0.0410	0.0573	0.0808	0.1367	0.1732
0.2041	0.0007	0.0133	0.0128	0.0203	0.0267	0.0361	0.0553	0.0993	0.1370
0.2959	0.0003	0.0071	0.0064	0.0109	0.0111	0.0225	0.0352	0.0672	0.0931
0.3814	0.0002	0.0052	0.0022	0.0058	0.0081	0.0121	0.0199	0.0387	0.0584
0.4492	0.0007	0.0022	0.0007	0.0024	0.0033	0.0051	0.0085	0.0164	0.0258
0.4901	0.0010	0.0005	-0.000[illegible]	0.0006	0.0006	0.0010	0.0017	0.0027	0.0057

TANGENTIAL INDUCED VELOCITY COMPONENT

RX/RO	0.2500	0.3000	0.4000	0.5000	0.6000	0.7000	0.8000	0.9000	0.9500
X/LT									
0.0099	-0.1014	-0.1112	-0.0998	-0.0926	-0.0839	-0.0777	-0.0786	-0.0914	-0.0900
0.0508	-0.0828	-0.0893	-0.0772	-0.0700	-0.0613	-0.0556	-0.0556	-0.0670	-0.0749
0.1186	-0.0674	-0.0718	-0.0602	-0.0533	-0.0441	-0.0394	-0.0389	-0.0512	-0.0587
0.2041	-0.0517	-0.0545	-0.0446	-0.0384	-0.0314	-0.0269	-0.0271	-0.0373	-0.0463
0.2959	-0.0359	-0.0374	-0.0301	-0.0253	-0.0194	-0.0172	-0.0174	-0.0252	-0.0315
0.3814	-0.0213	-0.0220	-0.0172	-0.0144	-0.0112	-0.0095	-0.0099	-0.0145	-0.0197
0.4492	-0.0096	-0.0095	-0.0072	-0.0062	-0.0047	-0.0040	-0.0042	-0.0061	-0.0087
0.4901	-0.0025	-0.0019	-0.0012	-0.0013	-0.0009	-0.0008	-0.0009	-0.0010	-0.0020

INDUCED DOWNWASH DUE TO ALL BLADES

RX/RO	0.2500	0.3000	0.4000	0.5000	0.6000	0.7000	0.8000	0.9000	0.9500
X/LT									
0.0099	0.0927	0.1190	0.1127	0.1222	0.1354	0.1546	0.1941	0.2649	0.2814
0.0508	0.0712	0.0901	0.0783	0.0844	0.0893	0.1035	0.1329	0.1922	0.2338
0.1186	0.0559	0.0689	0.0555	0.0576	0.0567	0.0684	0.0895	0.1459	0.1829
0.2041	0.0409	0.0486	0.0376	0.0376	0.0382	0.0439	0.0614	0.1060	0.1446
0.2959	0.0283	0.0320	0.0236	0.0227	0.0189	0.0275	0.0392	0.0718	0.0983
0.3814	0.0168	0.0195	0.0123	0.0125	0.0123	0.0150	0.0222	0.0413	0.0617
0.4492	0.0079	0.0084	0.0050	0.0053	0.0051	0.0063	0.0095	0.0175	0.0272
0.4901	0.0026	0.0017	0.0005	0.0012	0.0010	0.0012	0.0019	0.0029	0.0060

RX/RO	0.2500	0.3000	0.4000	0.5000	0.6000	0.7000	0.8000	0.9000	0.9500
P/D	0.9875	0.9875	0.9875	0.9875	0.9875	0.9875	0.9875	0.9875	0.9875
L.E.	1.3533	1.4880	1.7240	1.8480	1.8560	1.7400	1.4800	1.0720	0.7452
CHORD	2.7213	2.9760	3.4400	3.6960	3.7120	3.4800	2.9600	2.1440	1.4943

CAMBER DISTRIBUTION

X/LT									
0.0099	0.0019	0.0024	0.0022	0.0022	0.0021	0.0020	0.0019	0.0017	0.0011
0.0125	0.0024	0.0030	0.0028	0.0028	0.0026	0.0025	0.0023	0.0021	0.0014
0.0250	0.0045	0.0058	0.0052	0.0052	0.0049	0.0046	0.0044	0.0039	0.0028
0.0500	0.0083	0.0106	0.0093	0.0092	0.0087	0.0082	0.0078	0.0071	0.0053
0.1000	0.0147	0.0186	0.0158	0.0155	0.0143	0.0136	0.0131	0.0122	0.0095
0.2000	0.0247	0.0306	0.0251	0.0241	0.0217	0.0208	0.0204	0.0201	0.0162
0.3000	0.0315	0.0385	0.0308	0.0292	0.0259	0.0251	0.0250	0.0255	0.0211
0.4000	0.0357	0.0432	0.0339	0.0320	0.0280	0.0275	0.0276	0.0286	0.0241
0.5000	0.0372	0.0449	0.0348	0.0329	0.0288	0.0283	0.0285	0.0297	0.0251

CAMBER RATIO

X/LT									
0.0099	0.0007	0.0008	0.0007	0.0006	0.0006	0.0006	0.0006	0.0008	0.0008
0.0125	0.0009	0.0010	0.0008	0.0007	0.0007	0.0007	0.0008	0.0010	0.0010
0.0250	0.0017	0.0019	0.0015	0.0014	0.0013	0.0013	0.0015	0.0018	0.0019
0.0500	0.0031	0.0035	0.0027	0.0025	0.0024	0.0024	0.0026	0.0033	0.0035
0.1000	0.0054	0.0062	0.0046	0.0042	0.0038	0.0039	0.0044	0.0057	0.0068
0.2000	0.0091	0.0103	0.0073	0.0065	0.0059	0.0060	0.0069	0.0094	0.0109
0.3000	0.0116	0.0129	0.0090	0.0079	0.0070	0.0072	0.0084	0.0119	0.0141
0.4000	0.0131	0.0145	0.0099	0.0087	0.0075	0.0079	0.0093	0.0134	0.0161
0.5000	0.0137	0.0151	0.0101	0.0089	0.0078	0.0081	0.0096	0.0138	0.0168

NOTES: 1 Calculation based on five blades.

2. Calculated camber in inches.

APPENDIX A

EVALUATION OF INTEGRALS

It has been stated in the text that the integrals of Equation [16] have a singularity at $r = r_0$ and $\theta = \theta_0$ (or $\phi = 0$). The integrals are integrated numerically with this singular point isolated. The justification for this procedure is that the contribution to the final mean line due to the small region that includes the singular point is negligible. To show that this is indeed the case, we shall first take a look at the induced velocities and then their contributions to the final mean line.

INDUCED VELOCITIES

The integral to be investigated which represents the contribution of the small area to the induced velocity components is in the following general form:

$$I_n(r_0, \theta_0) = \int_{r_0-\delta_0}^{r_0+\delta_0} \int_{\theta_0-\epsilon_0}^{\theta_0+\epsilon_0} L_n(r, \theta)\, K_n(r_0, \theta_0, r, \theta)\, d\theta\, dr$$

where $\delta_0 \ll 1$, $\epsilon_0 \ll 1$, $L_n(r, \theta)$ represents the loading function, and $K_n(r_0\ \theta_0, r, \theta)$ is the kernel function which has the form

$$K_n(r_0, \theta_0, r, \theta) = \frac{F_n(r, \theta)}{[r_0^2 + r^2 - 2 r_0 r \cos(\theta - \theta_0) + (p/\pi)^2 (\theta - \theta_0)^2]^{3/2}}$$

To facilitate the evaluation, we introduce a limiting process of $\lim_{X \to 0}$ such that

$$I_n(r_0, \theta_0) = \lim_{X \to 0} \left\{ \int_{r_0-\delta_0}^{r_0+\delta_0} \int_{\theta_0-\epsilon_0}^{\theta_0+\epsilon_0} \frac{L_n(r, \theta)\, F_n(r, \theta)\, d\theta\, dr}{[X^2 + r_0^2 + r^2 - 2 r_0 r \cos(\theta - \theta_0) + (p/\pi)^2 (\theta - \theta_0)^2]^{3/2}} \right\}$$

Physically, the introduction of this limiting process means that mathematical evaluations are performed over an area on a surface which is X distance away from the control point on the lifting surface, and that in the limit the fictitious area is brought infinitesimally close to the control point. This means that the velocity induced on the surface $X = 0$ is a continuous function of X including $X = 0$.

With this procedure in mind, we shall attempt to deal with each of the four integrals involved.

Equation [16a]

$$V_{ba}(r_0, \theta_0) = I_1(r_0, \theta_0)$$

$$= \lim_{X \to 0} \left\{ -\frac{r_0}{4\pi} \int_{r_0-\delta_0}^{r_0+\delta_0} \int_{\theta_0-\epsilon_0}^{\theta_0+\epsilon_0} \frac{\gamma(r) \sin(\theta-\theta_0)\, d\theta\, dr}{[X^2 + r_0^2 + r^2 - 2r_0 r \cos(\theta-\theta_0) + (p/\pi)^2 (\theta-\theta_0)^2]^{3/2}} \right\}$$

For a small ϵ_0, we may substitute $\theta-\theta_0$ for $\sin(\theta-\theta_0)$ and $1 - \frac{1}{2}(\theta-\theta_0)^2$ for $\cos(\theta-\theta_0)$, and for a linear approximation we can express

$$\gamma(r) = \gamma(r_0) + \gamma'(r_0)(r-r_0)$$

Let

$$\epsilon = \theta - \theta_0, \quad |\epsilon| \ll 1$$

$$\delta = r - r_0, \quad |\delta| \ll 1$$

we have

$$I_1(r_0, \theta_0) = \lim_{X \to 0} \left\{ -\frac{r_0}{4\pi} \int_{-\delta_0}^{\delta_0} \int_{-\epsilon_0}^{\epsilon_0} \frac{[\gamma(r_0) + \gamma'(r_0)\delta]}{[X^2 + \delta^2 + a^2 \epsilon^2]^{3/2}}\, d\epsilon\, d\delta \right\}$$

where

$$a^2 = r_0^2 + (p/\pi)^2$$

The integration of the second term with respect to δ is zero, which justifies the omission of the second term in the calculation for the mid-zone, and the integration of the first term also vanishes for $\theta_l - \epsilon_0 \geq \theta_0 \geq \theta_t + \epsilon_0$. Therefore, we only have to consider the cases of $\theta_0 > \theta_l - \epsilon_0$ and $\theta_0 < \theta_t + \epsilon_0$, i.e., the end points. Integrating the first integral with respect to ϵ and assuming $\theta_l \leq \theta_0 \leq \theta_l - \epsilon_0$, we obtain

$$I_1(r_0, \theta_0) = \lim_{X \to 0} \left\{ -\frac{r_0 \gamma(r_0)}{4\pi} \int_{-\delta_0}^{\delta_0} \frac{1}{a^2 (X^2 + \delta^2 + a^2 \epsilon^2)^{1/2}} \Bigg|_{\theta_l - 2\epsilon_0 - \theta_0}^{\theta_l - \theta_0} d\delta \right\}$$

$$= \lim_{X \to 0} \left\{ - \frac{r_0 \gamma(r_0)}{4\pi a^2} \left[\int_{-\delta_0}^{\delta_0} \frac{d\delta}{[X^2 + \delta^2 + a^2 (\theta_l - \theta_0)^2]^{1/2}} \right. \right.$$

$$\left. \left. - \int_{-\delta_0}^{\delta_0} \frac{d\delta}{[X^2 + \delta^2 + a^2 (\theta_l - \theta_0 - 2\epsilon_0)^2]^{1/2}} \right] \right\}$$

$I_1 (r_0, \theta_0) = 0$ when $\theta_0 = \theta_l - \epsilon_0$.

Integrating and taking the limit, we finally obtain

$$I_1 (r_0, \theta_0) = - \frac{r_0 \gamma(r_0)}{4a^2\pi} \left\{ \ln \left[\delta_0 + \sqrt{\delta_0^2 + a^2 (\theta_l - \theta_0)^2} \right] \right.$$

$$- \ln \left[-\delta_0 + \sqrt{\delta_0^2 + a^2 (\theta_l - \theta_0)^2} \right]$$

$$- \ln \left[\delta_0 + \sqrt{\delta_0^2 + a^2 (\theta_l - \theta_0 - 2\epsilon_0)^2} \right]$$

$$\left. + \ln \left[-\delta_0 + \sqrt{\delta_0^2 + a^2 (\theta_l - \theta_0 - 2\epsilon_0)^2} \right] \right\}$$

or

$$I_1 (r_0, \theta_0) = \frac{r_0 \gamma(r_0)}{4a^2\pi} \ln \left[-\delta_0 + \sqrt{\delta_0^2 + a^2 (\theta_l - \theta_0)^2} \right]$$

since the second term is certainly the most important term as $\theta_0 \to \theta_l$. As expected, the induced velocity components have logarithmic singularity at the leading edge.

Equation [16b]

$V_{bt} (r_0, \theta_0) = I_2 (r_0, \theta_0)$

$$= \lim_{X \to 0} \left\{ \frac{1}{4\pi^2} \int_{r_0 - \delta_0}^{r_0 + \delta_0} \int_{\theta_0 - \epsilon_0}^{\theta_0 + \epsilon_0} \frac{\gamma(r)(\theta - \theta_0)[p \cos(\theta - \theta_0) + p'(r_0 - r \cos(\theta - \theta_0))]}{[X^2 + r_0^2 + r^2 - 2r_0 r \cos(\theta - \theta_0) + (p/\pi)^2 (\theta - \theta_0)^2]^{3/2}} d\theta\, dr \right\}$$

Following the same procedure and neglecting the p' term, we obtain

$$I_2(r_0 \theta_0) = - \frac{p \gamma(r_0)}{4a^2 \pi^2} \ln \left[- \delta_0 + \sqrt{\delta_0^2 + a^2 (\theta_l - \theta_0)^2} \right]$$

Equation [16c]

$$V_{fa}(r_0, \theta_0) = I_3(r_0, \theta_0)$$

$$= \lim_{X \to 0} \left\{ -\frac{1}{4\pi} \int_{r_0-\delta_0}^{r_0+\delta_0} \int_{\theta_0-\epsilon_0}^{\theta_0+\epsilon_0} \frac{\Gamma_\theta(r, \theta)\, r\, [r - r_0 \cos(\theta - \theta_0)]}{[X^2 + r_0^2 + r^2 - 2r_0 r \cos(\theta - \theta_0) + (p/\pi)^2 (\theta - \theta_0)^2]^{3/2}}\, d\theta\, dr \right\}$$

Let

$$\Gamma_\theta(r, \theta) = \Gamma_\theta(r_0, \theta) + \Gamma_\theta'(r_0, \theta)(r - r_0)$$

we have

$$I_3(r_0, \theta_0) = \lim_{X \to 0} \left\{ -\frac{r_0}{4\pi} \int_{-\epsilon_0}^{\epsilon_0} \int_{-\delta_0}^{\delta_0} \frac{\Gamma_\theta(r_0, \epsilon) + \Gamma_\theta'(r_0, \epsilon)\delta}{(X^2 + \delta^2 + a^2 \epsilon^2)^{3/2}}\, \delta\, d\delta\, d\epsilon \right\}$$

$$= \lim_{X \to 0} \left\{ -\frac{r_0}{4\pi} \int_{-\epsilon_0}^{\epsilon_0} \int_{-\delta_0}^{\delta_0} \frac{\Gamma_\theta(r_0, \epsilon) + C(r_0)\,\delta - \gamma'(r_0)\epsilon\delta}{(X^2 + \delta^2 + a^2 \epsilon^2)^{3/2}}\, \delta\, d\delta\, d\epsilon \right\}$$

since $\Gamma_\theta'(r_0, \epsilon)$ can be expressed as the sum of $C(r_0)$ and $-\gamma'(r_0)\epsilon$ where $C(r_0)$ represents quantities evaluated at r_0, a constant.

The integration of the first term with respect to δ and that of the third term with respect to ϵ vanish, and the only remaining term is the second term. Therefore

$$I_3(r_0, \theta_0) = \lim_{X \to 0} \left\{ -\frac{r_0 C(r_0)}{4\pi} \int_{-\epsilon_0}^{\epsilon_0} \int_{-\delta_0}^{\delta_0} \frac{\delta^2}{(X^2 + \delta^2 + a^2 \epsilon^2)^{3/2}}\, d\delta\, d\epsilon \right\}$$

$$= \lim_{X \to 0} \left\{ -\frac{r_0 C(r_0)}{4\pi} \int_{-\epsilon_0}^{\epsilon_0} \left[\frac{-2\delta_0}{(X^2 + \delta_0^2 + a^2 \epsilon^2)^{1/2}} + \ln\left(\delta_0 + \sqrt{X^2 + \delta_0^2 + a^2 \epsilon^2}\right) \right.\right.$$

$$\left.\left. - \ln\left(-\delta_0 + \sqrt{X^2 + \delta_0^2 + a^2 \epsilon^2}\right) \right] d\epsilon \right\}$$

Here again we observe that the most important term is the last term. Carrying out the integration, taking the limit, and using the approximation of

$$-\delta_0 + (\delta_0^2 + a^2 \epsilon^2)^{1/2} \to \delta_0 \frac{a^2}{2}\left(\frac{\epsilon}{\delta_0}\right)^2$$

we finaliy have

$$I_3(r_0, \theta_0) = \frac{r_0 C(r_0)}{4\pi}\left[\epsilon \ln \frac{a^2}{2\delta_0} + 2\epsilon (\ln \epsilon - 1)\right]_{-\epsilon_0}^{\epsilon_0}$$

which vanishes as $\epsilon_0 \to 0$.

Equation [16d]

$$V_{ft}(r_0, \theta_0) = I_4(r_0, \theta_0)$$

$$= \lim_{X \to 0}\left\{\frac{1}{4\pi^2}\int_{r_0-\delta_0}^{r_0+\delta_0}\int_{\theta_0-\epsilon_0}^{\theta_0+\epsilon_0} \frac{p\Gamma_\theta(r_0, \theta)\,[r_0 - r\cos(\theta-\theta_0) - r(\theta-\theta_0)\sin(\theta-\theta_0)]}{[X^2 + r_0^2 + r^2 - 2r_0 r\cos(\theta-\theta_0) + (p/\pi)^2(\theta-\theta_0)^2]^{3/2}}\right\} d\theta\, dr$$

$$= \lim_{X \to 0}\left\{\frac{1}{4\pi^2}\int_{-\epsilon_0}^{\epsilon_0}\int_{-\delta_0}^{\delta_0} \frac{-p\Gamma_\theta(r_0, \epsilon)\,\delta}{[X^2 + \delta^2 + a^2\epsilon^2]^{3/2}}\, d\delta\, d\epsilon\right\}$$

which vanishes by following the same produced as for I_3.

This shows that the only contribution is from I_1 and I_2.

CONTRIBUTION TO MEAN LINE

The contribution to the mean line due to the small area in the close neighborhood of the singular point when $\theta_l \geq \theta_0 \geq \theta_l - \epsilon_0$ is

$$\Delta C_m(r_0, \epsilon_0) = \frac{D\, r_0}{2V\cos\beta_i}\int_{\theta_l-\epsilon_0}^{\theta_l} v_n(r_c, \theta_0)\, d\theta_0$$

where v_n is the induced downwash, which can be expressed as

$$v_n(r_0, \theta_0) = I_1(r_0, \theta_0) \cos \beta_i(r_0) - I_2(r_0, \theta_0) \sin \beta_i(r_0)$$

Substituting the results of I_1 and I_2 and making the following approximation

$$-\delta_0 + \sqrt{\delta_0^2 + a^2 (\theta_l - \theta_0)^2} \rightarrow \delta_0 \frac{a^2}{2} \left(\frac{\theta_l - \theta_0}{\delta_0} \right)^2$$

we get

$$v_n(r_0, \theta_0) = f(r_0) \ln \left[\frac{\delta_0 a^2}{2} \left(\frac{\theta_l - \theta_0}{\delta_0} \right)^2 \right]$$

where

$$f(r_0) = \frac{\gamma(r_0)}{4 a^2 \pi} \left[r_0 \cos \beta_i(r_0) + (p(r_0)/\pi)^2 \sin \beta_i(r_0) \right]$$

Performing the integration, we obtain

$$\Delta C_m(r_0, \epsilon_0) = \frac{D r_0}{2 V \cos \beta_i} f(r_0) \epsilon_0 \left[\ln \frac{\delta_0 a^2}{2} + 2 \left(\ln \frac{\epsilon_0}{\delta_0} - 1 \right) \right]$$

Since $\epsilon_0 << 1$, this contribution to the mean line is indeed negligible. An estimate for a case where $\epsilon_0 = 0.001$ and $\delta_0 = 0.005$ shows that the contribution of this small area as compared to that of the remaining area is in the order of tenths of 1 percent. These values of ϵ_0 and δ_0 are actually used in the computing program.

APPENDIX B

PREPARATION OF INPUT DATA

The input data consists mainly of two parts: (1) program controls and (2) propeller data. The following discussion is outlined in the order of the input data format; see Figure 16.

Card 1	Format 9I8
NL	Number of radial stations in the common network of field points (maximum number of radial stations in the tip or hub zones) Specify NL = 18
Card 2	Format 8F9.5
DY	δ_0, half-width of mid-zone Specify DY = 0.005
DFD	Minimum chordwise spacing, $(\Delta\phi)_{min}$ in the common network of field points in degrees Specify DFD = 0.1*
FDFD	Maximum chordwise spacing, $(\Delta\phi)_{max}$ in the common network of field points in degrees Specify FDFD = 2.0*
DFFD	Maximum range of ϕ in the common network of field points in degrees Specify DFFD = 150.0*
Card 3	(more than one card) Format 9F8.5
SPR	Spacings of radial stations in the common network of field points. Total number of entries should equal NL. The following set of numbers may be specified: 0.005, 0.010, 0.016, 0.024, 0.035, 0.050, 0.070, 0.096, 0.129, 0.170, 0.220, 0.280, 0.352, 0.440, 0.552, 0.709, 0.945, 1.000

If Cards 1, 2, and 3 as specified are used, no entry for these cards is necessary.

Card 4	Format 12A6
	Propeller identification not more than 72 digits. (This is the first line in the print out.)
Card 5	Format 9I8
NN	Number of blades
NKN	Number of chordwise coordinates θ_0 at which induced velocities are calculated.

*Total number of chordwise stations on either side of control point should not exceed 90.

NCL — Number of chordwise coordinates x/L_T at which camber distribution is calculated.

NCTR — Program control.
When calculation for a given set of input data is completed, if:
NCTR = 1, the computer reads another completed set of input data (cards 4 through 9) and proceeds to compute.
NCTR = −1, the computer reads another set of data for NN, NCTR, NPT, KSP, VM, DY, SM, SW and proceeds to compute.
NCTR = 0, program terminates.

KRN — Number of radial coordinates r_0 at which induced velocities and camber distribution are calculated.

NPT — Specify NPT = 0. Program control for print out. (See Appendix C.)

KSP — Specify KSP = 0. Program control for print out. (See Appendix C.)

Card 6 — Format 9F8.5

DK — Used to calculate chordwise coordinates at which induced velocities are calculated. The j^{th} chordwise coordinate θ_0^j is calculated by using the formula:
$\theta_0^j = \theta_l(r_0) - \mathrm{DK}(j)\,\theta_T(r_0)$.
Total number of entries should equal NKN.

Card 7 — Format 9F8.5

XL — Chordwise coordinates at which camber distribution is calculated.
Total number of entries should equal NCL.

Card 8 — (9 cards) Format 9F8.5
Propeller data:

1st card – Radii r at which input data is given in the following four cards.

2nd card – Dimensionless leading edge coordinate from reference line at r, L_l/D.

3rd card – Dimensionless chord length at r, L_T/D.

4th card – Tangent of hydrodynamic pitch angle at r, $\tan\beta_i$, taken from the lifting line calculation output.*

5th card – Dimensionless bound circulation distribution $\Gamma(r)$ based on ship speed taken from the lifting-line calculation output.*

6th card – Radii r_0 at which induced velocities and camber distribution are calculated. Total number of entries should equal KRN.

7th card – Advance velocity at r_0, V_x.

8th card – Axial induced velocity u_a at r_0 taken from the lifting-line calculation output.*

9th card – Tangential induced velocity u_t at r_0 taken from the lifting-line calculation output.*

*AML Problem No. 106, "Moderately Loaded Propellers Using Induction Factors."

Card 9 Format 9F8.5

VM Scale factor for chord length used for calculating the camber for different expanded area ratios with respect to a reference EAR.
Specify VM = 1.0 if the input data L_T/D (third card of Card 8) give the required EAR. For other values of EAR it is only necessary to change the value of VM, e.g., VM = 1.25 represents an EAR which is 25 percent larger.

AJ Coefficient of advance, based on ship velocity.

DIA Propeller diameter.

SM Specify SM = 1.0.
If only the camber due to bound circulation is to appear in the print out, specify SM = 0.

SW Specify SW = 1.0.
If only the camber due to free circulation is to appear in the print out, specify SW = 0.

Note 1. The program is written so that more than one problem can be handled at one time. The computer performs complete sets of calculations, one for each problem, successively. The problem could be

a. for entirely different propellers, in which case one set of the input data Cards 4 through 9 for each propeller will be required,
b. for a propeller the same as the one specified in the immediate preceding set except that the expanded area ratio (EAR) is different,
c. for the same propeller as specified in the immediate preceding set except calculation is to be performed with different NN, NPT, KSP or SM, or
d. for a combination of b and c.

For either b, c, or d, a set of two input cards will be required. They specify the quantities involved in the following order:

Card i NN, NCTR, NPT, KSP (Format 4I8)

Card ii VM, DY, SM, SW (Format 4F8.5).

In each case, appropriate values of NCTR should be specified. The sets of input cards are to be arranged consecutively in an appropriate order.

Note 2. The computing time depends mainly on the number of blades, the shape of blade outline, and the fineness of network of field points, i.e., the number of stations. For a conventional propeller as the one shown in Figure 16, the computing time required is tabulated for various values for Z, NL, $(\Delta\phi)_{min}$, $(\Delta\phi)_{max}$, and maximum range of ϕ:

Z	NL	$(\Delta\phi)_{min}$	$(\Delta\phi)_{max}$	Range of ϕ	Time
1	20	0.10°	2.0°	150°	9.4 min
1	11	0.10°	2.0°	150°	6.0 min
1	11	0.10°	3.0°	220°	5.5 min
5	20	0.10°	2.0°	150°	11.4 min

APPLIED MATHEMATICS LABORATOR PROBLEM XPLU
PROPELLER DESIGN BASED ON LIFTING SURFACE THEORY
UNIFORM CHORDWISE LOAD DISTRIBUTION

PROPELLER 3916A XPLU Card 4 (see Appendix B for explanation)

INPUT DATA

Data	Card	Quantity
18	Card 1	
0.00500 0.10000 2.00000150.00000	Card 2	
0.00500 0.01000 0.01600 0.02400 0.03500 0.05000 0.07000 0.09600 0.12900	Card 3	
0.17000 0.22000 0.28000 0.35200 0.44000 0.55200 0.70900 0.94500 1.00000		
5 8 9 0 9 6 3		
0.00993 0.05083 0.11862 0.20414 0.29586 0.38138 0.44917 0.49007	Card 5	
0.00993 0.01250 0.02500 0.05000 0.10000 0.20000 0.30000 0.40000 0.50000	Card 6	
0.20000 0.30000 0.40000 0.50000 0.60000 0.70000 0.80000 0.90000 1.00000	Card 7	
0.15400 0.18600 0.21550 0.23100 0.23200 0.21750 0.18500 0.13400 0.02000	Card 8	r
0.30800 0.37200 0.43000 0.46200 0.46400 0.43500 0.37000 0.26800 0.04000		$L_l(r)/D$
1.64210 1.22835 0.90766 0.70429 0.56622 0.46392 0.38698 0.32722 0.27960		$L_t(r)/D$
		$\tan \beta_i(r)$
0. 0.01730 0.02266 0.02428 0.02283 0.01936 0.01463 0.00898-0.		$\Gamma(r)$
0.25000 0.30000 0.40000 0.50000 0.60000 0.70000 0.80000 0.90000 0.95000		r_o
1.00000 1.00000 1.00000 1.00000 1.00000 1.00000 1.00000 1.00000 1.00000		$V_x(r_o)$
0.14500 0.16902 0.20861 0.22173 0.20765 0.17661 0.13584 0.08937 0.06500		$u_a(r_o)$
0.16010 0.16678 0.16039 0.13704 0.10517 0.07483 0.04889 0.02767 0.01770		$u_t(r_o)$
1.00000 0.82600 8.00000 1.00000 1.00000	Card 9	

OUTPUT

AXIAL INDUCED VELOCITY COMPONENT

RX/RO	0.2500	0.3000	0.4000	0.5000	0.6000	0.7000	0.8000	0.9000	0.9500
X/LT									
0.0099	0.0590	0.1047	0.1314	0.1541	0.1522	0.1460	0.1385	0.1259	0.1146
0.0508	0.0421	0.0765	0.0903	0.1091	0.1084	0.0995	0.0954	0.0887	0.0919
0.1186	0.0305	0.0568	0.0662	0.0759	0.0774	0.0662	0.0651	0.0665	0.0724
0.2041	0.0214	0.0403	0.0448	0.0540	0.0524	0.0488	0.0466	0.0481	0.0570
0.2959	0.0141	0.0264	0.0285	0.0343	0.0337	0.0313	0.0303	0.0324	0.0372
0.3814	0.0083	0.0149	0.0154	0.0191	0.0188	0.0175	0.0172	0.0186	0.0245
0.4492	0.0043	0.0064	0.0061	0.0082	0.0079	0.0074	0.0074	0.0079	0.0109
0.4901	0.0019	0.0013	0.0006	0.0018	0.0016	0.0015	0.0015	0.0013	0.0026

TANGENTIAL INDUCED VELOCITY COMPONENT

RX/RO	0.2500	0.3000	0.4000	0.5000	0.6000	0.7000	0.8000	0.9000	0.9500
X/LT									
0.0099	-0.1699	-0.1953	-0.1730	-0.1480	-0.1142	-0.0849	-0.0620	-0.0450	-0.0360
0.0508	-0.1404	-0.1578	-0.1353	-0.1147	-0.0877	-0.0623	-0.0447	-0.0333	-0.0290
0.1186	-0.1150	-0.1277	-0.1073	-0.0889	-0.0671	-0.0454	-0.0323	-0.0253	-0.0230
0.2041	-0.0885	-0.0974	-0.0805	-0.0664	-0.0486	-0.0336	-0.0232	-0.0184	-0.0180
0.2959	-0.0614	-0.0671	-0.0547	-0.0447	-0.0323	-0.0220	-0.0153	-0.0124	-0.0119
0.3814	-0.0363	-0.0391	-0.0315	-0.0257	-0.0184	-0.0125	-0.0087	-0.0071	-0.0078
0.4492	-0.0163	-0.0168	-0.0132	-0.0111	-0.0078	-0.0053	-0.0038	-0.0030	-0.0035
0.4901	-0.0043	-0.0034	-0.0022	-0.0024	-0.0015	-0.0010	-0.0008	-0.0005	-0.0009

INDUCED DOWNWASH DUE TO ALL BLADES

RX/RO	0.2500	0.3000	0.4000	0.5000	0.6000	0.7000	0.8000	0.9000	0.9500
X/LT									
0.0099	0.1740	0.2175	0.2136	0.2112	0.1887	0.1682	0.1516	0.1339	0.1201
0.0508	0.1400	0.1707	0.1578	0.1553	0.1376	0.1164	0.1051	0.0947	0.0964
0.1186	0.1125	0.1348	0.1212	0.1132	0.1004	0.0791	0.0724	0.0710	0.0759
0.2041	0.0854	0.1010	0.0873	0.0824	0.0696	0.0584	0.0519	0.0514	0.0598
0.2959	0.0588	0.0687	0.0579	0.0538	0.0453	0.0376	0.0337	0.0347	0.0391
0.3814	0.0348	0.0397	0.0325	0.0304	0.0254	0.0211	0.0192	0.0199	0.0257
0.4492	0.0159	[illegible]	0.0134	0.0131	0.0107	0.0090	0.0082	0.0084	0.0115
0.4901	0.0046	[illegible]	0.0020	0.0029	0.0021	0.0018	0.0017	0.0014	0.0027

RX/RO	0.2500	0.3000	0.4000	0.5000	0.6000	0.7000	0.8000	0.9000	0.9500
P/D	1.1560	1.1577	1.1406	1.1063	1.0673	1.0202	0.9726	0.9252	0.8976
L.E.	1.3533	1.4880	1.7240	1.8480	1.8560	1.7400	1.4800	1.0720	0.7452
CHORD	2.7213	2.9760	3.4400	3.6960	3.7120	3.4800	2.9600	2.1440	1.4943

CAMBER DISTRIBUTION

X/LT									
0.0099	0.0035	0.0044	0.0042	0.0038	0.0029	0.0022	0.0015	0.0008	0.0005
0.0125	0.0044	0.0055	0.0052	0.0047	0.0037	0.0027	0.0018	0.0011	0.0006
0.0250	0.0084	0.0105	0.0099	0.0089	0.0069	0.0050	0.0034	0.0020	0.0012
0.0500	0.0157	0.0194	0.0180	0.0162	0.0125	0.0090	0.0061	0.0035	0.0022
0.1000	0.0283	0.0346	0.0314	0.0280	0.0216	0.0151	0.0103	0.0061	0.0039
0.2000	0.0483	0.0585	0.0519	0.0455	0.0348	0.0238	0.0163	0.0099	0.0067
0.3000	0.0624	0.0751	0.0656	0.0572	0.0433	0.0297	0.0202	0.0125	0.0087
0.4000	0.0709	0.0849	0.0735	0.0639	0.0482	0.0330	0.0225	0.0140	0.0099
0.5000	0.0740	0.0882	0.0760	0.0661	0.0497	0.0341	0.0232	0.0145	0.0104

CAMBER RATIO

X/LT									
0.0099	0.0013	0.0015	0.0012	0.0010	0.0008	0.0006	0.0005	0.0004	0.0003
0.0125	0.0016	0.0018	0.0015	0.0013	0.0010	0.0008	0.0006	0.0005	0.0004
0.0250	0.0031	0.0035	0.0029	0.0024	0.0019	0.0014	0.0012	0.0009	0.0008
0.0500	0.0058	0.0065	0.0052	0.0044	0.0034	0.0026	0.0021	0.0016	0.0015
0.1000	0.0104	0.0116	0.0091	0.0076	0.0058	0.0043	0.0035	0.0020	0.0026
0.2000	0.0177	0.0197	0.0151	0.0123	0.0094	0.0068	0.0055	0.0046	0.0045
0.3000	0.0229	0.0252	0.0191	0.0155	0.0117	0.0085	0.0068	0.0058	0.0058
0.4000	0.0261	0.0285	0.0214	0.0173	0.0130	0.0095	0.0076	0.0065	0.0066
0.5000	0.0272	0.0296	0.0221	0.0179	0.0134	0.0098	0.0078	0.0068	0.0069

Figure 16 – Sample Computer Output (for Propeller 3916A)

APPENDIX C

SAMPLES OF OUTPUT

The program prints out the following information in tabular form; see Figure 16.

Axial induced velocity component.
Tangential induced velocity component.
Induced downwash.
Camber distribution (in unit same as propeller diameter).
Camber ratio.

In addition, the program has a feature of printing out certain intermediate information when desired; see Figure 17. It will print out the chordwise integrated values of the axial and tangential induced velocity components in the following general order:

At $r_0 = r_0^1$

Tip-zone

$r = r_1$

chordwise integrated values of v_a at various θ_0
chordwise integrated values of v_t at various θ_0

$r = r_2$

(same print out as for $r = r_1$)

. . . .

etc.

Hub-zone

$r = r_1$

(same print out as in the tip-zone)
etc.
Integrated values of v_a in mid-zone at various θ_0
Integrated values of v_t in mid-zone at various θ_0

At $r = r_0^2$

(same print out for $r_0 = r_0^1$)

etc.

Also printed out are the values of integrands in the equations expressing the induced velocity components (Equation [16]) for any specified control point $P(r_0^i, \theta_0^j)$ in the following order:

At $r = r_0^i$ and $\theta_0 = \theta_0^j$

Tip- and Hub-Zones

At $r = r_1$

Chordwise stations ϕ, PHI

Axial components due to superimposed lifting line (to be exact, the second term of Equation [16c]) corresponding to ϕ, UHH

Tangential components due to superimposed lifting line (the second term of Equation [16d]) corresponding to ϕ, VHH

Axial components due to free system (the first term of Equation [16c]) corresponding to ϕ – leading edge portion (from P to leading edge), UHL

Axial component due to free system – trailing edge portion (from P to trailing edge), UHT

Tangential component due to free system (the first term of Equation [16d]) corresponding to ϕ – leading edge portion, VHL

Tangential component due to free system – trailing edge portion, VHT

Axial component due to bound system (Equation [16a]) corresponding to ϕ – leading edge portion, UBL

Axial component due to bound system – trailing edge portion, UBT

Tangential component due to bound system (Equation [16b]) corresponding to ϕ & leading edge portion, VBL

Tangential component due to bound system – trailing edge portion, VBT

Value of r_1

Chordwise integrated values of v_a at various θ_0

Chordwise integrated values of v_t at various θ_0

At $r = r_2$

(similar print out as for $r = r_1$)

Mid-Zone

(similar print out for the axial and tangential components as in the tip- and hub-zones.)

Integrated values of v_a at various θ_0

Integrated values of v_t at various θ_0

Figure 16 shows the output for a typical problem.

Figure 17 shows the partial output of the same problem as in Figure 16, except intermediate information for point P at $r_0 = r_0^6 = 0.7$ and $\theta_0 = \theta_0^3$, i.e., NPT = 6, KSP = 3, is also printed.

```
CHORDWISE INTEGRATED VALUES OF VA AND VT AT RO=.2500
TIP-ZONE
R=.2450
-0.92330E 02 -0.88920E 02 -0.76231E 02 -0.59221E 02 -0.40714E 02 -0.23373E 02 -0.96042E 01 -0.12934E 01
 0.12463E 03  0.12039E 03  0.10310E 03  0.79949E 02  0.54884E 02  0.31479E 02  0.12926E 02  0.17336E 01
R=.2600
-0.43474E 02 -0.42415E 02 -0.36732E 02 -0.28635E 02 -0.19690E 02 -0.11264E 02 -0.45621E 01 -0.51539E 00
 0.53491E 02  0.52674E 02  0.45597E 02  0.35442E 02  0.24303E 02  0.13577E 02  0.56111E 01  0.62383E 00
R=.2650
-0.27650E 02 -0.26974E 02 -0.23570E 02 -0.18440E 02 -0.12681E 02 -0.72284E 01 -0.28839E 01 -0.25932E-00
 0.3[illegible]E 02  0.30613E 02  0.26603E 02  0.20897E 02  0.14317E 02  0.81378E 01  0.32361E 01  0.27870E-00
R=.2710
-0.18773E 02 -0.18244E 02 -0.16081E 02 -0.12634E 02 -0.86913E 01 -0.49327E 01 -0.19321E 01 -0.11851E-00
 0.18613E 02  0.18477E 02  0.16404E 02  0.12848E 02  0.87964E 01  0.49722E 01  0.19356E 01  0.10324E-00
R=.2790
-0.12769E 02 -0.12348E 02 -0.10976E 02 -0.86697E 01 -0.59673E 01 -0.3[illegible]687E 01 -0.12885E 01 -0.30404E-01
 0.10670E 02  0.10628E 02  0.96099E 01  0.75864E 01  0.51929E 01  0.29138E 01  0.11008E 01  0.64386E-02
R=.2900
-0.86030E 01 -0.82547E 01 -0.73858E 01 -0.58724E 01 -0.40470E 01 -0.22715E 01 -0.84486E 00  0.18607E-01
 0.55540E 01  0.55438E 01  0.51422E 01  0.41175E 01  0.28226E 01  0.15689E 01  0.56807E 00 -0.36890E-01
R=.3050
-0.57757E 01 -0.55001E 01 -0.49364E 01 -0.39543E 01 -0.27333E 01 -0.15289E 01 -0.55646E 00  0.32799E-01
 0.[illegible]4654E 01  0.24804E 01  0.23945E 01  0.19710E 01  0.13599E 01  0.74806E 00  0.25614E-00 -0.41402E-01
R=.3[illegible]250
-0.3[illegible]345E 01 -0.37260E 01 -0.33443E 01 -0.27002E 01 -0.18794E 01 -0.10567E 01 -0.38838E-00  0.17191E-01
 0.[illegible]78565E 00  0.81850E 00  0.86667E 00  0.76249E 00  0.53796E 00  0.29408E-00  0.94912E-01 -0.26149E-01
R=.3510
-0.27583E 01 -0.26069E 01 -0.23398E 01 -0.19063E 01 -0.13445E 01 -0.77153E 00 -0.30233E-00 -0.16820E-01
-0.21427E-01  0.19507E-01  0.10946E-00  0.14947E-00  0.12002E-00  0.67050E-01  0.20969E-01 -0.70912E-02
R=.3840
-0.19466E 01 -0.18439E 01 -0.16612E 01 -0.13699E 01 -0.98560E 00 -0.58511E 00 -0.25316E-00 -0.50310E-01
-0.36189E-00 -0.32050E-00 -0.22770E-00 -0.13562E-00 -0.77593E-01 -0.40323E-01 -0.13105E-01  0.30270E-02
R=.4250
-0.12396E 01 -0.11825E 0[illegible] -0.10776E 01 -0.90568E 00 -0.66841E 00 -0.41163E-00 -0.19434E-00 -0.60573E-01
-0.48537E-00 -0.44828E-00 -0.36607E-00 -0.26283E-00 -0.17013E-00 -0.93214E-01 -0.33322E-01  0.29725E-02
R=.4750
-0.48479E-00 -0.47437E-00 -0.45143E-00 -0.39982E-00 -0.30965E-00 -0.19871E-00 -0.99283E-01 -0.36932E-01
-0.50934E 00 -0.47852E-00 -0.41042E-00 -0.31307E-00 -0.21085E-00 -0.11915E-00 -0.45986E-01 -0.33592E-02
R=.5350
 0.26920E-00  0.24622E-00  0.18772E-00  0.12158E-00  0.67230E-01  0.32020E-01  0.11463E-01  0.62007E-03
-0.47020E-00 -0.44832E-00 -0.39421E-00 -0.31059E-00 -0.21381E-00 -0.12291E-00 -0.51212E-01 -0.80420E-02
R=.6070
 0.87715E 00  0.80378E 00  0.69260E 00  0.53207E 00  0.36193E-00  0.20795E-00  0.88375E-01  0.17508E-01
-0.38850E-00 -0.36828E-00 -0.32879E-00 -0.26298E-00 -0.18292E-00 -0.10551E-00 -0.44063E-01 -0.73862E-02
R=.6950
 0.12581E 01  0.11588E 01  0.97708E 00  0.78258E 00  0.53912E 00  0.30983E-00  0.12771E-00  0.17830E-01
-0.27872E-00 -0.26327E-00 -0.23118E-00 -0.18790E-00 -0.13159E-00 -0.76142E-01 -0.31659E-01 -0.46009E-02
R=.8070
 0.14985E 01  0.13791E 01  0.11787E 01  0.91945E 00  0.64975E 00  0.37749E-00  0.15960E-00  0.28209E-01
-0.16825E-00 -0.15780E-00 -0.13844E-00 -0.11082E-00 -0.79373E-01 -0.46670E-01 -0.19740E-01 -0.33492E-02
R=.9640
 0.22769E 01  0.21293E 01  0.18186E 01  0.14191E 01  0.97915E 00  0.56103E 00  0.24208E-00  0.40819E-01
-0.96521E-01 -0.90102E-01 -0.78728E-01 -0.63117E-01 -0.44669E-01 -0.26020E-01 -0.11284E-01 -0.19084E-02
R=.9999
 0.35523E 01  0.32648E 01  0.27879E 01  0.21730E 01  0.15050E 01  0.88792E 00  0.38283E-00  0.57501E-01
-0.12182E-00 -0.11358E-00 -0.99279E-01 -0.79526E-01 -0.56407E-01 -0.33789E-01 -0.14664E-01 -0.22053E-02
HUB-ZONE
R=.2450
 0.11191E 03  0.96770E 02  0.81272E 02  0.62740E 02  0.43119E 02  0.24910E 02  0.10499E 02  0.18078E 01
-0.17782E 03 -0.15463E 03 -0.13021E 03 -0.10075E 03 -0.69354E 02 -0.40103E 02 -0.16910E 02 -0.29149E 01
R=.2400
 0.58851E 02  0.50487E 02  0.42074E 02  0.32396E 02  0.22261E 02  0.12893E 02  0.54902E 01  0.10278E 01
-0.10081E 03 -0.87487E 02 -0.73373E 02 -0.56769E 02 -0.39141E 02 -0.22712E 02 -0.96795E 01 -0.18136E 01
R=.2350
 0.39929E 02  0.35000E 02  0.29040E 02  0.22317E 02  0.15331E 02  0.88974E 01  0.38204E 01  0.76114E 00
-0.74085E 02 -0.65768E 02 -0.55128E 02 -0.42684E 02 -0.29478E 02 -0.17157E 02 -0.73750E 01 -0.14697E 01
R=.2290
 0.28988E 02  0.26033E 02  0.21597E 02  0.16574E 02  0.11383E 02  0.66166E 01  0.28607E 01  0.59852E 00
-0.59481E 02 -0.53998E 02 -0.45422E 02 -0.35231E 02 -0.24377E 02 -0.14228E 02 -0.61607E 01 -0.12885E 01
R=.2210
 0.21292E 02  0.19671E 02  0.16440E 02  0.12618E 02  0.86615E 01  0.50365E 01  0.21841E 01  0.46701E-00
-0.50405E 02 -0.46791E 02 -0.39726E 02 -0.30921E 02 -0.21443E 02 -0.12540E 02 -0.54499E 01 -0.11645E 01
R=.2100
 0.15763E 02  0.14654E 02  0.12640E 02  0.97364E 01  0.66762E 01  0.38680E 01  0.16602E 01  0.33166E-00
-0.45977E 02 -0.43212E 02 -0.37220E 02 -0.29140E 02 -0.20247E 02 -0.11823E 02 -0.50903E 01 -0.10169E 01
R=.2001
 0.12794E 02  0.12185E 02  0.10558E 02  0.81820E 01  0.56004E 01  0.32168E 01  0.13416E 01  0.21329E-00
-0.48627E 02 -0.43075E 02 -0.37490E 02 -0.29495E 02 -0.20487E 02 -0.11878E 02 -0.49729E 01 -0.79124E 00
INTEGRATED VA,VT IN MID-ZONE
 0.43029E-02 -0.78018E-03 -0.12828E-02 -0.11450E-02 -0.82964E-03 -0.48787E-03 -0.20401E-03 -0.30532E-04
-0.82402E-02 -0.59352E-03  0.41177E-03  0.54312E-03  0.43664E-03  0.26657E-03  0.11250E-03  0.16235E-04
```

(Similar print out for Ro = 0.3, 0.4, ..., 0.95)

Figure 17 – Sample Computer Output with Intermediate Information

```
CHORDWISE INTEGRATED VALUES OF VA AND VT AT RO=.7000
TIP-ZONE
THETASUBO  3
INTERMEDIATE INFORMATION OF PHI.UHH.VHH.UHL.UHT.VHL.VHT.UBL.UBT.VBL.VBT AT R 1
 0.          0.17454E-02  0.52361E-02  0.10472E-01  0.17454E-01  0.26180E-01  0.36652E-01  0.48870E-01  0.62833E-01
 0.78541E-01  0.95994E-01  0.11519E-00  0.13762E-00  0.15883E-00  0.18326E-00  0.20944E-00  0.23737E-00  0.26704E-00
 0.29846E-00  0.33162E-00  0.36652E-00  0.40143E-00  0.43634E-00  0.47125E-00  0.50615E 00  0.54106E 00  0.57597E 00
 0.61087E 00  0.64578E 00  0.68069E 00  0.71559E 00  0.75050E 00  0.78541E 00  0.82032E 00  0.85522E 00  0.89013E 00
 0.92504E 00  0.95994E 00  0.98762E 00
 0.74907E 04  0.67493E 04  0.35233E 04  0.10951E 04  0.32120E 03  0.10872E 03  0.43490E 02  0.20254E 02  0.10782E 02
 0.64313E 01  0.42682E 01  0.30716E 01  0.26057E 01  0.19244E 01  0.16315E 01  0.14283E 01  0.12818E 01  0.11725E 01
 0.10888E 01  0.10233E 01  0.97094E 00  0.93025E 00  0.89774E 00  0.87109E 00  0.84867E 00  0.82926E 00  0.81188E 00
 0.79571E 00  0.78005E 00  0.76424E 00  0.74769E 00  0.72989E 00  0.71039E 00  0.68892E 00  0.66536E 00  0.63985E 00
 0.61277E 00  0.58460E 00  0.56255E 00
-0.34444E 04 -0.31009E 04 -0.16186E 04 -0.50275E 03 -0.14714E 03 -0.49492E 02 -0.19515E 02 -0.88341E 01 -0.44786E 01
-0.24857E 01 -0.14796E 01 -0.92665E 00 -0.71041E 00 -0.59141E-00 -0.25161E-00 -0.15202E-00 -0.77208E-01 -0.18118E-01
 0.30867E-01  0.73399E-01  0.11197E-00  0.14671E-00  0.17919E-00  0.21044E-00  0.24110E-00  0.27156E-00  0.30200E-00
 0.33240E-00  0.36255E-00  0.39202E-00  0.42015E-00  0.44605E-00  0.46861E-00  0.48651E-00  0.49838E-00  0.50289E 00
 0.49897E-00  0.48605E-00  0.46942E-00
-0.37433E 04 -0.33701E 04 -0.17592E 04 -0.54675E 03 -0.16036E 03 -0.54273E 02 -0.21709E 02 -0.10109E 02 -0.53808E 01
-0.32190E 01 -0.21294E 01 -0.15322E 01 -0.12996E 01
-0.37433E 04 -0.33702E 04 -0.17594E 04 -0.54685E 03 -0.16041E 03 -0.54298E 02 -0.21723E 02 -0.10118E 02 -0.53869E 01
-0.32236E 01 -0.21330E 01 -0.15353E 01 -0.13026E 01 -0.96225E 00 -0.81598E 00 -0.71453E 00 -0.64138E 00 -0.58687E 00
-0.54514E 00 -0.51247E 00 -0.48641E-00 -0.46617E-00 -0.45002E-00 -0.43680E-00 -0.42569E-00 -0.41608E-00 -0.40749E-00
-0.39950E-00 -0.39176E-00 -0.38194E-00 -0.37574E-00 -0.36691E-00 -0.35722E-00 -0.34653E-00 -0.33478E-00 -0.32205E-00
-0.30852E-00 -0.29452E-00 -0.28339E-00
 0.17199E 04  0.15484E 04  0.80815E 03  0.25101E 03  0.73457E 02  0.24707E 02  0.97410E 01  0.44092E 01  0.22350E 01
 0.12403E 01  0.73819E 00  0.46222E-00  0.35432E-00
 0.17199E 04  0.15484E 04  0.80822E 03  0.25102E 03  0.73480E 02  0.24719E 02  0.97475E 01  0.44130E 01  0.22375E 01
 0.12420E 01  0.73946E 00  0.46318E-00  0.35513E-00  0.19572E-00  0.12584E-00  0.76048E-01  0.38634E-01  0.90685E-02
-0.15454E-01 -0.36759E-01 -0.56095E-01 -0.73518E-01 -0.89824E-01 -0.10552E-00 -0.12093E-00 -0.13626E-00 -0.15158E-00
-0.16689E-00 -0.18208E-00 -0.19694E-00 -0.21114E-00 -0.22423E-00 -0.23564E-00 -0.24472E-00 -0.25076E-00 -0.25311E-00
-0.25122E-00 -0.24479E-00 -0.23647E-00
 0.37451E-05 -0.94873E 03 -0.14831E 04 -0.91637E 03 -0.44145E 03 -0.21771E 03 -0.11592E 03 -0.66498E 02 -0.40620E 02
-0.26122E 02 -0.17519E 02 -0.12163E 02 -0.98989E 01
-0.37451E-05  0.94873E 03  0.14831E 04  0.91637E 03  0.44145E 03  0.21771E 03  0.11592E 03  0.66498E 02  0.40620E 02
 0.26122E 02  0.17519E 02  0.12163E 02  0.98989E 01  0.63559E 01  0.47404E 01  0.35913E 01  0.27541E 01  0.21304E 01
 0.16560E 01  0.12878E 01  0.99629E 00  0.77067E 00  0.59095E 00  0.44331E-00  0.31921E-00  0.21270E-00  0.11973E-00
 0.37578E-01 -0.35539E-01 -0.10062E-00 -0.15807E-00 -0.20779E-00 -0.24926E-00 -0.28171E-00 -0.30421E-00 -0.31592E-00
-0.31637E-00 -0.30535E-00 -0.28906E-00
 0.          0.44014E 03  0.68805E 03  0.42510E 03  0.20477E 03  0.10097E 03  0.53748E 02  0.30823E 02  0.18820E 02
 0.12097E 02  0.81099E 01  0.56293E 01  0.45817E 01
-0.          -0.44014E 03 -0.68805E 03 -0.42510E 03 -0.20477E 03 -0.10097E 03 -0.53748E 02 -0.30823E 02 -0.18820E 02
-0.12097E 02 -0.81099E 01 -0.56293E 01 -0.43817E 01 -0.29454E 01 -0.22021E 01 -0.16761E 01 -0.12957E 01 -0.10157E 01
-0.80637E 00 -0.64822E 00 -0.52796E 00 -0.44030E-00 -0.37600E-00 -0.32926E-00 -0.29636E-00 -0.27492E-00 -0.26339E-00
-0.26083E-00 -0.26665E-00 -0.28047E-00 -0.30200E-00 -0.33087E-00 -0.36652E-00 -0.40805E-00 -0.45409E-00 -0.50276E 00
-0.55163E 00 -0.59790E 00 -0.63078E 00
R=.7050
 0.29173E 02  0.34360E 01  0.12850E 01  0.61892E 00  0.29588E-00  0.98491E-01 -0.31545E-01 -0.10533E-00
-0.13466E 02 -0.15538E 01 -0.54315E 00 -0.22687E-00 -0.84029E-01 -0.10912E-01  0.29587E-01  0.30868E-01
THETASUBO = 3
INTERMEDIATE INFORMATION OF PHI.UHH.VHH.UHL.UHT.VHL.VHT.UBL.UBT.VBL.VBT AT R 2
 0.          0.34907E-02  0.87268E-02  0.15708E-01  0.24435E-01  0.34907E-01  0.47125E-01  0.61087E-01  0.76796E-01
 0.94249E-01  0.11345E-00  0.12144E-00  0.15708E-00  0.18152E-00  0.20770E-00  0.23562E-00  0.26529E-00  0.29671E-00
 0.32987E-00  0.36478E-00  0.39969E-00  0.43459E-00  0.46950E-00  0.50441E 00  0.53931E 00  0.57422E 00  0.60913E 00
 0.64404E 00  0.67894E 00  0.71385E 00  0.74876E 00  0.78366E 00  0.81857E 00  0.85348E 00  0.88838E 00  0.92329E 00
 0.95820E 00  0.98147E 00
 0.19153E 04  0.17231E 04  0.10909E 04  0.49377E 03  0.19924E 03  0.83594E 02  0 38475E 02  0.19611E 02  0.11028E 02
 0.67913E 01  0.45405E 01  0.39576E 01  0.24954E 01  0.20092E 01  0.16870E 01  0.14640E 01  0.13061E 01  0.11893E 01
 0.11011E 01  0.10330E 01  0.99166E 00  0.94177E 00  0.90993E 00  0.88384E 00  0.86187E 00  0.84275E 00  0.82548E 00
 0.80922E 00  0.79321E 00  0.77679E 00  0.75936E 00  0.74042E 00  0.71959E 00  0.69669E 00  0.67174E 00  0.64507E 00
 0.61725E 00  0.59846E 00
-0.87132E 03 -0.78383E 03 -0.49610E 03 -0.22429E 03 -0.90231E 02 -0.37588E 02 -0.17046E 02 -0.84555E 01 -0.45447E 01
-0.26125E 01 -0.15839E 01 -0.13170E 01 -0.64398E 00 -0.41707E-00 -0.26386E-00 -0.15497E-00 -0.73590E-01 -0.96606E-02
 0.43115E-01  0.88849E-01  0.12847E-00  0.16441E-00  0.19816E-00  0.23069E-00  0.26258E-00  0.29413E-00  0.32544E-00
 0.35634E-00  0.38648E-00  0.41523E-00  0.44174E-00  0.46489E-00  0.48341E-00  0.49589E-00  0.50099E 00  0.49760E-00
 0.48507E-00  0.47162E-00
-0.95283E 03 -0.85715E 03 -0.54263E 03 -0.24557E 03 -0.99073E 02 -0.41560E 02 -0.19125E 02 -0.97457E 01 -0.54789E 01
-0.33731E 01 -0.22543E 01 -0.19646E 01
-0.95283E 03 -0.85725E 03 -0.54279E 03 -0.24570E 03 -0.99158E 02 -0.41611E 02 -0.19156E 02 -0.97665E 01 -0.54936E 01
-0.33842E 01 -0.22632E 01 -0.19730E 01 -0.12448E 01 -0.10027E 01 -0.84231E 00 -0.73172E 00 -0.65277E 00 -0.59472E 00
-0.55092E 00 -0.51717E 00 -0.49176E-00 -0.47207E-00 -0.45638E-00 -0.44357E-00 -0.43280E-00 -0.42345E-00 -0.41603E-00
-0.40710E-00 -0.39929E-00 -0.39126E-00 -0.38271E-00 -0.37338E-00 -0.36310E-00 -0.35175E-00 -0.33936E-00 -0.32606E-00
-0.31221E-00 -0.30282E-00
 0.43306E 03  0.38991E 03  0.24676E 03  0.11155E 03  0.44868E 02  0.18688E 02  0.84730E 01  0.42019E 01  0.22579E 01
 0.12975E 01  0.78641E 00  0.65379E 00
 0.43346E 03  0.38996E 03  0.24683E 03  0.11161E 03  0.44906E 02  0.18710E 02  0.84870E 01  0.42109E 01  0.22639E 01
 0.13018E 01  0.78953E 00  0.65657E 00  0.32124E-00  0.20814E-00  0.13174E-00  0.77409E-01  0.36779E-01  0.48308E-02
-0.21572E-01 -0.44482E-01 -0.64359E-01 -0.82411E-01 -0.99390E-01 -0.11577E-00 -0.13186E-00 -0.14779E-00 -0.16362E-00
-0.17927E-00 -0.19455E-00 -0.20914E-00 -0.22263E-00 -0.23444E-00 -0.24392E-00 -0.25037E-00 -0.25310E-00 -0.25154E-00
-0.24535E-00 -0.23864E-00
 0.37022E-05 -0.23696E 03 -0.37414E 03 -0.30281E 03 -0.18747E 03 -0.10959E 03 -0.65356E 02 -0.40579E 02 -0.26269E 02
-0.17660E 02 -0.12265E 02 -0.10717E 02
-0.37022E-05  0.23696E 03  0.37414E 03  0.30281E 03  0.18747E 03  0.10959E 03  0.65356E 02  0.40579E 02  0.26269E 02
 0.17660E 02  0.12265E 02  0.10717E 02  0.64013E 01  0.47700E 01  0.36108E 01  0.27670E 01  0.21392E 01  0.16622E 01
 0.12925E 01  0.10001E 01  0.77429E 00  0.59422E 00  0.44658E-00  0.32255E-00  0.21616E-00  0.12330E-00  0.41211E-01
-0.31902E-01 -0.97081E-01 -0.15475E-00 -0.20484E-00 -0.24684E-00 -0.27998E-00 -0.30330E-00 -0.31594E-00 -0.31728E-00
-0.30724E-00 -0.29451E-00
 0.          0.10993E 03  0.17357E 03  0.14047E 03  0.86949E 02  0.50817E 02  0.30296E 02  0.18803E 02  0.12166E 02
 0.81756E 01  0.56770E 01  0.49604E 01
-0.          -0.10993E 03 -0.17357E 03 -0.14047E 03 -0.86949E 02 -0.50817E 02 -0.30296E 02 -0.18803E 02 -0.12166E 02
-0.81756E 01 -0.56770E 01 -0.49604E 01 -0.29663E 01 -0.22155E 01 -0.16846E 01 -0.13010E 01 -0.10169E 01 -0.80823E 00
-0.64916E 00 -0.52826E 00 -0.44014E-00 -0.37548E-00 -0.32842E-00 -0.29522E-00 -0.27347E-00 -0.26162E-00 -0.25871E-00
-0.26417E-00 -0.27762E-00 -0.29881E-00 -0.32738E-00 -0.36283E-00 -0.40430E-00 -0.45048E-00 -0.49952E-00 -0.54904E 00
-0.59624E 00 -0.62493E 00
R=.7100
 0.21869E 02  0.41084E 01  0.14477E 01  0.71692E 00  0.37526E-00  0.16912E-00  0.33854E-01 -0.42853E-01
-0.10027E 02 -0.18523E 01 -0.60918E 00 -0.26517E-00 -0.11612E-00 -0.41025E-01  0.38338E-03  0.22122E-01
```

(Similar print out for R = 0.715, 0.721, ..., 0.9999)

Figure 17 (Continued)

```
SUB-ICASE
THETASUBO  3
INTERMEDIATE INFORMATION OF PHI.UPH.VPH.UHL.UHT.VHL.VHT.UBL.UBT.VBL.VBT AT R15
 0.             0.17454E-02   0.52361E-02   0.10472E-01   0.17454E-01   0.26180E-01   0.36652E-01   0.48870E-01   0.62833E-01
 0.78541E-01    0.95994E-01   0.11519E-00   0.13614E-00   0.15979E-00   0.18326E-00   0.20944E-00   0.23737E-00   0.26704E-00
 0.29846E-00    0.33162E-00   0.36652E-00   0.40143F-00   0.43634E-00   0.47125E-00   0.50615E 00   0.54106E 00   0.57597E 00
 0.61087E 00    0.64578E 00   0.68069E 00   0.71559E 00   0.75050E 00   0.78541E 00   0.82032E 00   0.85522E 00   0.89013E 00
 0.92504E 00    0.95994E 00   0.99485E 00   0.99973E 00
-0.71780E 04   -0.64636E 04  -0.33798E 04  -0.10474E 04  -0.29756E 03  -0.94919E 02  -0.34052E 02  -0.13171E 02  -0.51449E 01
-0.17798E 01   -0.27934E-00   0.41438E-00   0.73744E 00   0.77066E 00   0.93952E 00   0.95256E 00   0.94385E 00   0.92494E 00
 0.90186E 00    0.87779E 00   0.85430E 00   0.83312E 00   0.81413E 00   0.79698E 00   0.78127E 00   0.76656E 00   0.75238E 00
 0.73827E 00    0.72378E 00   0.70843E 00   0.69180E 00   0.67351E 00   0.65327E 00   0.63092E 00   0.60650E 00   0.58029E 00
 0.55282E 00    0.52466E 00   0.49737E-00   0.49362E-00
 0.33626E 04    0.30280E 04   0.15835E 04   0.48875E 03   0.13987E 03   0.44951E 02   0.16439E 02   0.66557E 01   0.28953E 01
 0.13190E 01    0.61706E 00   0.29362E-00   0.14470E-00   0.12962E-00   0.57704E-01   0.57088E-01   0.67961E-01   0.85090E-01
 0.10583E-00    0.12892E-00   0.15383E-00   0.17916E-00   0.20494E-00   0.23127E-00   0.25821E-00   0.28580F-00   0.31396E-00
 0.34251E-00    0.37111E-00   0.39926E-00   0.42623E-00   0.45110E-00   0.47275E-00   0.48987E-00   0.50110E 00   0.50517E 00
 0.50107E 00    0.48826E-00   0.46685E-00   0.46321E-00
 0.36111E 04    0.32518E 04   0.17004E 04   0.52446E 03   0.14972E 03   0.47762E 02   0.17136E 02   0.66288E 01   0.25897E 01
 0.89595E 00    0.14064E-00  -0.20867E-00  -0.37142E-00  -0.38816E-00
 0.36111E 04    0.32517E 04   0.17002E 04   0.52437E 03   0.14967E 03   0.47741E 02   0.17126E 02   0.66233E 01   0.25869E 01
 0.89477E 00    0.14042E-00  -0.20827E-00  -0.37057E-00  -0.38725E-00  -0.47193E-00  -0.47837E-00  -0.47389E-00  -0.46427E-00
-0.45257E-00   -0.44036E-00   -0.42846E-00  -0.41771E-00  -0.40807E-00  -0.39936E-00  -0.39137E-00  -0.38389E-00  -0.37668E-00
-0.36950E-00   -0.36214E-00   -0.35436E-00  -0.34594E-00  -0.33669E-00  -0.32648E-00  -0.31521E-00  -0.30292E-00  -0.28975E-00
-0.27595E-00   -0.26192E-00   -0.24812E-00  -0.23624E-00
-0.16916E 04   -0.15233E 04   -0.79668E 03   -0.24590E 03   -0.70376E 02   -0.22619E 02   -0.82724E 01   -0.33497E 01   -0.14574E 01
-0.66402E 00   -0.31065E-00   -0.14766E-00   -0.72678E-01   -0.65265E-01
-0.16916E 04   -0.15233E 04   -0.79661E 03   -0.24586E 03   -0.70355E 02   -0.22609E 02   -0.82674E 01   -0.33470E 01   -0.14558E 01
-0.66314E 00   -0.31015E-00   -0.14757E-00   -0.72712E-01   -0.65132E-01   -0.28985E-01   -0.28669E-01   -0.34121E-01   -0.42711E-01
-0.53110E-01   -0.64678E-01   -0.77149E-01   -0.89827E-01   -0.10272E-00   -0.11589E-00   -0.12935E-00   -0.14313E-00   -0.15716E-00
-0.17143E-00   -0.18569E-00   -0.19971E-00   -0.21314E-00   -0.22551E-00   -0.23626E-00   -0.24474E-00   -0.25028E-00   -0.25224E-00
-0.25012E-00   -0.24365E-00   -0.23290E-00   -0.23107C-00
 0.38287E-05   -0.95016E 03   -0.14931E 04   -0.92667E 03   -0.44753E 03   -0.22091E 03   -0.11767E 03   -0.67519E 02   -0.41247E 02
-0.26526E 02   -0.17791E 02   -0.12352E 02   -0.88239E 01   -0.83638E 01
-0.38287E-05    0.95016E 03    0.14931E 04    0.92667E 03    0.44753E 03    0.22091E 03    0.11767E 03    0.67519E 02    0.41247E 02
 0.26526E 02    0.17791E 02    0.12352E 02    0.88239E 01    0.83638E 01    0.48136E 01    0.36466E 01    0.27963E 01    0.21627E 01
 0.16808E 01    0.13064E 01    0.10107C 01    0.78177E 00    0.59905E 00    0.44916L-00    0.32322E-00    0.21521E-00    0.12105E-00
 0.37952E-01   -0.35846E-01   -0.10136E-00   -0.15899E-00   -0.20864E-00   -0.24981C-00   -0.28173E-00   -0.30354E-00   -0.31446C-00
-0.31406E-00   -0.30242E-00   -0.28037E-00   -0.27654E-00
 0.             0.44080E 03    0.69268E 03    0.42988E 03    0.20759E 03    0.10246E 03    0.54562E 02    0.31296E 02    0.19111E 02
 0.12285E 02    0.82358E 01    0.57166E 01    0.40850E 01    0.38725E 01
-0.            -0.44080E 03   -0.69268E 03   -0.42988E 03   -0.20759E 03   -0.10246F 03   -0.54562E 02   -0.31296E 02   -0.19111E 02
-0.12285E 02   -0.82358E 01   -0.57166E 01   -0.40850E 01   -0.38725F 01   -0.22364E 01   -0.17022E 01   -0.13159E 01   -0.10315E 01
-0.81891E 00   -0.65830E 00   -0.53619E 00   -0.44718E-00   -0.38189E-00   -0.33443E-00   -0.30102E-00   -0.27922E-00   -0.26746E-00
-0.26475E-00   -0.27047E-00   -0.28421E-00   -0.30562E-00   -0.33430E-00   -0.36961E-00   -0.41061E-00   -0.45587E-00   -0.50347E 00
-0.55100E 00   -0.59570E 00   -0.63470E 00   -0.63955E 00
R=.6930
 0.75944E 01    0.27298E 01    0.13224E 01    0.77237E 00    0.48859E-00    0.31300E-00    0.19714E-00    0.13113E-00
-0.35871Z 01   -0.12513F 01   -0.57860E 00   -0.31229E-00   -0.18301E-00   -0.11581E-00   -0.78770E-01   -0.59363E-01
THETASUBO  3
INTERMEDIATE INFORMATION OF PHI.UPH.VPH.UHL.UHT.VHL.VHT.UBL.UBT.VBL.VBT AT R16
 0.             0.34907E-02   0.87266E-02   0.15708E-01   0.24435E-01   0.34907E-01   0.47125E-01   0.61087E-01   0.76796E-01
 0.94249E-01    0.11345E-00   0.13439E-00   0.14579E-00   0.18152E-00   0.20770E-00   0.23562E-00   0.26529E-00   0.29671E-00
 0.32987E-00    0.36478E-00   0.39969E-00   0.43459E-00   0.46950E-00   0.50441E 00   0.53931E 00   0.57422E 00   0.60913E 00
 0.64404E 00    0.67894E 00   0.71385E 00   0.74876E 00   0.78366E 00   0.81857E 00   0.85348F 00   0.88838E 00   0.92329E 00
 0.95820E 00    0.99311E 00   0.10057E 01
-0.17538E 04   -0.15796E 04   -0.10026E 04   -0.45169E 03   -0.17825E 03   -0.71252E 02   -0.30096E 02   -0.13337E 02   -0.60167E 01
-0.26082E 01   -0.93665E 00   -0.84473E-01    0.17869E-00    0.59551E 00    0.71752E 00    0.77782E 00    0.80383E 00    0.81071E 00
 0.80703E 00    0.79766E 00    0.78599E 00    0.77355E 00    0.76101E 00    0.74856E 00    0.73614E 00    0.72355E 00    0.71049E 00
 0.69664E 00    0.68162E 00    0.66509E 00    0.64673E 00    0.62630E 00    0.60373E 00    0.57910F 00    0.55274E 00    0.52525E 00
 0.49741E-00    0.47022E-00    0.46077E-00
 0.82988E 03    0.74749E 03    0.47462E 03    0.21411E 03    0.84799E 02    0.34192E 02    0.14725E 02    0.67969E 01    0.33335E 01
 0.17213E 01    0.93149E 00    0.53022E 00    0.40701E-00    0.21526E-00    0.16262E-00    0.14050E-00    0.13609E-00    0.14240E-00
 0.15557E-00    0.17352E-00    0.19405E-00    0.21639E-00    0.24018E-00    0.26519E-00    0.29127E-00    0.31822E-00    0.34578E-00
 0.37356E-00    0.40103E-00    0.42746E-00    0.45190E-00    0.47323E-00    0.49016E-00    0.50136E 00    0.50557E 00    0.50178E 00
 0.48945E-00    0.46868E-00    0.45925E-00
 0.88568E 03    0.79775E 03    0.50638E 03    0.22817E 03    0.90057E 02    0.36005E 02    0.15211E 02    0.67426E 01    0.30426E 01
 0.13193E 01    0.47395E-00    0.42759E-01   -0.90470E-01
 0.88568E 03    0.79765E 03    0.50623E 03    0.22805E 03    0.89981E 02    0.35961E 02    0.15186E 02    0.67283E 01    0.30344E 01
 0.13150E 01    0.47208E-00    0.42560E-01   -0.90012E-01   -0.29978E-00   -0.36104E-00   -0.39119E-00   -0.40406E-00   -0.40730E-00
-0.40522E-00   -0.40027E-00   -0.39417E-00   -0.38769E-00   -0.38118F-00   -0.37471E-00   -0.36827E-00   -0.36174E-00   -0.35500E-00
-0.34786E-00   -0.34016E-00   -0.33170E-00   -0.32234E-00   -0.31197E-00   -0.30054F-00   -0.28810E-00   -0.27482E-00   -0.26099E-00
-0.24701E-00   -0.23336E-00   -0.22862E-00
-0.41910E 03   -0.37751E 03   -0.23973E 03   -0.10816E 03   -0.42842E 02   -0.17278E 02   -0.74423E 01   -0.34361E 01   -0.16857E 01
-0.87068E 00   -0.47134E-00   -0.26839E-00   -0.20608E-00
-0.41910E 03   -0.37747E 03   -0.23965E 03   -0.10810E 03   -0.42806E 02   -0.17257E 02   -0.74301E 01   -0.34288E 01   -0.16812E 01
-0.86783E 00   -0.46948E-00   -0.26714E-00   -0.20503E-00   -0.10836E-00   -0.81829E-01   -0.70664E-01   -0.68411E-01   -0.71542E-01
-0.78115E-01   -0.87070E-01   -0.97313E-01   -0.10845E-00   -0.12030E-00   -0.13275E-00   -0.14571F-00   -0.15909E-00   -0.17277E-00
-0.18654E-00   -0.20013E-00   -0.21319E-00   -0.22524E-00   -0.23572E-00   -0.24401E-00   -0.24943E-00   -0.25137E-00   -0.24933E-00
-0.24305E-00   -0.23259E-00   -0.22786E-00
 0.38725E-05   -0.23764E 03   -0.37799E 03   -0.30855E 03   -0.19209E 03   -0.11263E 03   -0.67269E 02   -0.41800E 02   -0.27072E 02
-0.18204E 02   -0.12645E 02   -0.90301E 01   -0.76714E 01
-0.38725E-05    0.23764F 03    0.37799E 03    0.30855E 03    0.19209E 03    0.11263E 03    0.67269E 02    0.41800E 02    0.27072E 02
 0.18204E 02    0.12645E 02    0.90301E 01    0.76714E 01    0.49179E 01    0.37224E 01    0.28521E 01    0.22045E 01    0.17124E 01
 0.13310E 01    0.10293E 01    0.79636E 00    0.61063E 00    0.45845E-00    0.33072E-00    0.22131E-00    0.12602E-00    0.42038E-01
-0.32467E-01   -0.98536E-01   -0.15860E-00   -0.20656E-00   -0.24797E-00   -0.28007E-00   -0.30203E-00   -0.31311E-00   -0.31288C-00
-0.30146E-00   -0.27968E-00   -0.26957E-00
 0.             0.11025E 03    0.17535E 03    0.14313E 03    0.89093E 02    0.52225E 02    0.31183E 02    0.19369E 02    0.12539E 02
 0.84279E 01    0.58532E 01    0.41808E 01    0.35531E 01
-0.            -0.11025E 03   -0.17535E 03   -0.14313E 03   -0.89093E 02   -0.52225E 02   -0.31183E 02   -0.19369E 02   -0.12539E 02
-0.84279E 01   -0.58532E 01   -0.41808E 01   -0.35531E 01   -0.22847E 01   -0.17372E 01   -0.13417E 01   -0.10508E 01   -0.83353E 00
-0.66950E 00   -0.54484E 00   -0.45399E-00   -0.38733E-00   -0.33881E-00   -0.30457E-00   -0.28209E-00   -0.26976E-00   -0.26655E-00
-0.27181E-00   -0.28510E-00   -0.30606E-00   -0.33425E-00   -0.36905E-00   -0.40948E-00   -0.45412E-00   -0.50107F 00   -0.54795E 00
-0.59202E 00   -0.63048E 00   -0.64246E 00
R=.6900
 0.50337E 01    0.23473E 01    0.11840E 01    0.68056E 00    0.41196E-00    0.24396E-00    0.13277E-00    0.69373E-01
-0.23239E 01   -0.10780E 01   -0.52308E 00   -0.27679E-00   -0.15231E-00   -0.86512E-01   -0.50042E-01   -0.30903E-01
```

(Similar print out for R = 0.685, 0.680, ..., 0.2001)

Figure 17 (Continued)

```
TASUBO  3
ERMEDIATE INFORMATION OF PHI,UPH,VHH,UHL,UHT,VHL,VHT,UBL,UBT,VBL,VBT IN MID ZONE
17454E-02  0.52361E-02  0.10472E-01  0.17454E-01  0.26180E-01  0.36652E-01  0.48870E-01  0.62833E-01  0.78541E-01
95994E-01  0.11519E-00  0.13374E-00  0.15883E-00  0.18326E-00  0.20944E-00  0.23737E-00  0.26704E-00  0.29846E-00
33162E-00  0.36652E-00  0.40143E-00  0.43634E-00  0.47125E-00  0.50615E 00  0.54106E 00  0.57597E 00  0.61087E 00
54578E 00  0.68069E 00  0.71559E 00  0.75050E 00  0.78541E 00  0.82032E 00  0.85522E 00  0.89013E 00  0.92504E 00
95994E 00  0.99370E 00
56907E 00  0.20416E-00  0.11276E-00  0.73859E-01  0.51331E-01  0.37340E-01  0.28250E-01  0.22079E-01  0.17711E-01
14513E-01  0.12106E-01  0.10435E-01  0.87917E-02  0.76229E-02  0.66729E-02  0.58899E-02  0.52377E-02  0.46883E-02
42214E-02  0.38214E-02  0.34910E-02  0.32137E-02  0.29775E-02  0.27740E-02  0.25969E-02  0.24414E-02  0.23037E-02
21810E-02  0.20710E-02  0.19718E-02  0.18819E-02  0.18001E-02  0.17253E-02  0.16567E-02  0.15935E-02  0.15352E-02
14812E-02  0.14326E-02
68503E-02 -0.31023E-01 -0.38048E-01 -0.30575E-01 -0.22646E-01 -0.16083E-01 -0.12915E-01 -0.10148E-01 -0.81626E-02
66975E-02 -0.55895E-02 -0.48172E-02 -0.40560E-02 -0.35130E-02 -0.30706E-02 -0.27051E-02 -0.23998E-02 -0.21418E-02
19218E-02 -0.17326E-02 -0.15756E-02 -0.14432E-02 -0.13298E-02 -0.12316E-02 -0.11455E-02 -0.10695E-02 -0.10017E-02
94091E-03 -0.88593E-03 -0.83595E-03 -0.79027E-03 -0.74830E-03 -0.70958E-03 -0.67369E-03 -0.64030E-03 -0.60913E-03
57993E-03 -0.55336E-03
28521E-00 -0.10232E-00 -0.56514E-01 -0.37017E-01 -0.25726E-01 -0.18714E-01 -0.14158E-01 -0.11065E-01 -0.88762E-02
72734E-02 -0.60672E-02 -0.52296E-02
28521E-00 -0.10232E-00 -0.56515E-01 -0.37018E-01 -0.25727E-01 -0.18714E-01 -0.14159E-01 -0.11066E-01 -0.88767E-02
72739E-02 -0.60678E-02 -0.52301E-02 -0.44066E-02 -0.38208E-02 -0.33446E-02 -0.29522E-02 -0.26253E-02 -0.23500E-02
21160E-02 -0.19155E-02 -0.17499E-02 -0.16109E-02 -0.14925E-02 -0.13906E-02 -0.13018E-02 -0.12238E-02 -0.11549E-02
10934E-02 -0.10382E-02 -0.98851E-03 -0.94346E-03 -0.90246E-03 -0.86498E-03 -0.83059E-03 -0.79893E-03 -0.76970E-03
74262E-03 -0.71827E-03
34333E-02  0.15548E-01  0.19069E-01  0.15324E-01  0.11350E-01  0.84615E-02  0.64726E-02  0.50859E-02  0.40909E-02
33566E-02  0.28013E-02  0.24142E-02
34333E-02  0.15548E-01  0.19070E-01  0.15324E-01  0.11350E-01  0.84618E-02  0.64728E-02  0.50862E-02  0.40911E-02
33569E-02  0.28015E-02  0.24145E-02  0.20329E-02  0.17608E-02  0.15391E-02  0.13559E-02  0.12029E-02  0.10736E-02
96332E-03  0.86847E-03  0.78979E-03  0.72341E-03  0.66659E-03  0.61736E-03  0.57425E-03  0.53614E-03  0.50218E-03
47169E-03  0.44413E-03  0.41908E-03  0.39618E-03  0.37515E-03  0.35574E-03  0.33775E-03  0.32102E-03  0.30540E-03
29076E-03  0.27744E-03
14034E 03 -0.37680E 02 -0.12745E 02 -0.50582E 01 -0.23277E 01 -0.12047E 01 -0.68216E 00 -0.41404E-00 -0.26545E-00
17786E-00 -0.12357E-00 -0.91688E-01
14034E 03  0.37680E 02  0.12745E 02  0.50582E 01  0.23277E 01  0.12047E 01  0.68216E 00  0.41404E-00  0.26545E-00
17786E-00  0.12357E-00  0.91688E-01  0.64999E-01  0.48806E-01  0.37348E-01  0.29057E-01  0.22938E-01  0.18343E-01
14838E-01  0.12128E-01  0.10093E-01  0.85264E-02  0.72948E-02  0.63091E-02  0.55078E-02  0.48478E-02  0.42975E-02
38340E-02  0.34399E-02  0.31020E-02  0.28100E-02  0.25561E-02  0.23339F-02  0.21382E-02  0.19651E-02  0.18111E-02
16726E-02  0.15540E-02
65108E 02  0.17480E 02  0.59124E 01  0.23462E 01  0.10795E 01  0.55851E 00  0.31608E-00  0.19170E-00  0.12276E-00
82131E-01  0.56943E-01  0.42153E-01
65108E 02 -0.17480E 02 -0.59124E 01 -0.23462E 01 -0.10795E 01 -0.55851E 00 -0.31608E-00 -0.19170E-00 -0.12276E-00
82131E-01 -0.56943E-01 -0.42153E-01 -0.29771E-01 -0.22259E-01 -0.16943E-01 -0.13097E-01 -0.10258E-01 -0.81261E-02
65002E-02 -0.52426E-02 -0.42984E-02 -0.35716E-02 -0.30002E-02 -0.25428E-02 -0.21709E-02 -0.18646E-02 -0.16092E-02
13940E-02 -0.12111E-02 -0.10542E-02 -0.91859E-03 -0.80064E-03 -0.69738E-03 -0.60645E-03 -0.52597E-03 -0.45437E-03
39040E-03 -0.33479E-03
EGRATED VA,VT IN MID-ZONE
10796E-01  0.23058E-02  0.94946E-03  0.49127E-03  0.27033E-03  0.13979E-03  0.56447E-04  0.95776E-05
49694E-02 -0.10363E-02 -0.41224E-03 -0.20608E-03 -0.11042E-03 -0.56245E-04 -0.22633E-04 -0.39378E-05
```

Figure 17 (Continued)

APPENDIX D

FORTRAN LISTING OF COMPUTER PROGRAM

The FORTRAN listing of the computer program is included in the following pages. The computer also uses the subroutine MATINV and the function SIMPUN.

```
      PROPELLER DESIGN BASED ON LIFTING SURFACE THEORY WITH UNIFORM
      CHORDWISE LOAD DISTRIBUTION
      XPLU(6-22-64)
      DIMENSION DK(20),XL(20),B(9,9),CO(9),AH(10,9),CD(10,9),FAH(20,20)
     1,EAH(20,18),
     XDB(9,16),DC(9),HA(9),BP( 3,9),DE(9),BV(16),DWSH(9,20),
     X                  XX(20,20),ZZ(20,18),TIT(12),CM(20,18),CMR(20,18)
      DIMENSION XY(50),YX(50),BB(16,50),SY(90),        SAG(50),
     1AGS(50),AB(9,9),                  DWSHT(9,20),          SAGT(50),
     XAGST(50),BO(16  ),         VRE(20),  BPP(20)
      DIMENSION H(25),T(25),SPR(20),A(25,90),NF(25),AS(25,90),AC(25,90),
     XSYS(90),SYC(90),UHH(90),VHH(90),UHL(90),UHT(90),VHL(90),VHT(90),
     XUBL(90),UBT(90),VBL(90),VBT(90)
      DIMENSION WT(20),QT(20),Z(5,90),P(9),VP(90)
      DIMENSION DSA(10,35),DSAT(10,35),R(5,90),YS(90)
      READ 3,NL
      READ  7,DY,DFD,FDFD,DFFD
      READ 4,(SPR(J),J=1,NL)
      CALCULATE ANGLE FE, SINE(FE),AND COSINE(FE) TABLES
      DF=DFD/57.295
      FDF=FDFD/57.295
      DFF=DFFD/57.295
      K=1
      A(K,1)=0.
      AS(K,1)=0.
      AC(K,1)=1.
      I=2
  173 FD=FLOATF(I-1)*DF
      IF(FD-FDF)171,172,172
  172 FD=FDF
  171 A(K,I)=A(K,I-1)+FD
      SS=SINF(FD)
      CC=COSF(FD)
      AC(K,I)=CC*AC(K,I-1)-SS*AS(K,I-1)
      AS(K,I)=CC*AS(K,I-1)+SS*AC(K,I-1)
      I=I+1
      IF(A(K,I-1)-DFF)173,174,174
  174 NF(1)=I
      NFN=NF(1)
      DO 170 K=2,NL
      DO 176 J=K,NFN
      N=J-K+1
      A(K,N)=A(1,J)-A(1,K)
      AS(K,N)=AS(1,J)*AC(1,K)-AC(1,J)*AS(1,K)
      AC(K,N)=AC(1,J)*AC(1,K)+AS(1,J)*AS(1,K)
  176 CONTINUE
      NF(K)=N
  170 CONTINUE
  101 READ 2,TIT
      READ 3, NN,    NKN,NCL,NCTR,KRN,     NPT,KSP
      READ 4,(DK(J),J=1,NKN)
      READ 4,(XL(J),J=1,NCL)
      READ 4,((B(K,J),J=1,9),K=1,9)
      READ  4,VM,AJ,DIA,SM,SW
    1 FORMAT (1H012A6)
    2 FORMAT (12A6)
    3 FORMAT (9I8)
    4 FORMAT (9F8.5)
    7 FORMAT(8F9.5)
 2000 FORMAT(9E13.5)
      PRINT 2999
 2999 FORMAT (1H1,33X,44H APPLIED MATHEMATICS LABORATORY PROBLEM XPLU)
      PRINT 3000
 3000 FORMAT(30X,50H PROPELLER DESIGN BASED ON LIFTING SURFACE THEORY )
      PRINT 3002
 3002 FORMAT(36X,38H UNIFORM CHORDWISE LOAD DISTRIBUTION  )
      PRINT 1,TIT
      PRINT 3001
 3001 FORMAT(11H0INPUT DATA)
      PRINT3,NL
      PRINT 7,DY,DFD,FDFD,DFFD
      PRINT4,(SPR(J),J=1,NL)
      PRINT 3,NN,    NKN,NCL,NCTR,KRN,     NPT,KSP
      PRINT 4,(DK(J),J=1,NKN)
      PRINT 4,(XL(J),J=1,NCL)
      PRINT 4,((B(K,J),J=1,9),K=1,9)
      PRINT 4,VM,AJ,DIA,SM,SW
      DO 2800 J=1,9
 2800 B(4,J)=B(4,J)*3.1416*B(1,J)
      PRINT 2998
 2998 FORMAT(7H0OUTPUT)
C     CALCULATE COEFFICIENTS OF DATA INTERPOLATING MATRIX
 1061 DO 5J=1,9
      AB(2,J)=B(2,J)*VM
      AB(3,J)=B(3,J)*VM
      AB(5,J)=B(5,J)*6.2832
      CO(J)=3.1416*B(1,J)/SQRTF((3.1416*B(1,J))**2+B(4,J)**2)
      AH(2,J)=(1.+B(1,1)-2.*B(1,J))/(1.-B(1,1))
      CD(2,J)=SQRTF(1.-AH(2,J)**2)
      AH(1,J)=1.
    5 CD(1,J)=0.
      AH(2,1)=1.
      AH(2,9)=-1.
      CD(2,1)=0.
      CD(2,9)=0.
      DO 6 J=3,10
      L=J-1
      DO 6K=1,9
      AH(J,K)=AH(L,K)*AH(2,K)-CD(L,K)*CD(2,K)
    6 CD(J,K)=CD(L,K)*AH(2,K)+AH(L,K)*CD(2,K)
  106 DO 9J=1,9
      DO 11K=1,9
   11 FAH(J,K)=AH(K,J)
      EAH(J,1)=AB(2,J)
      EAH(J,2)=AB(3,J)
      EAH(J,3)=B(4,J)
      FT=CO(J)*2./B(1,J)
      EAH(J,4)=AB(5,J)
      EAH(J,5)=CO(J)
      EAH(J,6)=AB(2,J)*FT
      EAH(J,7)=AB(3,J)*FT
      EAH(J,8)=AB(5,J)/EAH(J,7)
    9 CONTINUE
      ERASE ZZ
      XH=B(1,1)
      CALL MATINV(FAH,9,EAH,8,V,ID)
      GOTO (1000,184),ID
```

```
  184 PRINT 1002
      GOTO 84
 1000 DO 15J=1,9
      DO 15K=1,8
   15 DB(J,K)=EAH(J,K)
      ERASE DWSH,DWSHT
      KR=1
   20 RP=B(6,KR)
      IF(NPT)200,200,2997
 2997 PRINT 2996,RP
 2996 FORMAT(48H0CHORDWISE INTEGRATED VALUES OF VA AND VT AT RO=F5.4)
      PRINT 2993
 2993 FORMAT(9H TIP-ZONE)
C     SET UP RADIAL STATIONS OF FIELD POINTS FOR POINT P
  200 J=1
      T(1)=RP+DY
  201 J=J+1
      T(J)=T(1)+SPR(J-1)
      IF(T(J)-.9999)201,202,202
  202 T(J)=.9999
      LT=J
      J=1
      H(1)=RP-DY
  203 J=J+1
      H(J)=H(1)-SPR(J-1)
      IF(H(J)-XH-.0001)204,204,203
  204 H(J)=XH+.0001
      LH=J
      LTH=LT+LH
      LTH1=1+LTH
      DO 205 J=1,LT
  205 XY(J)=T(J)
      DO 206 J=1,LH
      JJ=J+LT
  206 XY(JJ)=H(J)
      XY(LTH1)=RP
C     INTERPOLATE INPUT DATA AT RADIAL STATIONS OF FIELD POINTS
  427 ERASE BB
      DO 405 L=1,LTH1
      X=XY(L)
   21 CY=(1.+XH-2.*X)/(1.-XH)
      SZ=SQRTF(1.-CY*CY)
      HA(1)=1.
      HA(2)=CY
      DC(1)=0.
      DC(2)=SZ
      DO 17J=3,9
      I=J-1
      HA(J)=HA(I)*HA(2)-DC(I)*DC(2)
   17 DC(J)=DC(I)*HA(2)+HA(I)*DC(2)
      DO 19 J=1,9
   19 DE(J)=-FLOATF(J-1)*DC(J)
      DO 22J=1,9
      DO 22K=1,8
   22 DB(J,K+8)=DB(J,K)*DE(J)
   23 DO 25 K=1,8
      DO 25J=1,9
      BB(K+8,L)=BB(K+8,L)+DB(J,K+8)*2./((1.-XH)*DC(2))
   25 BB(K,L)=BB(K,L)+DB(J,K)*HA(J)
  405 CONTINUE
      DO 1405 K=1,3
 1405 BP(K,KR)=BB(K,LTH1)
      ERASE DSA,DSAT
C     SET UP CHORDWISE STATIONS OF FIELD POINTS
      NM=1
      N=1
 7601 L=N
  760 Y=XY(N)
      ALT=ABSF(BB(6,LTH1)-BB(6,N)+BB(7,N))
      ATL=ABSF(BB(6,N)-BB(6,LTH1)+BB(7,LTH1))
      ACT=ALT
      IF(ALT-ATL) 700,701,701
  700 ACT=ATL
  701 DO 411 J=1,16
  411 BV(J)=BB(J,N)
      ERASE Z
      M7=1
      M=1
  231 FMP=6.2832*FLOATF(M-1)/FLOATF(NN)
      FMPS=SINF(FMP)
      FMPC=COSF(FMP)
      J=1
  702 SX=AS(L,J)*FMPC+AC(L,J)*FMPS
      CX=AC(L,J)*FMPC-AS(L,J)*FMPS
      S=A(L,J)
      YRPS=ABSF(Y*Y+RP*RP-2.*Y*RP*CX+(BV(3)*S/3.1416)**2)
      VP(J)=YRPS**1.5
      Z(1,J)=Z(1,J)-SX*RP/VP(J)
      Z(5,J)=Z(5,J)+S*CX/VP(J)
      Z(2,J)=Z(2,J)+S*(RP-Y*CX)/VP(J)
      Z(3,J)=Z(3,J)+(RP-Y*(CX+S*SX))/VP(J)
      Z(4,J)=Z(4,J)+Y*(Y-RP*CX)/VP(J)
      GO TO (704,705,706),M7
  704 J=J+1
      IF(A(L,J)-ACT)702,702,710
  710 M=M+1
      IF(M-NN) 231,231,730
  730 DO 719 K=1,5
  719 P(K)=Z(K,1)
      P(6)=AS(L,1)
      P(7)=AC(L,1)
      P(8)=A(L,1)
      P(9)=VP(1)
      KS=1
  758 FP=BB(6,LTH1)-DK(KS)*BB(7,LTH1)
      YL=BB(6,N)-FP
      YT=FP+BB(7,N)-BB(6,N)
      SL=ABSF(YL)
      ST=ABSF(YT)
      SL1=SL
      SL2=ST
      IF(SL-ST) 520,520,521
  521 SL1=ST
      SL2=SL
  520 J=1
  523 DO 703 K=1,5
```

```
  703 R(K,J)=Z(K,J)
      SY(J)=A(L,J)
      J=J+1
      IF(A(L,J)-SL1) 523,523,5241
 5241 JS1=J-1
      SL1A=SL1-A(L,JS1)
      IF(SL1A-.0005)1714,524,524
 1714 SL1=SL1+.0005
  524 M7=2
      J1=J
      DO 708 K=1,5
  708 Z(K,1)=0.
      AS(L,1)=SINF(SL1)
      AC(L,1)=COSF(SL1)
      A(L,1)=SL1
      SY(J1)=SL1
      M=1
      GO TO 231
  705 M=M+1
      IF(M-NN)231,231,712
  712 DO 713 K=1,5
  713 R(K,J1)=Z(K,1)
      JK=J1
      IF(SL-S7)525,526,525
  525 J=J1+1
 5251 IF(A(L,J)-SL2)527,527,5281
 5281 JS2=J-1
      SL2A=SL2-A(L,JS2)
      IF(SL2A-.0005)1716,528,528
 1716 SL2=SL2+.0005
      GO TO 528
  527 DO 714 K=1,5
  714 R(K,J)=Z(K,J)
      SY(J)=A(L,J)
      J=J+1
      GO TO 5251
  528 M7=3
      J2=J
      DO 715 K=1,5
  715 Z(K,1)=0.
      SY(J2)=SL2
      AS(L,1)=SINF(SL2)
      AC(L,1)=COSF(SL2)
      A(L,1)=SL2
      M=1
      JK=J2
      GO TO 231
  706 M=M+1
      IF(M-NN)231,231,720
  720 DO 721 K=1,5
  721 R(K,J2)=Z(K,1)
  526 J2=JK
      DO 1721 K=1,5
 1721 Z(K,1)=P(K)
      VP(1)=P(9)
      AS(L,1)=P(6)
      AC(L,1)=P(7)
      A(L,1)=P(8)
```

```
C     CALCULATE INDUCED VELOCITY COMPONENTS IN TIP AND HUB ZONES
      ERASE UHL,VHL,UHT,VHT,UBL,VBL,UBT,VBT,UHH,VHH
      JS=1
      SLM=1.
      STM=1.
      IF(YL)722,724,723
  722 DO 7221 J=1,J1
      UHH(J)=-BV(12)*R(4,J)
 7221 VHH(J)=-BV(12)*R(3,J)*BV(3)/3.1416
      JS=J1
  724 SLM=0.
  723 TT=1.
      IF(YT)725,790,727
  725 DO 7251 J=1,J1
      UHH(J)=-BV(12)*R(4,J)
 7251 VHH(J)=-BV(12)*R(3,J)*BV(3)/3.1416
      JS=J1
      TT=-1.
  790 STM=0.
  727 CONTINUE
      KL=J2
      KT=J1
      IF(SL-ST)533,534,534
  533 KT=J2
      KL=J1
  534 CONTINUE
      DO 535  J=JS,J2
      IF(J-KT)536,536,537
  536 UHH(J)=-BV(12)*R(4,J)
      VHH(J)=-BV(12)*R(3,J)*BV(3)/3.1416
  537 S=SY(J)
      SFL=(BV(4)*BV(14)+(YL-S)*(BV(12)-BV(4)/BV(7)*BV(15)))/BV(7)
      SFT=(BV(4)*BV(14)+(YL+S)*(BV(12)-BV(4)/BV(7)*BV(15)))/BV(7)
      UH=R(4,J)
      UHL(J)=SLM*SFL*UH
      UHT(J)=STM*SFT*UH
      VH=BV(3)*R(3,J)/3.1416
      VHL(J)=SLM*SFL*VH
      VHT(J)=STM*SFT*VH
      VB=(BV(3)*R(5,J)+R(2,J)*BV(11)    )*BV(8)/(3.1416)
      VBL(J)=SLM*VB
      VBT(J)=-STM*VB
      UB=BV(8)*R(1,J)
      UBL(J)=SLM*UB
      UBT(J)=-STM*UB
  535 CONTINUE
 4103 IF(KR-NPT)711,2005,711
 2005 IF(KS-KSP)711,2004,711
 2004 PRINT 4104,KS
 4104 FORMAT(11H THETASUBO ,I2)
      PRINT 4102,N
 4102 FORMAT(77H INTERMEDIATE INFORMATION OF PHI,UHH,VHH,UHL,UHT,VHL,VHT
     X,UBL,UBT,VBL,VBT AT R,I2)
      PRINT 2000,( SY(JP),JP=1,J2)
      PRINT 2000,(UHH(JP),JP=1,KT)
      PRINT 2000,(VHH(JP),JP=1,KT)
      PRINT 2000,(UHL(JP),JP=1,KL)
      PRINT 2000,(UHT(JP),JP=1,KT)
```

```
      PRINT 2000,(VHL(JP),JP=1,KL)
      PRINT 2000,(VHT(JP),JP=1,KT)
      PRINT 2000,(UBL(JP),JP=1,KL)
      PRINT 2000,(UBT(JP),JP=1,KT)
      PRINT 2000,(VBL(JP),JP=1,KL)
      PRINT 2000,(VBT(JP),JP=1,KT)
  711 CONTINUE
C     CHORDWISE INTEGRATION AT R
      IF(SLM)7112,7111,7112
 7111 DO 7113 J=1,J2
      UHH(J)=UHH(J)+UHT(J)
 7113 VHH(J)=VHH(J)+VHT(J)
      GO TO 7115
 7112 IF(STM)7115,7114,7115
 7114 JJ=J1-1
      DO 7116 J=1,JJ
      UHL(J)=UHH(J)*TT
 7116 VHL(J)=VHH(J)*TT
 7115 DSA (KS,N)=SM*(SIMPUN(SY,UHH,KT)*STM+SIMPUN(SY,UHL,KL)
     X+SIMPUN(SY,UHT,KT)*SLM)+SW*(SIMPUN(SY,UBL,KL)+SIMPUN(SY,UBT,KT))
      DSAT(KS,N)=SM*(SIMPUN(SY,VHH,KT)*STM+SIMPUN(SY,VHL,KL)
     X+SIMPUN(SY,VHT,KT)*SLM)+SW*(SIMPUN(SY,VBL,KL)+SIMPUN(SY,VBT,KT))
      KS=KS+1
      IF(KS-NKN)758,758,7591
 7591 CONTINUE
      IF(NPT)759,759,2994
 2994 PRINT 2989,Y
 2989 FORMAT(3H R=F5.4)
      PRINT 2000,(DSA (KS,N),KS=1,NKN)
      PRINT 2000,(DSAT(KS,N),KS=1,NKN)
  759 N=N+1
      GO TO (770,771),NM
  770 IF(N-LT)7601,7601,773
  771 IF(N-LTH)772,772,761
  773 NM=2
      IF(NPT)772,772,2990
 2990 PRINT 2991
 2991 FORMAT(9H HUB-ZONE)
  772 L=N-LT
      GO TO 760
  761 CONTINUE
      DO 5392 KS=1,NKN
      DO 539 J=1,LH
      K=LT+J
      YX(J)=XY(K)
      AGS(J)=DSA(KS,K)
      AGST(J)=DSAT(KS ,K)
  539 CONTINUE
      DO 5391 J=1,LT
      SAG(J)=DSA (KS,J)
 5391 SAGT(J)=DSAT(KS,J)
      DWSH(KR,KS)=SIMPUN(XY,SAG,LT)-SIMPUN(YX,AGS,LH)
      DWSHT(KR,KS)=SIMPUN(XY,SAGT,LT)-SIMPUN(YX,AGST,LH)
      DWSH(KR,KS)=DWSH(KR,KS)/12.5664
      DWSHT(KR,KS)=DWSHT(KR,KS)/12.5664
 5392 CONTINUE
C     CALCULATE INDUCED VELOCITY COMPONENTS IN MID ZONE OF THE FIRST
C     BLADE
      ERASE Z,R,SYC,SYS,SY,YS
      ERASE UHL,VHL,UHT,VHT,UBL,VBL,UBT,VBT,UHH,VHH
      WT=0.
      QT=0.
      DO 811 K=1,16
  811 BQ(K)=UB(K,LTH1)
      KS=1
 4501 FP=BQ(6)-DK(KS)*BQ(7)
      YL=BQ(6)-FP
      YT=FP+BQ(7)-BQ(6)
      R1=RP-DY
      R2=RP+DY
      M8=1
      J=2
  731 S=A(1,J)
      SY(J)=S
      CX=AC(1,J)
      SX=AS(1,J)
      SYS(J)=SX
      SYC(J)=CX
  733 PP=(BQ(3)*S/3.1416)**2
      ZP=(RP*SX)**2+PP
      SQ1=SQRTF(ABSF(RP*RP+R1*R1-2.*RP*R1*CX+PP))
      SQ2=SQRTF(ABSF(RP*RP+R2*R2-2.*RP*R2*CX+PP))
      Z(4,J)=((R2-RP*CX)/SQ2-(R1-RP*CX)/SQ1)/ZP
      Z(1,J)= LOGF(ABSF((R2-RP*CX+SQ2)/(R1-RP*CX+SQ1)))-R2/SQ2+R1/SQ1
      Z(2,J)= (RP*(SX*SX-S*CX*SX)*(R2/SQ2-R1/SQ1)+(RP*RP*S*SX+(CX+S*SX)
     X*PP)*(1./SQ2-1./SQ1))/ZP
      Z(3,J)=BQ(3)*CX*Z(4,J)+   (RP*BQ(11)*Z(4,J)+(BQ(11)*CX*((RP*RP+PP
     X)*(1./SQ2-1./SQ1)-RP*CX*(R2/SQ2-R1/SQ1)) /ZP))
      GO TO (735,736,750),M8
  735 J=J+1
      IF(A(1,J)-BQ(7)) 731,732,732
  732 SY(J)=BQ(7)
      SL1=YL
      SL2=YT
      IF(YL-YT)741,742,742
  742 SL1=YT
      SL2=YL
  741 J=2
 1741 IF(SY(J)-SL1)744,745,745
  744 DO 743 K=1,4
  743 R(K,J)=Z(K,J)
      Z(5,J)=SY(J)
      J=J+1
      GO TO 1741
  745 J1=J
      DO 1745 K=1,4
 1745 P(K)=Z(K,J1)
      M8=2
      Z(5,J1)=SL1
      S=SL1
      CX=COSF(S)
      SX=SINF(S)
      SYS(J1)=SX
      SYC(J1)=CX
      GO TO 733
  736 DO 746 K=1,4
```

```
      R(K,J1)=Z(K,J1)
  746 Z(K,J1)=P(K)
      IF(YL-YT)1748,1750,1748
 1748 J=J1+1
 7481 IF(SY(J)-SL2)748,749,749
  748 DO 747 K=1,4
  747 R(K,J)=Z(K,J)
      Z(5,J)=SY(J)
      J=J+1
      GO TO 7481
  749 J2=J
      DO 1749 K=1,4
 1749 P(K)=Z(K,J2)
      M8=3
      Z(5,J2)=SL2
      S=SL2
      CX=COSF(S)
      SX=SINF(S)
      SYS(J2)=SX
      SYC(J2)=CX
      GO TO 733
  750 DO 751 K=1,4
      R(K,J2)=Z(K,J2)
  751 Z(K,J2)=P(K)
 1750 J2=J
      KL=J1
      KT=J2
      IF(YL-YT)752,752,753
  753 KL=J2
      KT=J1
  752 CONTINUE
      DO 1112 J=2,J2
 1112 YS(J)=Z(5,J)
      IF(YL)754,754,793
  793 DO 755 J=2,KL
      X1=R(1,J)
      X2=R(2,J)
      X3=R(3,J)
      X4=R(4,J)
      S=Z(5,J)
      SX=SYS(J)
      CX=SYC(J)
      SFL=              BQ(8)*BQ(14)+(YL-S)*(BQ(12)-BQ(8)*BQ(15))/BQ(7)
      UHL(J)= X1*SFL
      VHL(J)= X2*BQ(3)*SFL/3.1416
      VBL(J)= X3*BQ(8)*S/3.1416
  755 UBL(J)=-X4*RP*SX*BQ(8)
  754 IF(YT)765,765,756
  756 DO 757 J=2,KT
      X1=R(1,J)
      X2=R(2,J)
      X3=R(3,J)
      X4=R(4,J)
      S=Z(5,J)
      SX=SYS(J)
      CX=SYC(J)
      SFT=              BQ(8)*BQ(14)+(YL+S)*(BQ(12)-BQ(8)*BQ(15))/BQ(7)
      UHH(J)=-X1*BQ(12)
      VHH(J)=-X2*BQ(12)   *BQ(3)/3.1416
      UHT(J)= X1*SFT
      VHT(J)= X2*SFT*BQ(3) /3.1416
      VBT(J)=-X3*S*BQ(8)/3.1416
  757 UBT(J)= X4*RP*SX*BQ(8)
  765 CONTINUE
 4684 IF(KR-NPT)4682,4683,4682
 4683 IF(KS-XSP)4682,4681,4682
 4681 PRINT 4104,KS
      PRINT 25000
25000 FORMAT(69H INTERMEDIATE INFORMATION OF PHI,UHH,VHH,UHL,UHT,VHL,VHT
     X,UBL,UBT,VBL,VBT IN MID ZONE          )
      PRINT 2000,( YS(JP),JP=2,J2)
      PRINT 2000,(UHH(JP),JP=2,KT )
      PRINT 2000,(VHH(JP),JP=2,KT )
      PRINT 2000,(UHL(JP),JP=2,KL )
      PRINT 2000,(UHT(JP),JP=2,KT )
      PRINT 2000,(VHL(JP),JP=2,KL )
      PRINT 2000,(VHT(JP),JP=2,KT )
      PRINT 2000,(UBL(JP),JP=2,KL )
      PRINT 2000,(UBT(JP),JP=2,KT )
      PRINT 2000,(VBL(JP),JP=2,KL )
      PRINT 2000,(VBT(JP),JP=2,KT )
 4682 CONTINUE
      WT(KS)=(SIMPUN(YS,UHH,KT)    +SIMPUN(YS,UHL,KL)+SIMPUN(YS,UHT,KT))*
     XSM +(SIMPUN(YS,UBL,KL)+SIMPUN(YS,UBT,KT))*SW
      QT(KS) =(SIMPUN(YS,VHH,KT)    +SIMPUN(YS,VHL,KL)+SIMPUN(YS,VHT,KT))
     XSM +(SIMPUN(YS,VBL,KL)+SIMPUN(YS,VBT,KT))*SW
      WT(KS)=WT(KS)/12.5664
      QT(KS)=QT(KS)/12.5664
 4502 KS=KS+1
      IF(KS-NKN)4501,4501,450
  450 CONTINUE
      IF(NPT)467,467,4671
 4671 PRINT 4693
 4693 FORMAT(29H INTEGRATED VA,VT IN MID-ZONE)
      PRINT 2000,(WT(KS),KS=1,NKN)
      PRINT 2000,(QT(KS),KS=1,NKN)
  467 CONTINUE
      DO 5393 KS=1,NKN
      DWSH (KR,KS)= DWSH (KR,KS)+WT(KS)
      DWSHT(KR,KS)= DWSHT(KR,KS)+QT(KS)
 5393 CONTINUE
      KR=KR+1
      IF(KR-KRN)20,20,57
   57 DO 60J=1,NKN
      XX(J,1)=1.
      XX(J,2)=DK(J)
      DO 60 K=3,NKN
   60 XX(J,K)=XX(J,K-1)*XX(J,2)
      IF(SW)2017,2018,2017
 2018 PRINT 2019
 2019 FORMAT(30HODUE TO BOUND CIRCULATION ONLY)
      GO TO 12017
 2017 IF(SW) 12017,12018,12017
12018 PRINT 12019
12019 FORMAT(29HODUE TO FREE CIRCULATION ONLY     )
12017 PRINT 2020
```

```
 2020 FORMAT(33H0AXIAL INDUCED VELOCITY COMPONENT)
      PRINT 262,(B(6,J),J=1,KRN)
      PRINT 263
      DO 2021 J=1,NKN
 2021 PRINT 264,DK(J),(DWSH(K,J),K=1,KRN)
      PRINT 2022
 2022 FORMAT(38H0TANGENTIAL INDUCED VELOCITY COMPONENT)
      PRINT 262,(B(6,J),J=1,KRN)
      PRINT 263
      DO 2023 J=1,NKN
 2023 PRINT 264,DK(J),(DWSHT(K,J),K=1,KRN)
   82   JS=KRN
   83 DO 63J=1,KRN
      CCAA =3.1416*B(6,J)/SQRTF((3.1416*B(6,J))**2+B(4,J)**2)
      SBI=SQRTF(ABSF(1.-CCAA*CCAA))
      JJKRN=J+KRN
      DO 63K=1,NKN
   63 ZZ(K,J)=DWSH(J,K)*CCAA-DWSHT(J,K)*SBI
      IF(NN-1)12025,12024,12025
12024 PRINT 2024
 2024 FORMAT(41H0 INDUCED DOWNWASH DUE TO FIRST BLADE ONLY)
      GO TO 12026
12025 PRINT 2026
 2026 FORMAT(35H0 INDUCED DOWNWASH DUE TO ALL BLADES)
12026 PRINT 262,(B(6,J),J=1,KRN)
      PRINT 263
      DO 2027 J=1,NKN
 2027 PRINT 264,DK(J),(ZZ(J,K),K=1,KRN)
      CALL MATINV(XX,NKN,ZZ,JS,V,ID)
      GOTO (1001,183),ID
  183 PRINT 1002
      GOTO 84
 1001 ERASE CM
      DO 65 J=1,NKN
   65 XX(J,19)=FLOATF(J)
      DO 67J=1,JS
      DO 67K=1,NKN
   67 XX(K,J)=ZZ(K,J)/XX(K,19)
      DO 70J=1,NCL
      XX(1,20)=XL(J)
      DO 73K=2,NKN
   73 XX(K,20)=XX(K-1,20)*XL(J)
      DO 75JJ=1,JS
      DO 75KK=1,NKN
   75 CM(J,JJ)=XX(KK,JJ)*XX(KK,20)+CM(J,JJ)
   70 CONTINUE
      DO 78J=1,KRN
      BPP(J)=BP(2,J)
      VRE(J)=
     X     SQRTF((3.1416*B(6,J)/AJ-B(9,J))**2+(B(7,J)+B(8,J))**2)
   78 CONTINUE
      DO 77 J=1,JS
      DO 77K=1,NCL
      CMR(K,J)=CM(K,J)/VRE(J)
   77 CM(K,J)=CMR(K,J)*BPP(J)*DIA
      PRINT 262,(B(6,J),J=1,KRN)
  262 FORMAT( /12H      RX/RO ,9F12.4)
      PRINT 266,(BP(3,J),J=1,KRN)
  266 FORMAT(  12H       P/D   ,9F12.4)
      DO 2010 J=1,KRN
      BP(1,J)=DIA*BP(1,J)
 2010 BP(2,J)=DIA*BP(2,J)
   90 PRINT 267,(BP(1,J),J=1,KRN)
  267 FORMAT(  12H       L.E.  ,9F12.4)
      PRINT 268,(BP(2,J),J=1,KRN)
  268 FORMAT(  12H       CHORD ,9F12.4)
      PRINT 2711
 2711 FORMAT(20H0CAMBER DISTRIBUTION)
      PRINT 263
  263 FORMAT(5H X/LT)
      DO 261J=1,NCL
  261 PRINT 264,XL(J),(CMR(J,K),K=1,KRN)
      PRINT 270
  270 FORMAT(13H0CAMBER RATIO)
      PRINT 263
      DO 265 J=1,NCL
  265 PRINT 264,XL(J),(CMR(J,K),K=1,KRN)
  264 FORMAT(F8.4,F16.4,8F12.4)
 1002 FORMAT(19H MATRIX IS SINGULAR)
   84 IF(NCTR)102,100,101
  102 READ 104,NN,    NCTR,    NPT,KSP
  104 FORMAT(4I8)
      READ  4,VM,DY,SM,SW
      PRINT 108
  108 FORMAT(53H1CAMBER LINES FOR THE SAME INPUT DATA AS ABOVE EXCEPT)
      PRINT 107,NCTR,NN, VM,DY,SM,      NPT,KSP,SW
  107 FORMAT(6H0NCTR=I2,2X,3HNN=I2,2X, 3HVM=F8.5,2X,3HDY=F8.5,2X,3HSM=F8
     X.5,2X,4HNPT=I2,2X,4HKSP=I2,2X,3HSW=F8.5)
      GO TO 1061
  100 CALL END JOB
      STOP
      END
```

REFERENCES

1. Pien, P.C., "The Calculation of Marine Propellers Based on Lifting-Surface Theory," Journal of Ship Research, Vol. 5, No. 2., Sep 1961.

2. Eckhardt, M.K. and Morgan, W.B., "A Propeller Design Method," Trans. SNAME, Vol. 63, 1955.

3. Van Manen, J.D. and Bakker, A.R., "Numerical Results of Sparenberg's Lifting Surface Theory for Ship Screws," Fourth Symposium on Naval Hydrodynamics, ONR, ACR Vol. 1, 1962.

4. Kerwin, J.E. and Leopold, R., "Propeller-Incidence Correction Due to Blade Thickness," Journal of Ship Research, Vol. 7, No. 2, Oct 1961.

5. Kerwin, J.E. and Leopold, R., "User's Description, Program to Compute Propeller Pitch and Camber Corrections Due to Blade Thickness," MIT, Department of Naval Architecture and Marine Engineering, Dec 1963.

INITIAL DISTRIBUTION

Copies

10 CHBUSHIPS
- 3 Tech Lib (Code 210L)
- 1 Ship Des (Code 410)
- 1 Ship Silencing Br (Code 345)
- 1 Prelim Des (Code 420)
- 1 Hull Des (Code 440)
- 1 Sci & Res (Code 442)
- 1 Hull, Arrgts & Seamanship (Code 341B)
- 1 Prop, Shaft, & Bear (Code 644)

1 CHBUWEPS

5 CHONR
- 4 (Code 438)
- 1 (Code 466)

2 CDR, USNOL, White Oak
Attn: Lib

5 CDR, USNOTS, Pasadena
- 2 Tech Lib
- 2 Head, Thrust Producer Sec
- 1 (Code P-8063)

1 CDR, USNOTS, China Lake
Attn: Mr. D.M. Nelson

20 CDR, DDC

1 CO, USNROTC & NAVADMINU, MIT

2 DIR, ORL

1 DIR, USNRL
Attn: Code 2000

1 ONR, Boston

1 ONR, Chicago

1 ONR, Pasadena

1 ONR, New York

1 ONR, San Francisco

1 SNAME

2 ADMIN MARAD
- 1 Mr. V.L. Russo
  Office of Ship Construction
- 1 Mr. Caesar Tangerini
  Main Propulsion Sec
  Eng Specifi Br

Copies

1 NNSB & DD Co
Attn: Mr. John Kane

3 SIT, Davidson Lab, Hoboken
Attn: Dr. J.P. Breslin

2 Univ of Califomia, Berkeley
- 1 Dr. J.V. Wehausen, Dept of Eng
- 1 Prof. J.A. Schade, Dept of Eng Res

2 Univ of Notre Dame, Dept of Eng Mech, Indiana
Attn: Dr. A.G. Strandhagen

2 Univ of Michigan, Dept NAME, Ann Arbor
- 1 Dr. F.C. Michelsen
- 1 Prof. R.B. Couch

2 Univ of Minnesota, St Anthony Falls Hydraulic Lab, Minneapolis
- 1 Dr. L.G. Straub
- 1 Prof. C.S. Song

2 O in C, PGSCOL, Webb

1 DIR, Hydrodynamics Lab, CIT, Pasadena

2 MIT, Dept NAME, Cambridge, Mass

1 Bethlehem Steel, Quincy
Attn: Mr. Hollinshead De Luce

2 Gibbs & Cox

1 Reed Res, Washington
Attn: Mr. S. Reed

1 Editor, Engineering Index, Inc, New York

1 Librarian, Inst of Aero Sciences, New York

1 Editor, Applied Mechanics Review, San Antonio

1 Accurate Products Co., Hillside, N.J.
Attn: Dr. Peter Buehning

1 Cambridge Acoustic Assoc, Cambridge, Mass.
Attn: Dr. J.V. Rattaya

2 Douglas Aircraft Co., Inc., Aircraft Div, Long Beach, California
- 1 Mr. J. Hess
- 1 Mr. A.M.O. Smith

Copies

2 EB Div, Gen Dyn Corp
- 1 Mr. H.E. Sheets
- 1 Mr. R.J. McGrattan

2 GASL, Westbury, Long Island
- 1 Dr. Simon Slutsky
- 1 Mr. E. Lieberman

2 Grumman Aircraft Eng Corp
Bethpage, Long Island
- 1 Dr. S. Ciolkowski
- 1 Mr. C. Squires

3 Hydronautics, Inc, Laurel, Md
- 1 Mr. P. Eisenberg
- 1 Mr. M.P. Tulin
- 1 Mr. G.G. Cox

2 Iowa Inst of Hydraulic Res, Univ of Iowa
- 1 Dr. Hunter Rouse
- 1 Prof. L. Landweber

2 Technical Res Group, Inc, Syosset, N.Y.
- 1 Dr. J. Kotik
- 1 Dr. J. Lurye

1 Vidya, Palo Alto, California
Attn: Dr. A.H. Sacks

2 Therm, Inc, Therm Advance Res, Ithaca, N.Y.
- 1 Dr. A. Ritter
- 1 Dr. S.C. Ling

...ions of the computer program are also given.

David Taylor Model Basin. Report 1802.
HYDRODYNAMIC ASPECT OF PROPELLER DESIGN BASED ON LIFTING-SURFACE THEORY. PART I – UNIFORM CHORDWISE LOAD DISTRIBUTION, by Henry M. Cheng. Sep 1964. vii, 64p. illus., graphs, tables, refs. UNCLASSIFIED

This report presents a method of the propeller camber calculations for the case of uniform chordwise load distribution employing the lifting-surface theory. This is essentially a refinement of Pien's published work on propeller lifting-surface theory. Mathematical development pertinent to the numerical computation is reviewed. Details of the computational procedure and method are outlined, and results of sample calculations are included. A detailed instruction for preparation of input data for the computer, samples of the computer input data and output, and the FORTRAN listing of the computer program are also given.

1. Propellers--Design--Mathematical analysis
2. Propellers--Design--Hydrodynamic aspects
3. Propellers--Load distribution--Programming
4. FORTRAN (Computer program language)--Applications
I. Cheng, Henry M.

David Taylor Model Basin. Report 1802.
HYDRODYNAMIC ASPECT OF PROPELLER DESIGN BASED ON LIFTING-SURFACE THEORY. PART I – UNIFORM CHORDWISE LOAD DISTRIBUTION, by Henry M. Cheng. Sep 1964. vii, 64p. illus., graphs, tables, refs. UNCLASSIFIED

This report presents a method of the propeller camber calculations for the case of uniform chordwise load distribution employing the lifting-surface theory. This is essentially a refinement of Pien's published work on propeller lifting-surface theory. Mathematical development pertinent to the numerical computation is reviewed. Details of the computational procedure and method are outlined, and results of sample calculations are included. A detailed instruction for preparation of input data for the computer, samples of the computer input data and output, and the FORTRAN listing of the computer program are also given.

1. Propellers--Design--Mathematical analysis
2. Propellers--Design--Hydrodynamic aspects
3. Propellers--Load distribution--Programming
4. FORTRAN (Computer program language)--Applications
I. Cheng, Henry M.

David Taylor Model Basin. Report 1802.
HYDRODYNAMIC ASPECT OF PROPELLER DESIGN BASED ON LIFTING-SURFACE THEORY. PART I – UNIFORM CHORDWISE LOAD DISTRIBUTION, by Henry M. Cheng. Sep 1964. vii, 64p. illus., graphs, tables, refs. UNCLASSIFIED

This report presents a method of the propeller camber calculations for the case of uniform chordwise load distribution employing the lifting-surface theory. This is essentially a refinement of Pien's published work on propeller lifting-surface theory. Mathematical development pertinent to the numerical computation is reviewed. Details of the computational procedure and method are outlined, and results of sample calculations are included. A detailed instruction for preparation of input data for the computer, samples of the computer input data and output, and the FORTRAN listing of the computer program are also given.

1. Propellers--Design--Mathematical analysis
2. Propellers--Design--Hydrodynamic aspects
3. Propellers--Load distribution--Programming
4. FORTRAN (Computer program language)--Applications
I. Cheng, Henry M.

David Taylor Model Basin. Report 1802.
HYDRODYNAMIC ASPECT OF PROPELLER DESIGN BASED ON LIFTING-SURFACE THEORY. PART I – UNIFORM CHORDWISE LOAD DISTRIBUTION, by Henry M. Cheng. Sep 1964. vii, 64p. illus., graphs, tables, refs. UNCLASSIFIED

This report presents a method of the propeller camber calculations for the case of uniform chordwise load distribution employing the lifting-surface theory. This is essentially a refinement of Pien's published work on propeller lifting-surface theory. Mathematical development pertinent to the numerical computation is reviewed. Details of the computational procedure and method are outlined, and results of sample calculations are included. A detailed instruction for preparation of input data for the computer, samples of the computer input data and output, and the FORTRAN listing of the computer program are also given.

1. Propellers--Design--Mathematical analysis
2. Propellers--Design--Hydrodynamic aspects
3. Propellers--Load distribution--Programming
4. FORTRAN (Computer program language)--Applications
I. Cheng, Henry M.